NTNU

Norwegian University of
Science and Technology

Simplified Adaptive Control of Centrifugal Compressors

Andrzej Tomasz Jerzak

Master of Science in Cybernetics and Robotics
Submission date: January 2017
Supervisor: Jan Tommy Gravdahl, ITK

Norwegian University of Science and Technology
Department of Engineering Cybernetics

Summary

In this thesis adaptive surge control in axial and centrifugal compressor with unknown characteristic was studied. The compressor to be viewed as the control target, was a part of the compression system which also included the plenum and a throttling device, both located downstream to the compressor.

The literature offers already several research papers dealing with adaptive control of compressors, where the knowledge of the compressor map is not needed in advance. Summaries of some of the papers has been offered in this thesis. The author proposed a simplified version of an adaptive controller where the controller gain is being calculated by estimating the compressor characteristic. The estimation was carried out by using the most basic identification techniques: method of steepest decent and the least-squares.

Both strategies estimated the unknown coefficients of the compressor characteristic by processing input/output data of the latter on-line. The input signal for the estimation scheme consisted of a flow measurement at the compressor duct while the pressure rise at the compressor would constitute the output signal. Occasionally, the flow at the compressor duct will be unavailable for measurement. As a solution, the compression system will was coupled with an observer which predicted the behaviour of the compressor duct flow by considering the model for entire compression system. The observer originated from [12] where it has been proven that the flow is being predicted in a exponentially stable manner. The core of each of the estimation methods was the adaptive law, which will continuously updates the estimates of the unknown coefficients. The trajectories of the estimates was all said to be bounded functions. Strictly speaking, they are considered as elements of $\mathcal{L}_\infty$ and $\mathcal{L}_2$ spaces. This was verified with stability analysis where Lyapunov's direct method was applied. The stability analysis was previously published in [33] and has were included in this report.

Two types of actuators for surge control were considered: closed-coupled valve (CCV) and a piston. The resulting control law for both actuators was a basic proportional controller which recovered the compression system from surge and bring it towards global asymptotic stability. The controller operating CCV required feedback from compressor mass flow measurement while the piston was being run by the controller that required feedback from pressure measurements at the compressor discharge and at the plenum. By assigning the actuator and the controllers, the compressor was brought to global asymptotic stability even if it was operating at the unstable area in the first place. In the past, the gain for each controller was constructed by the coefficients used to describe the compressor characteristic. In subject to not knowing the compressor characteristic, the coefficients appearing in the controller would be replaced by their estimates which were generated by the earlier mentioned adaptive laws. The implementation of the adaptive laws depended on the knowledge of the coordinates of the system equilibrium. Yet another adaptive law was implemented to estimate the coordinates. The estimation was needed for equilibrium , since the computation of the latter is restricted to knowing the compressor characteristic. Linearization of the compression system augmented with the adaptive controller and the equilibrium estimation was used as a tool to demonstrate that under specific conditions the overall systems becomes locally asymptotically stable.

Preface

This thesis is submitted in partial fulfillment of the requirements for the master's degree in Engineering Cybernetics at the Norwegian University of Science and Technology.
The work on the thesis spanned from September 2016 to January 2017.

First of all, I would like to thank my supervisor Professor Jan Tommy Gravdahl. This thesis would never take place without his involvement. Not only did he let me work on the field of adaptive control of compressors, but throughout the period of the thesis, he has answered my questions of different issues.

I am also grateful to Nur Uddin, a PhD graduate from Department of Engineering Cybernetics at NTNU, for willingly sharing his knowledge on piston actuation.

My best regards and acknowledgements goes to Tor Wilhelm Seim, chief executive officer at Albaran AS, for providing a working place for me and for his effort of creating a warm and inclusive atmosphere so that I could fully concentrate on my thesis.

Finally, I would like to express my love to my brother Alexander and to my parents, Harald Damhaug and Ewa Jerzak-Damhaug.

Andrzej Jerzak
January 2017

Table of Contents

List of Tables

List of Figures

Abbreviations

MPC = **M**odel **P**redictive **C**ontrol

LQR = **L**inear **Q**uadratic **R**egulator

SAS = **S**urge **A**voidance **S**ystem

ASCS = **A**ctive **S**urge **C**ontrol **S**ystem

SL = **S**urge **L**ine

SCL = **S**urge **C**ontrol **L**ine

SM = **S**urge **M**argin

CCV = **C**losed-**C**oupled **V**alve

PAASC = **P**iston **A**ctuated **A**ctive **S**urge **C**ontrol

LMI = **L**inear **M**atrix **Inequality**

SPR = **S**trictly **P**ositive **R**eal

Chapter 1

Introduction and Motivation

1.1 Background

The compressor can be viewed as a mechanic device that has the potential of increasing the pressure of the fluid passing through it. A way of achieving such pressure rise is by basically decreasing the fluids volume. The bellow ideal gas law can be studied as an explanation to this phenomena:

$$p = \frac{mRT}{V} \tag{1.1}$$

where R is the gas constant. Moreover, p is the pressure of the fluid, while m, T and V are its mass,temperature and volume. respectively. A point made by [10] is that due to the definition of density being $\rho = \frac{m}{V}$, the compressor can alternatively be viewed as a device that provides gain in fluid pressure by increasing the density of the fluid. Over the years, the compressors has been used in a wide range of applications [34]. They are essential in gas turbines for power generation (Brayton cycle) and jet engines in aircraft. One can also found them in many household appliances such as refrigerators and air conditioners. In addition the compressors are commonly applied in process industry, where they are used to transport fluids through pipelines, for example in chemical plants and/or oil and natural gas production installations.

There are various types of compressors, some of them being centrifugal compressors, axial compressors and the positive displacement pumps. The axial and centrifugal compressors (termed turbo compressors by [10]) works by somewhat equal principle of operation which mainly consists of two steps: first increase the velocity of the fluid ,something that is being done by running the fluid through a row of rotating blades, and secondly decelerate the gas in divergence channels in order to obtain a pressure rise. The author will follow [10] and explain the second step by Bernoulli equation:

$$p_1 + \frac{1}{2}\rho v_1^2 = p_2 + \frac{1}{2}v_2^2 \tag{1.2}$$

for the flow assumed to be frictionless incompressible along the pipeline. The subscript "1" refers to the state of the fluid where its velocity is high. Meanwhile, the subscript "2" denotes the state of the fluid where its velocity has been slowed down, i.e. $v_1 > v_2$.

Obviously, for the equality in Bernoulli equation to hold, p_2 must be greater that p_1. The assumption of incompressibility which will be followed through entire report clearly contradicts with the ideal gas law. However, [10] supports this assumption stating that it is "made to illustrate conversion to pressure by means of simple expression".

The axial compressor got its name from both receiving and discharged the flow in the axial direction, that is, parallel with the axis of rotation [13]. A compression of a fluid can be further increased by assigning an axial or centrifugal compressor of multiple stages. The multiple stages compressors are simply single stages compressors mounted in series and are driven by the same shaft Thus, they are being run by the same rotational speed. Figures provided by [13] shows that an industrial single stage axial compressor is able to obtain a pressure rise in order $1.05 : 1 - 1.2 : 1$ with the efficiency ranging from 88% to 92% . If several stages are added together, the axial compressors have the potential to obtain a pressure rise up to 40 times the original pressure. [13] claims that axial compressor will be frequently encountered in gas turbines, especially for those with power exceeding 5MW. Although research in this thesis is applicable for both axial and centrifugal compressor due to their similarities, this report will emphasize centrifugal compressor, because of its popularity in the industry. For that reason, a whole subsection will be devoted to discuss centrifugal compressors.

The positive displacement pumps differs significantly from turbo compressors in terms of working principle and applications. Instead of accelerating the fluid to a higher velocity like for turbo compressors, positive displacement pumps obtain a gain in pressure by capturing a fixed amount of fluid in a chamber where the volume will be reduced by a piston mechanism. Once the fluid is compressed to a higher pressure (recall the ideal gas law), the fluid is forced (or displaced) into a discharge pipe or a throttle from which it leaves the compressor. The principle of operation for the positive displacement pump has been demonstrated by Figure 1.1

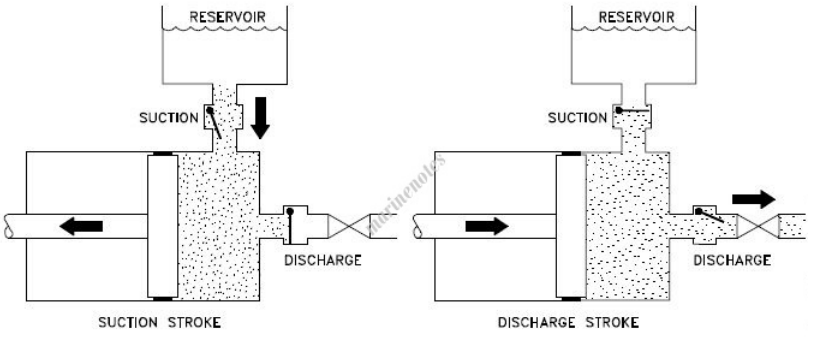

Figure 1.1: Positive displacement pump operation (Marine Notes, `http://marinenotes.blogspot.no`)

Because of its property of allowing fluid to pass with a low velocity, positive displacement pumps are consequently used in applications where one is requiring a combination of low flow rate and high pressure, such as pumping media containing fragile solids (Process Industry Forum, `http://www.processindustryforum.com/`).

Finally, positive displacement pumps operate at high efficiency and are the natural choice when dealing with high viscosity fluids.

1.2 Centrifugal Compressors

According to [14], the centrifugal compressors have three basic components which are the impeller, the diffuser and the volute (scroll) The impeller can be recognized as a rotating disk with curved blades (two-dimentional or three dimensional) and is driven by some device (typically a motor or a turbine) which generates a torque τ_d so that the compressor rotates with angular speed ω. While rotating, the impeller will increase the velocity of the incoming fluid and lead it radially outward through the diffuser. From the point of view of energy domain, one can say that the impeller converts its rotational energy to the kinetic energy in the flow. [48] calls the impeller "the most critical part of the centrifugal compressor", no matter which type of compressor it belongs to. It is further stated that the impeller stand for 70% of the total pressure rise considering a single stage. If the impeller is well-designed for the compressor, it can reach a efficiency of 96%. Another part of the compressor, the diffuser, comprises of vane passages and is responsible of slowing down the fluid and thus generating the pressure rise. The fluid with increased static pressure, is being collected by the volute which guides the fluid to the compressor outlet. The compound of the components making up the centrifugal compressor is being shown in Figure 1.2

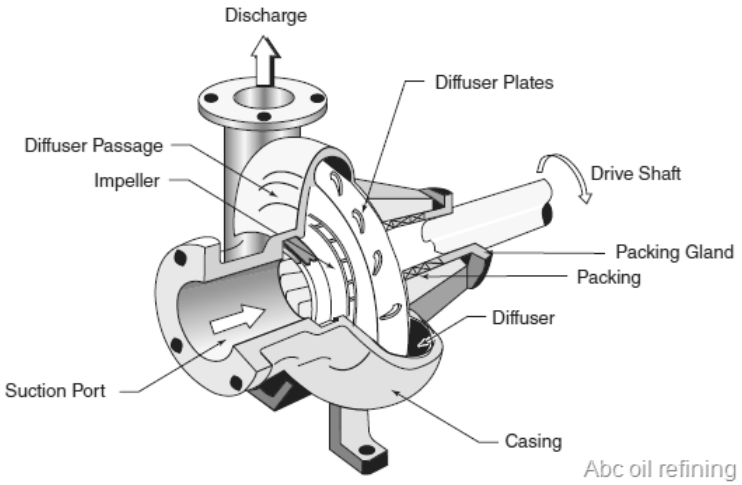

Figure 1.2: The components making up the centrifugal compressor (ME Mechanical, `http://me-mechanicalengineering.com`)

It is primary in the way of discharging the fluid out to the system, that the centrifugal compressor differs itself from the compressors of axial type. In contrast to axial compressors where the fluid is leaving in the axial direction, the fluid departs from the centrifugal compressor in the direction 90 degrees to the axis of rotating shaft, as proven by Figure 1.2. Besides, for the axial compressor, the deceleration of the fluid will take place in the stator blade passages, instead of the diffuser. The centrifugal compressors are limited to handling much lower flowrates then axial compressors, but in return are capable of delivering much higher pressure ratios. Nevertheless, the units used in the process industry have, according to [15], typically a pressure ratio around 1.3:1 per stage, so only slightly higher than for compressors of axial type. On other hand, the centrifugal compressors applied in gas turbines range in pressure ratios from 3:1 up to 7:1 for a single stage, clearly overcoming the axial compressors. Evaluation of Figure 7 in [14] shows that axial compressors beats centrifugal compressor when the overall efficiency is considered. According to [14], the centrifugal compressors can typically be found in following services of processes : combustion, distribution of natural gas, refrigeration and separation. The advantages of centrifugal compressors are that they are compact, robust and less affected by the performance degradation due to fowling [34]. In his master thesis, [42] states that this type of compressors is favoured in the process industry because they are more flexible and generate lower installation and maintenance costs.

1.3 Compressor Map

The relation between pressure at the compressor inlet, denoted by p_i and the pressure at the compressor outlet, denoted p_d is given as follows:

$$p_d = p_c(w_i, \omega)p_i \tag{1.3}$$

where

$$p_c(w_i, \omega) = \left(1 + \frac{\mu r_2^2\omega^2 - \frac{r_1}{2}(\omega - \alpha w_i)^2 - k_f\omega^2}{c_p T_{01}}\right)^{\frac{\kappa}{\kappa-1}} \tag{1.4}$$

is the pressure rise also to be addressed as the pressure ratio. Throughout the thesis, p_d will be equal to p_c. A very important thing to have in mind is that although $p_c(w_i)$ is not known as a function, a value of p_c at an arbitrary w_i is accessible. Notice that the pressure of the compressor rise for the centrifugal compressor depends both on rotation speed $\omega[\frac{rad}{s}]$ at the impeller and the flow $w_i[\frac{m^3}{s}]$ passing through the compressor. The flow w_i is termed inlet mass flow (inlet flow when non-dimensionalized). For the definitions of the constants appearing in eq. (1.4), the reader is referred to [26]. If the compressor rise is to be visualized as a function of inlet mass flow and impeller speed, the compressor characteristic (also known as compressor map) will be obtained. The map will often be presented as the collection of constant speed lines, as shown in Figure 1.3

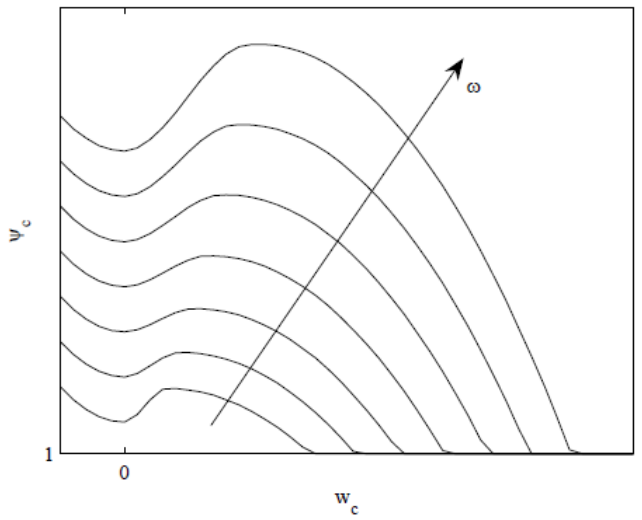

Figure 1.3: Compressor map [10]

As the name implies, the constant speed line will relate the pressure ratio to mass flow at a specific rotational speed. A single speed line can also be described by following cubic equation which has been provided by [39]:

$$p_c(w_i) = p_{c0} + H\left[1 + \frac{3}{2}\left(\frac{w_i}{W} - 1\right) - \frac{1}{2}\left(\frac{w_i}{W} - 1\right)^3\right] \tag{1.5}$$

where p_{c0} is the shut-off value of the axisymmetric characteristic, W is semi-width of the cubic axisymmetric compressor characteristic and H is the semi-height of the cubic axisymmetric compressor characteristic [51]. A detailed definition of the constant appearing in eq. (1.5) can be found in [39]. The compressor characteristic defines the operational domain of the compressor and should always be taken into account when selecting the size of the compressor [34]. It is unique for every compressor and will typically be provided by the manufacturer when purchasing the device. Alternatively, it can be retrieved by the compressor performance test, a procedure described in [52] and which also will be summarized later in this section. By analysing Figure 1.3, it can be observed that by either reducing the flow rate passing through the compressor (this can be done by adjusting the throttle opening in the system) or operating the device at higher rotational speed, a greater compressor rise will be achieved. However, too low flow rate will generate the unwanted phenomena of surge which will drive the compressor to instability. Usually, a surge line is drawn at the compressor map with the purpose of separating the stable area in the compressor map with the area where the surge will develop.

Now, moving to the topic of compressor map test. Simply, it will be performed by first setting the compressor to constant speed, then defining several operating points by varying the throttle opening and finally recording data of compressor rise and inlet mass flow for each point. Figure 1.4 shows experimental results of the compressor test done by [52].

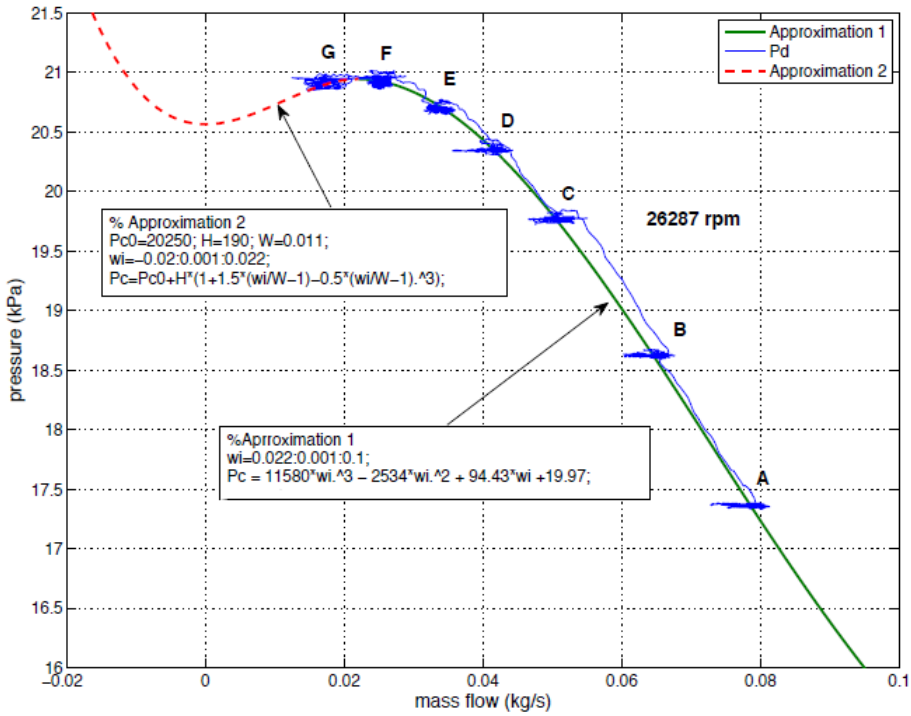

Figure 1.4: Compressor map obtained by the performance test [52]

The impeller was adjusted to a speed of 23978 RPM, and eight operating points were recorded and labelled sequentially by alphabet A to H. [52] reports that the first seven operating points were generated by gradually decreasing the throttle opening from 40% to 10%, resulted in a stable operation of the compressor, with point G approximately located at the surge line (referred to as the surge point) being the peak of the compressor characteristic. Point H, on the other hand, which was obtained by reducing the opening at the throttle to 5%, is said to be placed at the unstable area, thus bringing surge upon the compressor.

The cubic function in eq. (1.5) is being modelled by evaluating the instability conditions because of surge, making it valid over the unstable operating area of the compressor characteristic ("Approximation 2" in Figure 1.4). According to [52] the value of H is roughly equal to the amplitude of compressor outlet pressure oscillations (see Figure 4 in [52]), appearing due to the presence of surge. The inlet mass flow recorded for the surge point is being equal to 2W while the value of p_{c0} is a result of subtracting 2H from the pressure rise recorded for the surge point. Meanwhile, the compressor characteristic for the stable area can be approximated by considering operating point A to G. This approach, which have been labelled "Approximation 1" in Figure 1.4, can easily by done with polynomial curve fitting on the earlier mentioned point. The outcome will be a 3rd order polynomial function of inlet mass flow, as depicted in Figure 1.4.

1.4 Compressor Instability

1.4.1 Rotating Stall

Commonly, rotating stall is characterized by disturbance in uniform flow pattern [18]. In contrast to surge, rotating state will appear locally at the compressor. Strictly speaking, it tends to occur between the blade passages in the impeller (or rotor for axial compressors) where the flow may stall. The region of rotating stall may propagate exponentially along the blades until a certain state has been reached [18]. A row of axial compressor blades operating at a high angle of attack has been depicted in Figure 1.5.

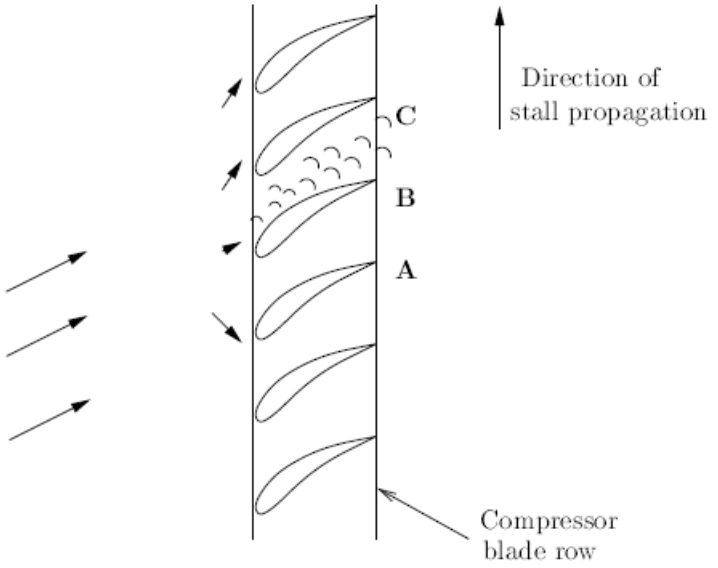

Figure 1.5: Physical mechanism for inception of rotating stall [23]

[23] describes the propagation mechanism as follows. "Suppose that there is non-uniformity in the inlet flow such that a locally higher angle of attack is produced on blade B which is enough to stall it. The flow now separates from the suction of the blade, producing a flow blockage between B and C. This blockage causes a diversion of the inlet flow away from B towards A and C, resulting in a increased angle of attack on C, causing it to stall. Thus the the stall propagate along the blade row".

Considering this scenario, the rotating stall can be classified into two types: part-span and full-span rotating stall. In a part-span rotating stall, only a limited region of the blade passage (the tip in most cases) will stall. For the full-span rotating stall, the stalling will occur at complete heigh of the annulus. Hence, the influence of the rotating stall may also be measured by the size of area the flow blockage is taking up in the compressor annulus [23]. For the centrifugal compressor, the stalling may be present in the parts of the impeller, in the diffuser or in the volute. The components may stall simultaneously or individually [18]. However, a stall in one component may not grow sufficiently in strength to spread to the other areas of the machine. As a consequence, several parts of the centrifugal com-

pressor may stall without the entire unit stalling [15]. It turned out that the rotating stall both in the impeller and the diffuser, may develop into surge for entire system. Nevertheless, the role of rotating stall in centrifugal compressors is still a matter of debate among the compressor researchers. [18] claims that rotating stall often will have little impact on pressure rise for centrifugal compressor and thus on surge. The significance of surge may also be questioned for single-stage axial compressors. For multi-stage axial compressors, rotating stall is more relevant for the applications where the shaft speed is relatively low.

1.4.2 Surge

The surge is a cyclical form of instability with the symptoms of large amplitude fluctuations both in pressure rise and mass flow in annulus (or duct). If not handled properly, this condition may further develop to *deep surge* where one may experience flow reversal [18]. The surge cycle, which generates the oscillations, have been illustrated in Figure 1.6.

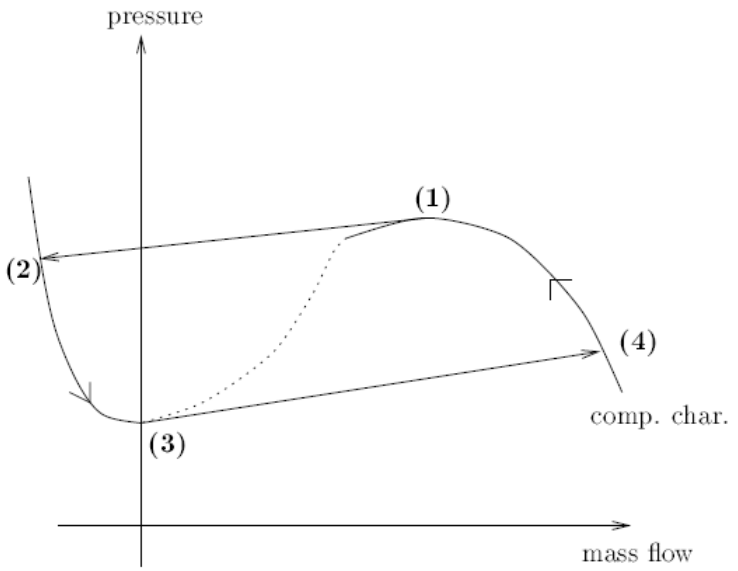

Figure 1.6: Surge cycle illustrated in a compressor map [56]

Initially, the compressor operates at steady-state in the stable area of the compressor. Then, a disturbance is applied on the system resulting in a flow deceleration. The compressor is now forced to operate at unstable point (1). The flow continues to decrease until it reaches its lower limit at point (2) where the flow now have a negative value and thus becomes reversal. Next, the flow accelerates first to point (3) (where it reaches a zero value) and then to (4) at the stable area. With no changes in the system, the cycle follows the compressor characteristic up to the point (1), meaning that the surge cycle repeats.

When the compressor is suffering from some local aerodynamic instability, say rotating stall, it will be unable to deliver sufficient pressure so that the flow moving downstream from the compressor will loose its continuous nature. This results in the incident of surge. Seen from other perceptive, the surge is a consequence of the compressor ,which is limited

to constant impeller speed, not keeping up with the excessive increase in system resistance such as decrease in throttle opening. [15]. The resistance will then reduce the flow, making it reversal and thus unsteady. The unsteady flow will interfere with other components besides the compressor, making the system unstable as a whole. As stated earlier, the rotating stall is often viewed as the inception of surge. Ironically, while the flow in pure rotating stall is known for its nonuniform mass deficit [18], the flow will retrieve its uniformity during the surge condition.

A phenomena of surge can, according to [18] be divided into four different types:

1. *Mild surge*: exhibits small pressure oscillations. No evidence of flow reversal.
2. *Classic surge*: will often have larger oscillations at lover frequency then mild surge. Still no flow reversal.
3. *Modified surge*: characterized by unsteady and non-axisymmetric flow. Combination of rotating stall and classic surge.
4. *Deep surge*: a most severe form for surge. Flow reversals are typical. The cycle described above occurs for deep surge

Notice that this terminology is not unique, and may vary through the literature. At least for axial compressors, several types of compressor surge may be experienced in a sequence [18]. The first step is mild surge, followed by rotating stall. From rotating stall, the system can possibly go over to classic surge or deep surge. Deep surge may itself convert into modified surge, presuming that the system is affected with some kind of nonaxisymmetric disturbances. Apart from mild surge, operation under surge condition is rather hazardous and should be avoided at all cost. Along with reduced pressure rise and degradation in efficiency, the surge may expose the impeller blades to vibrations and eventual damage. Not only will high-amplitude vibrations tear the compressor, they can also damage the system components surrounding it, in particular pipe connections [51]. Another consequence of surge, as well as rotating stall, is the fact that it may lead to heating of the impeller blades and temperature rise at the compressor outlet. Surprisingly, the instability of surge tends to appear quite often in the process industry. Disfunctionalities that have a possibility of inducing surge are: the compressor is not fulfilling the system requirements, inappropriate design of the compressor and failing anti-surge control system. Another factor is unfavourable arrangement of piping and process components that in some way are interconnected with the compressor.

1.5 Contributions

This thesis attempts to contribute on following areas:

(1) Performing a literature review on adaptive active control of compressors

(2) In the case of the compressor map being poorly known, the thesis will propose an adaptive version of the control law (18) for closed-coupled valve in [24]. Comparison of the adaptive and non-adaptive controller will be given by simulations.

(3) The knowledge of the compressor map is also necessary in order to find the gain for controller piston actuation. To compensate for that, the thesis will look for appropriate control law which in turn will be modified with adaptive extension. Comparison of the adaptive and non-adaptive controller will be given by simulations

(4) Real time measurement of mass flow may be unobtainable for feedback. The thesis will investigate if there is an observer type that can supply the adaptive controllers with an estimate of mass flow. The accuracy of the suggested observer will be studied by simulations. The possibility of having the controller that assumes feedback from pressure will also be looked into.

The adaptive controller developed in this thesis will estimate the coefficients of the compressor map. The estimates will later be used for construction of the controller in (2) and (3). Unless otherwise stated, the compressor is restricted to constant speed and the only disturbance will occur in reducing the throttle opening. Finally, all flows are regarded to have real and positive values.

1.6 Implementation

The simulations in this thesis were carried out in the software MATLAB 2016a along with its toolbox Simulink. Implementation of the adaptive controller derived by the gradient method was based on solution of Assignment 7 in the course TTK4215 at NTNU. Implementation of the adaptive controller derived by the method of least-squares was based on a simulation example dealing with the identification of the pendulum by method of least-squares with forgetting factor. The example was offered in the course TTK4215.

1.7 Outline of the Thesis

- **Chapter 2:** The compression model pioneered by Greitzer will be studied. At first, the brief history and advantages of the model will be given. The analysis will continue into describing the model in detail before demonstrating how the model can be derived by applying basic principles of physics. The analysis will end at investigating the the open-loop stability of the Greitzer model.

- **Chapter 3:** Two basic strategies on surge prevention will be reviewed. The actuation by closed-coupled valve and piston will being included into the Greitzer model. The control law for each choice of the actuator will also be presented. The thesis has managed to come up with the control law for piston that assumed feedback from pressure.

- **Chapter 4:** Design of the parameter estimator by considering two identification approaches. Stability analysis will follow for both of them. Stability analysis will be given for both of them. The theory in the chapter has been provided by [33].

- **Chapter 5:** A very brief review on the observers in the compressors will be given. Later, a GES observer which is applied in this thesis, will be studied and then non-dimentionalized. The chapter ends with mentioning the separation principle for the observer.

- **Chapter 6:** Examples of the adaptive surge controller will be presented.
- **Chapter 7:** The performance of the adaptive controllers and the accuracy of the observer will be validated by numerical simulations.
- **Chapter 8:** Discussion of the results in Section 8.
- **Chapter 9:** Concluding remarks

Chapter 2

The Model of Greitzer

2.1 Introduction

Over the years there have been published a large amount of literature that concerns the topic of compressor system modelling. However, it is the groundbreaking model of Greitzer that really stands out. The model, which was outlined for axial compressors, was presented in [28]. It is an improvement to its predecessor in [19] when it comes to capturing the phenomena of surge. The Greitzer model has maintained the non-linear nature of compression system as opposed to model given in [19] which has been derived by linearization. It allows model of Greitzer to display full-sized amplitude oscillations generated by the surge condition. This cannot be said about the model developed in [19] because, as the model departures further and further from its equilibrium, it becomes less and less accurate. Hence, it can only exhibit surge oscillations at relatively small amplitudes . Few years after the Greitzer model was first published, [31] made it also applicable for the centrifugal compressors. The invention of the Greitzer model allowed for developing a large amount of strategies with the aim of preventing both axial and centrifugal compressors to operate at the surge condition. More on this topic later. It is also worth mentioning that in his master thesis, [42] showed that the Greitzer model can be implemented as an equality constraint in the algorithm for the MPC-controller which is assigned to run the compressor in a optimal manner, that is, with maximum efficiency. The model of Greitzer belongs to the classification of compressor models that can be used to simulate both the surge and rotating stall ([10] reports that there exists some compressor models that are only able to capture the phenomena of surge). Whether one is dealing with surge or rotating stall in a Greitzer model can be determinated by considering a value of a special parameter, termed Greitzer B-parameter, that will be revealed later in the chapter when the model has been non-dimensionalized.

2.2 Description of the Greitzer Model

The compression system that is considered for the Greitzer model, contains mainly of three components: a compressor, a plenum and a throttle. As shown by the Figure 2.1, the flow w_i with the pressure p_i is being directed to the compressor through a upstream duct (called

compressor duct in the figure) with the length and section area denoted as L_c and A_c, respectively. The mass flow symbolized as w_d (which is equal to w_i at steady-state) with the pressure p_d (obtained by the pressure rise at the compressor) is now being discharged into the plenum of the fixed volume V_p, containing the pressure p_p and the temperature T_p. It is assumed that the thermodynamic properties are all uniform over the plenum volume. If the heat losses to the surroundings are small, compared with the total energy related to the plenum, the losses can be neglected, meaning that all processes taking place in the plenum can be regarded as isentropic. On the other side of the compression system, the throttle has been placed with the purpose of adjusting the outlet mass flow w_o from the plenum. Changes in the outlet mass flow are obtained by basically varying the throttle opening. Both, the upstream duct and the duct containing the throttling device, which is described as outlet duct in the figure, is assumed to contain flows at relative small velocities. Thus, one can model the flows as incompressible. Furthermore, the passing fluid at both ducts is assumed to contain velocity lines pointing in the same direction, allowing to establish the fact that the corresponding flows are one-dimensional. By neglecting the friction at the ducts, one can consider p_i and p_o equal to the pressures at station A (p_A) and station B (p_B), respectively. From the surge control point of view, the plenum pressure p_p and the flow at the compressor inlet flow w_i can be viewed as the system states. Meanwhile, the throttle opening can be both considered as a control input or as a disturbance, depending on the circumstances.

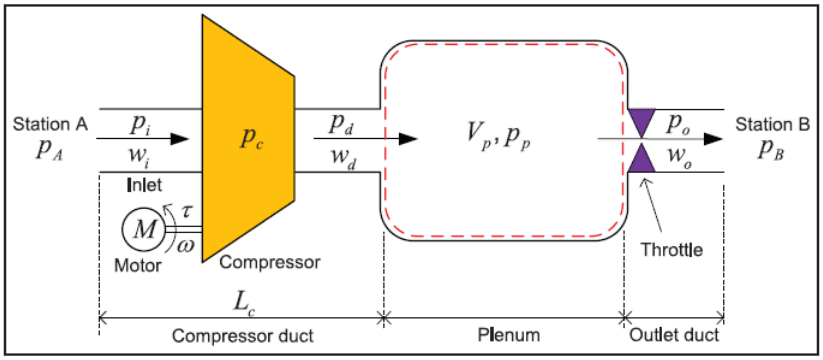

Figure 2.1: Model of a single compression system [51]

A reader that have some experience in the control engineering will know that the transient dynamics of the system states can be described by differential equations which are typically related to some laws of physics. Due to the lack of ability of adjusting impeller speed ω by varying the drive torque τ, the differential equation for impeller has been left out from the system equations. The differential equations of Greitzer compression model are:

$$\dot{w}_i = \frac{A_c}{L_c}(p_c(w_i) - p_p) \tag{2.1a}$$

$$\dot{p}_p = \frac{a_0^2}{V_p}(w_i - w_o(p_p)) \tag{2.1b}$$

The pressure rise $p_c(w_i)$ has replaced p_d in eq. (2.1a). Apart from the earlier defined parameters, a_0 is the speed of sound while $w_o(p_p)$ symbolize the outlet mass flow as the

function of the plenum pressure and is given by:

$$w_o(p_p) = u_T k_T \sqrt{p_p - p_o} \tag{2.2}$$

where k_T a constant specifying the throttle and u_T is the throttle opening ranging from 0 $\%$ to 100 $\%$. The throttle is assumed to contain no inertance. In other words, the relation between the pressure drop at the plenum and the rate of change of the outlet flow is neither effected by the length or the section area of the downstream duct. It will also be independent of the fluid density [55]. Now, p_i and p_0 have been set equal to the atmospheric pressure which is defined as a zero-reference for the gauge pressure. Hence, the equation for outlet mass flow may be simplified to:

$$w_o = u_T k_T \sqrt{p_p} \tag{2.3}$$

2.3 Derivation of the Dynamic Equations for the Greitzer Model

This section will give the reader an insight on the equations (2.1a) and (2.1b) can be obtained by applying the fluid dynamic laws of mass conservation and momentum balance, an approach originally considered by Greitzer when developing his model. The reader should be aware, that there exist other concepts from which the model for the compression system may be derived. For instance, [51] demonstrated that by evaluating the energy transfers between components, one can arrive at the same set of differential equations as for the Greitzer model. The presented procedure of deriving the equations has been based on the research in [10] and [26]. The second part which consists of the derivation of dynamic equation for w_i, was originally published in [34]. By accounting for fixed control volume and uniform density at the plenum, the volume integral describing the rate of mass flow is given by:

$$\frac{d}{dt}\int_{V_p(t)} \rho_p dV = \frac{d\rho_p}{dt}\int_{V_p(t)} dV = V_p \frac{d\rho_p}{dt} \tag{2.4}$$

which is equal to the mass balance:

$$V_p \dot{p}_p = w_i - w_0(p_p) \tag{2.5}$$

As previously mentioned, all processes in the plenum are isentropic. This property, along with evaluating the fluid as an ideal gas allows to establish the relation:

$$dp_p = a_0^2 d\rho_p \tag{2.6}$$

along with

$$a_0 = \sqrt{\kappa R T} \tag{2.7}$$

where R is now the mean radius of the compressor and $\kappa = \dfrac{c_p}{c_v}$ is the ratio of specific heats . Combination of equations (2.5), (2.6) and (2.7) yields:

$$\begin{aligned} \frac{dp}{dt} &= c_p^2 \frac{d\rho}{dt} \\ \frac{dp}{dt} &= c_p^2 \frac{1}{V_p}(w_i - w_o(p_p)) \\ \dot{p}_p &= \frac{c_p^2}{V_p}(w_i - w_o(p_p)) \end{aligned} \tag{2.8}$$

Thus, it has been verified that by taking into consideration the principle of mass balance, one can indeed arrive at the differential equation for the plenum pressure in (2.1b). To proceed with the derivation of the differential equation for the inlet mass flow, one can set up the momentum equation:

$$\frac{d}{dt}(m_d C) = A_c p_d - A_c p_p \tag{2.9}$$

where

$$m_d = L_c A_c \rho \tag{2.10}$$

is the mass of the flow passing through the compressor duct. By using the following expression for inlet mass flow

$$w_i = \rho A_c C \tag{2.11}$$

the velocity C can be defined as

$$C = \frac{w_i}{\rho A_c} \tag{2.12}$$

and by combining the equations (2.9), (2.10) and (2.12), the differential equation for the mass flow at the compressor inlet becomes:

$$\begin{aligned} \frac{d}{dt}\left(\frac{L_c A_c \rho w_i}{\rho A_c}\right) &= A_c p_d - A_c p_p \\ \frac{d}{dt}(L_c w_i) &= A_c p_d - A_c p_p \\ \dot{w_i} &= \frac{A_c}{L_c}(p_d - p_p) \end{aligned} \tag{2.13}$$

and the derivation differential equation for inlet mass flow in eq. (2.1a) has been completed. Remember that p_d has been replaced by $p_c(w_i)$ in the compressor models analyzed in this thesis.

2.4 Non-dimensionalization of the Greitzer model

There are several reasons why the non-dimensionalization of the dynamic equations for an arbitrary model is beneficial. Not only will one gain the reduction of the parameters constants occurring in the dynamic equations (from 4 to 1 in the case of the Greitzer model) but one can also more easily identify the dominant term in a equation. This property can turn out to be valuable, when performing sensitivity analysis of the model,[37] and [42]. As for the model of Greitzer, by non-dimensionalizing the dynamic equations one is allowed to operate with the *Greitzer's B-parameter* which is not only a useful tool for detecting instabilities in the compression system but may also be used to predict the size and shape of the surge cycles [41]. Non-dimensionalization will be performed by using the factors: $\frac{1}{2}\rho U^2$ for plenum pressure p_p, $\rho U A_c$ for the compressor inlet mass flow w_i (where U is the mean velocity of the rotor) and $1/\omega_H$ for time t. The arising non-dimension equivalents for the five system variables are:

$$\phi = \frac{w_i}{\rho U A_c} \;,\; \Phi_T(\psi) = \frac{w_o(p_p)}{\rho U A_c} \;,\; \psi = \frac{p_p}{\frac{1}{2}\rho U^2} \;,\; \Psi_c(\phi) = \frac{p_c(w_i)}{\frac{1}{2}\rho U^2} \text{ and } \tau = t\,\omega_H \tag{2.14}$$

with ω_H being the Helmholtz frequency:

$$\omega_H = a_0 \sqrt{\frac{A_c}{V_p L_c}} \tag{2.15}$$

The non-dimensionalization for the eq. (2.1a) yields:

$$\begin{aligned} \dot{w_i} &= \frac{A_c}{L_c}(p_c(w_i) - p_p) \\ \frac{\rho U A_c d\left(\frac{w_i}{\rho U A_c}\right)}{\frac{d\tau}{\omega_H}} &= \frac{1}{2}\rho U^2 \frac{A_c}{L_c}\left(\frac{p_c(w_i)}{\frac{1}{2}\rho U^2} - \frac{p_o}{\frac{1}{2}\rho U^2}\right) \\ \dot{\phi} &= \frac{U}{2\omega_H L_c}(\Psi_c(\phi) - \psi) \end{aligned} \tag{2.16}$$

By introducing the Greitzer B-parameter:

$$B = \frac{U}{2\omega_H L_c} \tag{2.17}$$

eq. (2.16) can be rewritten to:

$$\dot{\phi} = B\left(\Psi_c(\phi) - \psi\right) \tag{2.18}$$

Now, moving to non-dimentionalization of eq. (2.1b):

$$\begin{aligned} \dot{p_p} &= \frac{a_0^2}{V_p}(w_i - w_o(p_p) \\ \frac{\frac{1}{2}\rho U^2 d\left(\frac{p_p}{\frac{1}{2}\rho U^2}\right)}{\frac{d\tau}{\omega_H}} &= \rho U A_c \frac{c_p^2}{V_p}\left(\frac{w_i}{\rho u A_c} - \frac{w_o}{\rho u A_c}\right) \\ \dot{\psi} &= \frac{2\omega_H L_c}{U}(\phi - \Phi_T(\psi)) \end{aligned} \tag{2.19}$$

By considering the definition of the Greitzer B-parameter, one will get:

$$\dot{\psi} = \frac{1}{B}(\phi - \Phi_T(\psi)) \tag{2.20}$$

Putting together equations (2.18) and (2.20) results in the non-dimensional model of Greitzer:

$$\begin{aligned} \dot{\phi} &= B\left(\psi_c(\phi) - \psi\right) \\ \dot{\psi} &= \frac{1}{B}(\phi - \Phi_T(\psi) \end{aligned} \tag{2.21}$$

with $\Phi_T(\psi)$ is being defined as:

$$\Phi_T(\psi) = \gamma_T \sqrt{\psi} \tag{2.22}$$

where the throttle gain $\gamma_T = k_T u_T$ was defined for simplicity. A study of the B-parameter may help identify the mode of the compressor instability one will encounter during the stall time [28]. If the parameter is above some critical value, denoted as B_{crit}, the system will oscillate due to presence of surge. For the cases where the parameter is bellow B_{crit}, one may expect the compressor to suffer from rotating stall. As a closing remark, it needs to be mention that B_{crit} is unique for every single compressor [23].

2.5 Equilibrium Point and Open-Loop Stability

Let the equilibrium point of the system states in eq. (2.21) be denoted as $x_0 = [\psi_0 \quad \phi_0]^T$ so that:

$$\dot{\phi} = f(\psi_0) = 0$$
$$\dot{\psi} = f(\phi_0) = 0$$

A subject of equilibrium point has been concerned in [24], where it has been defined in visual manner as the intersection between the compressor characteristic $\Psi_c(\phi_o)$ and the throttle characteristic. The latter is defined as

$$\Psi_T(\phi) = \frac{1}{\gamma_T^2}\phi^2 \tag{2.23}$$

and can easily be obtained by rewriting the equation for $\Phi_T(\psi)$. When decreasing the opening at the throttle, something that will be achieved by reducing γ_T, the equilibrium point moves along the compressor characteristic toward lower flow values. Such scenario has been visualized in Figure 2.2.

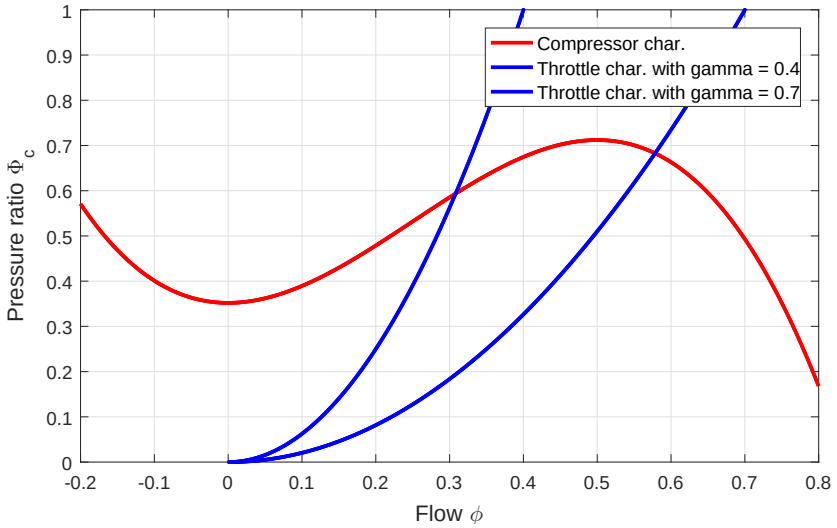

Figure 2.2: Compressor and throttle characteristic in the same coordinate system

If the equilibria is to the right of the peak of the compressor characteristic, the system will remain stable. However, equilibria placed to the left of the peak value, will lead

the system towards the surge condition Said differently, if the equilibrium is located at the positive slope of the compressor characteristic, the system will become unstable. The latter statement will be proven when open-loop stability of the compression system in (2.21) is analysed locally. Linearizing the model in (2.21) with respect to the equilibrium x_0, yields following model on state-space form:

$$\begin{bmatrix} \dot{\tilde{\psi}} \\ \dot{\tilde{\phi}} \end{bmatrix} = \begin{bmatrix} -\frac{1}{Bg_T} & \frac{1}{B} \\ -B & Bg_c \end{bmatrix} \begin{bmatrix} \tilde{\psi} \\ \tilde{\phi} \end{bmatrix} \tag{2.24}$$

where

$$A = \begin{bmatrix} -\frac{1}{Bg_T} & \frac{1}{B} \\ -B & Bg_c \end{bmatrix} \tag{2.25}$$

is the system matrix and

$$g_c = \frac{\partial \Psi_c}{\partial \phi} \text{ along with } g_T = \frac{\partial \Phi_T}{\partial \psi}$$

are slopes of the compressor characteristic and the throttle characteristic, respectively. Be aware that in this context, the throttle characteristic is equal to the outlet flow at the throttle. In addition, the variables $\tilde{\psi} = \psi - \psi_0$ and $\tilde{\phi} = \phi - \phi_0$ represent departures from the equilibrium and will play a important role later in the thesis. The stability of the linearized system can be studied by evaluating the eigenvalues of the matrix A. In order to obtain the eigenvalues , one has to solve the characteristic equation with respect to λ. The equation becomes:

$$\lambda^2 + \left(\frac{1}{Bg_T} - Bg_c\right)\lambda + \left(1 - \frac{g_c}{g_T}\right) = 0 \tag{2.26}$$

and the solution is found to be

$$\lambda = \frac{-\left(\frac{1}{Bg_T} - Bg_c\right) \pm \sqrt{\left(\frac{1}{Bg_T} - Bg_c\right)^2 - 4\left(1 - \frac{g_c}{g_T}\right)}}{2} \tag{2.27}$$

As stated by [25], the expression for the eigenvalues reveals that the stability of the compression system is bounded by a relation between the slope of compressor characteristic, the throttle characteristic and Greitzer B-parameter. Moreover, [25] distinguish between two types of instability for the compression system For the case where $\left(1 - \frac{g_c}{g_T}\right) < 0$, the slope of the compressor characteristic will be steeper then for throttle characteristic (g_c is greater than g_T) and the system becomes statically unstable. Furthermore, $-\left(\frac{1}{Bg_T} - Bg_c\right) < 0$ implies that the slope of compressor characteristic will be positive at the equilibrium. Consequentially, the dynamic instability will be released upon the system. As stated by [3], static instability is related to the departure from the original operating point to a new operating point because of the interference of small disturbances. Figure 2.2 might visualize this scenario, if the reduction in the throttle gain can be regraded as the system disturbance. Meanwhile, the dynamic instability acts as the criterion that induces the fluctuations in the plenum pressure and inlet flow. A remark made by

[3] is that static instability is necessary but may not be sufficient alone to induce the dynamic instability. [42] reports that if the compression system is to be stabilized, g_c must be upper-bounded by:

$$g_c < \frac{1}{B^2 g_T} \tag{2.28}$$

along with

$$g_c < g_T \tag{2.29}$$

at the equilibrium point. The stabilization schemes discussed in the next chapter will all try to satisfy those criteria.

Chapter 3

Surge Control

3.1 Introduction

The drawbacks associated with surge made the control community to came up with various approaches, so that this instability would not enter the system. Such techniques can commonly be divided into two groups: surge avoidance system (SAS) and active surge control system (ASCS). The chapter begins with description of both of them, although the emphasis will be on active surge control since this method is far more pertinent for this thesis. Later, two variants of ASCS are to be mentioned and their relevance to adaptive extension will be shown. The derivation based stability analysis for both variants are left to their respective authors. This is no secret, hoverer, that each of them will use standard P-controllers to maintain a global asymptotic stability for the overall system. A later modification of both controller will require the knowledge of the equilibrium point. It may however be unobtainable in advance. As a solution, the author will propose an adaptive scheme for the equilibrium, originating from [6].

A reliable detection is necessary for proper anti surge control and [18] addresses this issue in some extent. Primarily, one should focus on monitoring the physical quantities that can easily indicate the presence of surge. A reasonable choice for measurement would in such case be the inlet mass flow and the plenum pressure. Another important factor of properly detecting surge is selection of suitable instruments. To quickly counteract the effects of surge, sensors and actuators are required to have small time constants and delays. The importance of short reaction time to surge occurrence is emphasized by [18], since the compressor may enter into deep surge in a short period of time if not taken care off. It is preferable to choose instruments that are not intrusive, and if they are for some reason, they should be placed downstream to the compressor instead of upstream. Finally, one should limit the instrumentation to smallest possible extent in order to keep down the investments and maintenance costs in addition to simplifying possible future repairs, [18].

3.2 Surge Avoidance System (SAS)

Traditionally, one has managed to keep the compressor away from the instability of surge by equipping the compression system with SAS. The surge avoidance system is based on the idea of preventing the compressor to operate near or beyond the surge line (SL) at the compressor map. For this purpose, a *surge control line* (SCL) has been introduced and has been placed to the right of the SL. It cannot under any circumstances be crossed by the compressor while in operation. The distance between the SL and SCL is denoted *surge margin* (SM) and is defined as:

$$\text{SM} = \frac{w_{SCL} - w_{SL}}{w_{SCL}} \tag{3.1}$$

where w_{SL} is the mass flow at SL while w_{SCL} is the mass flow at SCL. [18] suggests 10% as a descent value for the surge margin. The way the compressor escapes from operating at the unstable area is being illustrated by Figure 3.1

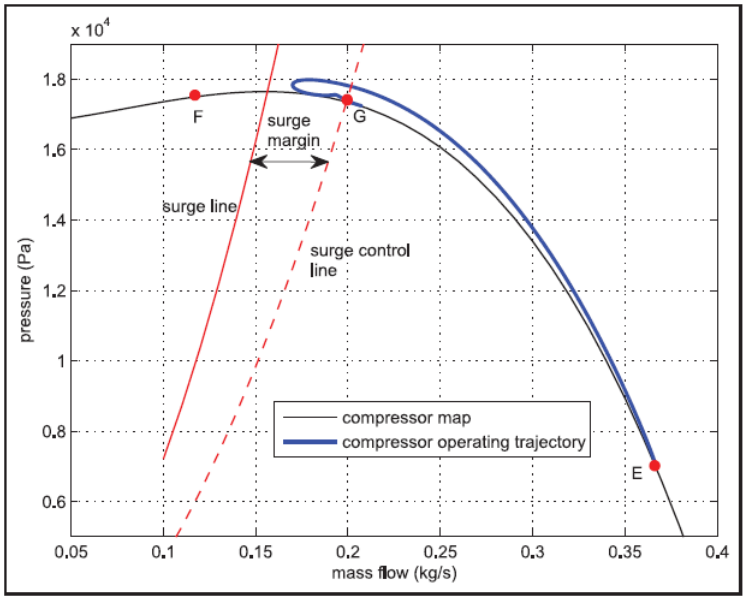

Figure 3.1: Trajectory of the compressor system prevented from going into surge [51]

At the beginning, the compressor operates at steady-state (point E in the Figure 3.1) with the throttle opening at 100% Then, the opening at the throttle is being reduced to 20%, which will move the operating point of the compressor to F (in the surge area) if SAS has not been implemented in the compression system. Instead the operating point will move towards the surge area but while it crosses SCL, the fluid will be recycled from the plenum back to the compressor inlet (the SAS-controller has detected that $w_i < w_{SCL}$) and the compressor will be forced to operate at point G located at the SCL[34]. Hence, the compressor has been prevented from entering the unstable condition of surge. It needs to be noted, however, that the compensation for the disturbances and the uncertainty of the

compressor map (and hence the surge line) will require an extension of the surge margin. As a consequence of implementing the surge avoidance method, the feasible region of the compressor will be limited. What follows is restriction of the compressor capability since the point of peak pressure will often be located close the surge margin, which the compressor is unable to cross. Another significant drawback of the surge avoidance is the fact that one will often need to resort to recycling or bleed in order to achieve it, two actuator strategies [18] deprecates to use since they will cause further efficiency losses. Those claims are supported by [10], who states that "same gas" will be compressed several times consuming even more energy. In terms of blowing off flow through the bleed valve, the already compressed flow is discharged downstream the compressor and into system surroundings, making the compression of it meaningless in the first place.

3.3 Active Surge/Stall Control System (ASCS)

Another method to overcome the compressor surge is active surge/stall control which became popular during the last two decades. [23] explains that its rising popularity must partially be credited to the introduction of the Moore - Greitzer model [39]. The model of Moore and Greitzer is a result of further developing the Greitzer model by including the rotating stall amplitude as a system state and not just incorporate it as a pressure drop like for some other models [23]. The method of active surge control differs fundamentally from surge avoidance. Hence, some of the drawbacks that are typical for SAS, will not be encountered in ASCS. Instead of not letting the compressor operate near the surge line one is allowing the compressor to operate at the unstable area and then recovering the system from surge by introducing an active element. Application of this strategy benefits in extension of the operating range of the compressor and thus improving its performance. This strategy of stabilizing rather than avoiding surge and rotating stall, will provide robustness to the system and the interfering disturbances that are capable of initiating the surge or the rotating will be handled without degenerating the efficiency of the compressor.

The method of active surge control was pioneered by [20]. Over the years, there have been proposed several actuators for ASCS with an overview given in [56]. The interesting proposals for the actuator that have been listed are movable wall [30], loudspeaker [57], suction-side valve [40] and air injection/bleed valve [58]. By taking into account how the actuators works to stabilize the surge, active surge control can according to [53] be divided into the concept of either increasing the pressure at the compressor upstream duct or decreasing the pressure at the plenum by flowing more fluid out of the plenum. This two approaches have in the control literature been commonly referred to as upstream energy injection and downstream energy dissipation, respectively. A controller based on downstream energy dissipation requires feedback from compressor mass flow while a controller based on upstream energy injection requires feedback from pressure measurement at the plenum [53].

This section will give examples of implementation of both types, where a *closed-couple valve* (CCV for short) will be used as a actuator for downstream energy dissipation while upstream energy will be carried out though *piston* actuation. Various strategies can be used to derive the control laws for both approaches of ASCS. Examples are nonlinear controller design using Lyapunov's method, feedback linearization, bifurcation theory and backstepping. The latter will be used to design the controller for CCV. As for the piston, several

design methodologies will be evaluated.

3.3.1 Closed-Couple Valve

The idea of using a closed-couple valve as a actuator was studied in various research papers, with [24], [43], [45] and [46] being among them. The impact of CCV on surge stabilization was verified by [24] which is the main contributor to this section. To quote [46]: " the term closed-couple implies that there is no significant mass storage (fluid capacitance) between the valve and the compressor". The idea of placing the control valve very close to the compressor is supported by [29] where it is argued that the stability effect of the control valve falls when the distance between the compressor and the control valve is enlarged. [43] persuades to position the control valve between the compressor and the plenum. This is to avoid the decrease in control efficiency for system characterized by a large B. A system with an increased B, is said to be more compliant which implies that the unsteady flow through the throttle is less coupled with the unsteady flow through the compressor.

[45] investigated the possibilities of coupling CCV with the feedback of either inlet flow or plenum pressure. The conclusion was that for the cases where a simple P-controller is chosen as the control structure, a feedback from inlet flow will ensure stabilization under any circumstances as long as the controller gain K is chosen sufficiently large. The ability of stabilizing the compressor surge by proportional feedback from plenum pressure will be limited by the values of the parameter B and the slope of the compressor characteristic g_c. More precisely, the feedback by plenum pressure will only be useful when the slope of the equivalent compressor characteristic ,given by $m_{Ce} = \frac{\partial(\Psi_c - \Psi_v)}{\partial\phi}$), is upper-bounded so that $m_{Ce} < \frac{1}{B^2 g_T}$ where Ψ_v is the pressure drop at CCV and is addressed as the CCV characteristic. The slope of the throttle characteristic tends to be in a order of 10-100 while the B-parameter exceeds unity in many application [45]. In such cases, the stabilization abilities of the proportional feedback by plenum pressure will be limited to a great degree. It needs to be remarked that those conclusions was based on the linearized version of the compressor model, so they may not hold over large perturbations from equilibrium. With the assumption of no flow stored between the CCV and the compressor, one can treat the two devices as one component, termed "equivalent compressor" by [46]. Furthermore, [46] defines the characteristic of the equivalent compressor as:

$$\Psi_e(\phi) = \Psi_c(\phi) - \Psi_v(\phi) \tag{3.2}$$

where $\Psi_v(\phi)$ is expressed by:

$$\Psi_v(\phi) = \frac{1}{\gamma_{cc}^2}\phi^2 \tag{3.3}$$

where $\gamma_{cc} > 0$ is proportional to the valve opening and will be considered later.

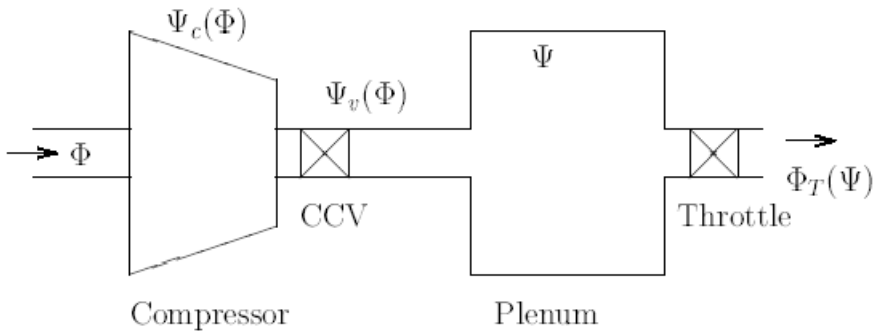

Figure 3.2: Single compression system extended with CCV [24]

The compression system in a serial configuration with CCV is being illustrated by Figure 3.2. The dynamics of the expanded system are determinated by the equation set:

$$\begin{aligned} \dot{\phi} &= B(\Psi_e(\phi) - \psi) \\ \dot{\psi} &= \frac{1}{B}(\phi - \Phi_T(\psi)) \end{aligned} \tag{3.4}$$

The extension of the system with CCV, shifts the equilibrium point to the intersection of the equivalent compressor characteristic defined in eq. (3.2) and the throttle characteristic. This allows to manipulate the slope of the equivalent characteristic at the equilibrium point, by adjusting $\gamma_c c$. Therefore, the pressure drop at the control valve will be regarded as the systems input, i.e. $u = \Psi_v$. Before assigning it with a specific control law, a transformation of system coordinates suggested by [46] will be performed. The transformation results in shifting the equilibrium to the origin and has been defined by [46] as:

$$\hat{\phi} = \phi - \phi_0 \tag{3.5}$$

$$\hat{\psi} = \psi - \psi_0 \tag{3.6}$$

The variables defined in equations (3.5) and (3.6) will from now on be referred as *deviation variables* since they measure the departure from the equilibrium. The system characteristics mapped with the new coordinates are:

$$\hat{\Psi}_e(\hat{\phi}) = \Psi_e(\hat{\phi} + \phi_0) - \Psi_e(\phi_0) = \Psi_e(\phi) - \Psi_e(\phi_0) \tag{3.7}$$

$$\hat{\Psi}_c(\hat{\phi}) = \Psi_c(\hat{\phi} + \phi_0) - \Psi_c(\phi_0) = \Psi_c(\phi) - \Psi_c(\phi_0) \tag{3.8}$$

$$u = \hat{\Psi}_v(\hat{\phi}) = \Psi_v(\hat{\phi} + \phi_0) - \Psi_v(\phi_0) = \Psi_v(\phi) - \Psi_v(\phi_0) \tag{3.9}$$

Applying the transformation to the model in (3.4) yields:

$$\begin{aligned} \dot{\hat{\phi}} &= B(\hat{\Psi}_c(\hat{\phi}) - \hat{\psi} - u) \\ \dot{\hat{\psi}} &= \frac{1}{B}(\hat{\phi} - \hat{\Phi}_T(\hat{\psi})) \end{aligned} \tag{3.10}$$

with

$$\hat{\Phi}_T(\hat{\psi}) = \gamma_T\sqrt{\hat{\psi} + \psi_0} - \gamma_T\sqrt{\psi_0} = \sqrt{\psi} - \gamma_T\sqrt{\psi_0} \tag{3.11}$$

$$\hat{\Psi}_c(\hat{\phi}) = -k_3\hat{\phi}^3 - k_2\hat{\phi}^2 - k_1\hat{\phi} \tag{3.12}$$

where for the latter equation

$$k_1 = \frac{3H\phi_0}{2W^2}\left(\frac{\phi_0}{W} - 2\right) \quad , \quad k_2 = \frac{3H}{2W^2}\left(\frac{\phi_0}{W} - 1\right) \quad , \quad k_3 = \frac{H}{2W^3} \tag{3.13}$$

Obviously, $k_3 > 0$ while $k_1 \leq 0$ if the equilibrium is unstable and $k_1 > 0$ otherwise. The sign of k_3 vary independently of the stability conditions. Motivation behind the change of variables is to get the insight on how the states deviates from their desired equilibrium point. Shifting the coordinates will also pay off in simplifying the expression for the compressor map ,as showed by eq. (3.12), which turns out to be essential in later design of the parameter estimator. [24] showed by applying the methodology of backstepping, that if the controller gain c_1 satisfies:

$$c_1 > \frac{k_2^2}{4k_3} - k_1 \tag{3.14}$$

the control law

$$u = c_1\hat{\phi} \tag{3.15}$$

will make the equilibrium of the closed-loop system in (3.10) globally uniformly asymptotic stable (GUAS). Due to pressure drop at the CCV being defined as the system input, one can establish the relation:

$$\begin{aligned} u = \hat{\Psi}_v(\hat{\phi}) &= \Psi_v(\hat{\phi} + \phi_0) - \Psi_v(\phi_0) = \Psi_v(\phi) - \Psi_v(\phi_0) \\ &= \frac{1}{\gamma_{cc}^2}\phi^2 - \frac{1}{\gamma_{cc}^2}\phi_0^2 \end{aligned} \tag{3.16}$$

By inserting

$$u = c_1\hat{\phi} = c_1(\phi - \phi_0) \tag{3.17}$$

following equation will be obtained:

$$c_1(\phi - \phi_0) = \frac{1}{\gamma_{cc}^2}\phi^2 - \frac{1}{\gamma_{cc}^2}\phi_0^2 \tag{3.18}$$

and when solved with respect to γ_{cc}, it is revealed that:

$$\gamma_{cc} = \sqrt{\frac{\phi + \phi_0}{c_1}} \tag{3.19}$$

Clearly, the control law will affect the equivalent compressor characteristic by adjusting the gain γ_{cc} of the closed-couple valve. The adaptive laws presented and analyzed in Chapter 4 will provide the control law in eq. (3.24) with estimates of k_1,k_2 and k_3, so that lower bound on c_1 can be specified.

3.3.2 Piston Actuation

Piston-actuated active surge control system, PAASCS for short, originate from [50]. Over the years,the literature has offered several improvements to PAASCS. Theoretical work of [49] showed that active surge control involving a piston can be realized with a *linear quadratic regulator* (LQR) which is related to the field of of optimal control. The linear quadratic regulator will further be modified with integral action to bring the piston drift

down to zero at steady-state. Although ASCS and SAS are commonly regarded as two distinguish anti-surge strategies, [49] proved by simulations that ASCS and SAS can be combined together where SAS will act as a back-up if ASCS should fail under some circumstances. The analysis given in this section will stick to a pure PAASCS and three design approaches are to be evaluated in order to derive a controller later to be made adaptive. The compression system extended with piston actuation is being shown by the Figure 3.3:

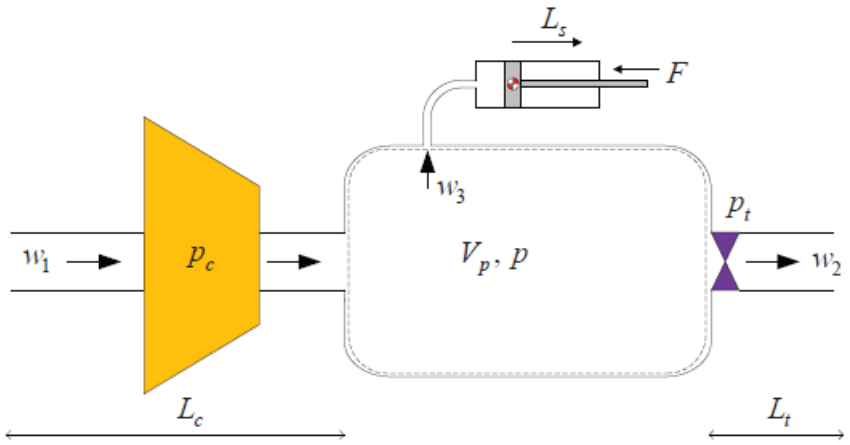

Figure 3.3: Compression system equipped with piston [50]

Key parameters of the presented system that have not been defined in previous section are: piston position L_s which is time-varying, mass of the piston denoted m_s and force F applied on the rod of the piston. The force F is being regarded as the system input. As the surge occurs, the movable piston wall will adjust the flow w_c directed out of the plenum, reduce the plenum pressure (recall the terminology of downstream energy dissipation) and bring the compressor to asymptotic stability. According to [50], the stiffness and the damping associated with the piston can be neglected due to being dominated by the pressure and actuating forces. Alternatively, they could be included in the model by being compensated for by the input force F, as stated by [50]. The assumption made for the compression system given by the Greitzer model will follow here. The bellow equations describes the dynamics of system depicted in figure 3.3.

$$\begin{aligned} \dot{w}_i &= \frac{A_c}{L_c}\left(p_c(w_i) - p_p\right) \\ \dot{p}_p &= \frac{a_o^2}{V_p}\left(w_i - w_o(p_p) - \rho A_s \frac{dL_s}{dt}\right) \\ m_s \frac{d^2 L_s}{dt^2} &= \rho A_s - F \end{aligned} \tag{3.20}$$

where w_i, w_o and p_p have replaced w_1, w_2 and p in order to follow earlier established notation. Finding the control law for the system represented by the equation set (3.20) can be quite challenging due to the systems complexity. Two control laws were proposed by [50] for this particular system. The first one has been designed by employing the backstepping method, and although not fully revealed by the authors, it will probably contain many

complicated terms, and consequently has been omitted from further discussion. The second law to be proposed, has been conducted with the aim of making the Jacobian matrix have eigenvalues in the right half-plane. A matrix with such properties, has been named Hurwitz matrix by the control community. What follows is a local asymptotic stability for the equilibrium point. Neither the second control law will be used, however, because it does not exploit the linear nature of the compressor characteristic (obtained by shifting the coordinates of the states) which makes it inconvenient to form the adaptive controller evolved this thesis. To continue the search for a more suited control law, there will be a need to look for a less complicated model. One way to achieve it is to treat the piston as an actuator with very fast transient dynamics so that the only contribution the piston will have to the system is through the outflow w_u. The simplified version of (3.20) is given by:

$$\begin{aligned} \dot{w_i} &= \frac{A_c}{L_c}(p_c(w_i) - p_p) \\ \dot{p_p} &= \frac{a_o^2}{V_p}(w_i - w_o - w_u) \end{aligned} \tag{3.21}$$

with w_u now being defined as the control input. By non-dimnsionalizing equation set (3.21) in the same manner as for the original Greitzer model, one will get the following:

$$\begin{aligned} \dot{\phi} &= B(\Psi_c(\phi) - \psi) \\ \dot{\psi} &= \frac{1}{B}(\phi - \Phi_T(\psi) - \phi_u) \end{aligned} \tag{3.22}$$

The coordinates for PAASCS will be transformed in the same way as they were for CCV. The model described by the equation set (3.22) expressed with the new coordinates will take the form:

$$\begin{aligned} \dot{\hat{\phi}}_1 &= B(\hat{\Psi}_c(\hat{\phi}) - \hat{\psi}) \\ \dot{\hat{\psi}} &= \frac{1}{B}(\hat{\phi} - \hat{\Phi}_T(\hat{\psi}) - \hat{\phi}_u) \end{aligned} \tag{3.23}$$

where $\hat{\phi}_u = \phi_u$ Now, consider the control law:

$$\hat{\phi}_u = -c_2 B^2(\hat{\Psi}_c - \hat{\psi}) \tag{3.24}$$

which has been designed by [53] for the system given in (3.23). [53] proved by applying Lyapunov stability method and Young's inequality that by choosing the controller gain c_2 within the bounds:

$$k_m \leq \frac{c_2}{2} \leq k_n \tag{3.25}$$

with $k_m = \left.\frac{\partial \hat{\Psi}_c}{\partial \hat{\phi}}\right|_{\max}$ and $k_n = \left.\frac{\partial \hat{\psi}}{\partial \hat{\Phi}_T}\right|_{\min}$, the global asymptotic stability of the operating point

will be ensured. Next, recall the definition of the compressor characteristic:

$$\hat{\Psi}_c(\hat{\phi}) = -k_3\hat{\phi}^3 - k_2\hat{\phi}^2 - k_1\hat{\phi} \tag{3.26}$$

Because of the cubic nature of the compressor characteristic, the maximum positive slope (as implied by the lower bound of the controller gain c_2) is located at at the inflection

point in the stable area of the compressor characteristic. Like for any twice differentiable function, the inflection point can be determinated by evaluating function's second derive at zero. For the compressor characteristic curve, the inflection point occurs at $\hat{\phi}_m$ equal to:

$$\frac{\partial^2 \hat{\Psi}_c}{\partial \hat{\phi}^2} = -6k_3\hat{\phi} - 2k_2 = 0 \Longrightarrow -6k_3\hat{\phi} = 2k_2 \Longrightarrow \hat{\phi}_m = -\frac{k_2}{3k_3}$$

and is given by:

$$k_m = \left.\frac{\partial \hat{\psi}_c}{\hat{\phi}}\right|_{\hat{\phi}=\hat{\phi}_m} = \frac{k_2^2}{4k_3} - k_1 \tag{3.27}$$

Appendix in [50] proved that

$$k_n = \left.\frac{2\hat{\psi}}{\hat{\Phi}_T}\right|_{\min} \tag{3.28}$$

Since k_n from eq. (3.28) is not expressed by the coefficients k_1,k_2 and k_3 from the compressor map, it will not be accounted for in this thesis. To avoid the violation of upper bound k_n, c_2 has been placed fairly closed to the lower bound k_m defined in (3.27). The adaptive laws presented and analyzed in Chapter 4 will provide the control law in eq. (3.24) with estimates of k_1,k_2 and k_3, so that k_m can be specified.

3.4 Determination of the Equilibrium Point

As a consequence of implementing the closed-loop compression system in (3.10) and (3.23) , the coordinates of the equilibrium point $x_0 = [\phi_0, \psi_0]^T$ has to be known prior to the simulation. For CCV, the coordinates may be determinated by first solving the following 3rd order equation originally given in [23]:

$$\begin{aligned} \Psi_c(\phi_0) - \Psi_v(\phi_0) &= \frac{1}{\gamma_{cc}^2}\phi_0^2 \\ \psi_{c0} + H\left(1 + \frac{3}{2}\left(\frac{\phi_0}{W} - 1\right) - \frac{1}{2}\left(\frac{\phi_0}{W} - 1\right)^3\right) - \frac{c_1\phi_0}{2} &= \frac{1}{\gamma_{cc}^2}\phi_0^2 \end{aligned} \tag{3.29}$$

which follows from

$$\begin{aligned} \Psi_v(\phi_0) &= (u + \Psi_v(\phi_0))|_{\phi=\phi_0} \\ &= \left(c_1(\phi - \phi_0) + \frac{c_1}{\phi + \phi_0}\phi_0^2\right)\Bigg|_{\phi=\phi_0} \\ &= \frac{c_1\phi_0}{2} \end{aligned} \tag{3.30}$$

Then, ϕ_0 can be found by using the formula for the throttle characteristic:

$$\psi_0 = \frac{1}{\gamma_T^2}\phi_0^2 \tag{3.31}$$

Regarding the actuation by piston, the equilibrium may be obtained by simply drawing $\Psi_c(\phi)$ and $\Psi_T(\phi)$ in the same coordinate system and locating the intersection between

them. Both approaches will depend on knowing the compressor characteristic. Since the compressor characteristic is assumed unobtainable, neither of the them can be applied. Alternatively, an approximation of the equilibrium coordinates may be used. In such case, the asymptotic stability cannot be guaranteed for the controller, but convergence to a set and avoidance of surge can be shown. The proof can be found in [23]. If neither this alternative is attractive,[6] provided following linear adaptation law linear adaptation law for the equilibrium point.

$$\dot{\hat{\theta}} = P(x - \hat{\theta}) \tag{3.32}$$

where

$$\hat{\theta} = \begin{bmatrix} \hat{\phi_0} \\ \hat{\psi_0} \end{bmatrix} \tag{3.33}$$

is the estimate of the unknown equilibrium point

$$\theta^* = \begin{bmatrix} \phi_0 \\ \psi_0 \end{bmatrix} \tag{3.34}$$

Furthermore,

$$P = \begin{bmatrix} p_1 & p_2 \\ p_3 & p_4 \end{bmatrix} \tag{3.35}$$

is the adaptive gain matrix to be designed and $x = [\phi \quad \psi]^T$ is earlier defined state vector. The performance of the adaptive law will be presented in section 7 The closed-loop compression systems in (3.10) and (3.23) , can both be expressed in more general manner as:

$$\dot{x} = f(x) + g(x)u \tag{3.36}$$

with the control law

$$u = \varphi(x - x_0) = \varphi(z) \tag{3.37}$$

Augmenting the closed-loop system (3.36) with the recently defined adaptive law in 3.32 gives the new and extended system

$$\dot{x} = f(x) + g(x)\varphi(x - \hat{\theta})$$
$$\dot{\hat{\theta}} = P(x - \hat{\theta})$$

What follows is a statement made by [6].

" Let $[x_0^T \ , \ \theta_0^T]^T$ denote an equilibrium of (3.38). The non singularity of P implies that all equilibria must satisfy $x_0 = \theta_0$, "Let the $[x_0^T \ , \ \theta_0^T]^T$ represent the equilibrium of (3.38). If P is chosen to be a non-singular matrix, all equilibria will have to satisfy $x_0 = \theta_0$ witch in turn implies that $\varphi(x_0 - \hat{\theta_0}) = 0$."

The statement will be revisited when the performance of the adaptive law is evaluated. The desired equilibrium x_0 along with any other possible equilibria will not depend on the parameters of the controller as long as asymptotic stability is secured. The rest of this section will be dedicated to discussing under which conditions the system in (3.38) will become asymptotically stable. First, let's begin with the singular perturbation analysis and define $x_{QSS} = h(\hat{\theta})$, so that:

$$f(x_{QSS}) + g(x_{QSS})\varphi(x_{QSS} - \hat{\theta}) = 0 \tag{3.38}$$

Furthermore, the boundary-layer system with constant $\hat{\theta}$ is defined to be:

$$\dot{x} = f(x) + g(x)\varphi(x - \hat{\theta}) \tag{3.39}$$

and

$$\dot{\hat{\theta}} = \epsilon P(h(\hat{\theta}) - \hat{\theta}) \tag{3.40}$$

is termed the reduced system. If slow adaptation is being chosen, the adaptive law for equilibrium will be on the form:

$$\dot{\hat{\theta}} = \epsilon P(x - \hat{\theta}) \tag{3.41}$$

where $0 < \epsilon \ll 1$. Next, consider the following theorem together with its corresponding proof [6]:

Theorem 1. *For a given equilibrium point x_0 assume that:*

(1) there exist a control law $u = \varphi(\phi - \phi_0)$ where $\varphi(0) = 0$ such that x_0 is an asymptotically stable equilibrium point of (3.36)

(2) $J_0 \triangleq \partial f/\partial x$ and $J_c \triangleq J_0 + g\,(\partial\varphi/\partial x)$ evaluated at $x = x_e$ are non-singular.

Under these conditions, there exist a matrix $P \in \mathbb{R}^{2x2}$ and a scalar $\epsilon^* > 0$ such that , $\forall\epsilon \in [0, \epsilon^*)$, x_0 is an exponentially stable equilibrium of the extended system (3.38)*.*

Proof. It follows from Assumption (1) that (3.39) has an exponetially stable equilibrium. Moreover, the linearization of the reduced system (3.40) around $\hat{\theta}_e = x_0$ is expressed as:

$$\dot{\hat{\theta}} = \epsilon P \left(\frac{\partial h}{\partial \hat{\theta}} - I \right) \hat{\theta} \tag{3.42}$$

Taking the derivative with respect to θ in (3.39) and noting that $\varphi(.)$ vanishes at the equilibrium gives:

$$\begin{aligned}
J_0 \frac{\partial h}{\partial \hat{\theta}} + g\frac{\partial \varphi}{\partial z}\left[\frac{\partial h}{\partial \hat{\theta}} - I\right] &= 0 \\
\frac{\partial h}{\partial \hat{\theta}}\left[J_0 + g\frac{\partial \varphi}{\partial z}\right] - g\frac{\partial \varphi}{\partial z} &= 0 \\
\frac{\partial h}{\partial \hat{\theta}} J_c - g\frac{\partial \varphi}{\partial z} &= 0 \\
\frac{\partial h}{\partial \hat{\theta}} &= J_c^{-1} g\frac{\partial \varphi}{\partial z} \\
\frac{\partial h}{\partial \hat{\theta}} - I &= J_c^{-1} g\frac{\partial \varphi}{\partial z} - I \\
&= J_c^{-1}\left[g\frac{\partial \varphi}{\partial z} - J_c\right] \\
&= -J_c^{-1} J_0
\end{aligned} \tag{3.43}$$

Lastly, the reduced system described by (3.40) can now be expressed as:

$$\hat{\theta} = -\epsilon \left(P J_c^{-1} J_0\right) \hat{\theta} \tag{3.44}$$

From Assumption (2),it follows that $J_c^{-1}J_0$ is non-singular. Therefore there exists a matrix P such that $PJ_c^{-1}J_0$ is Hurwitz, which in turn implies the local exponential stability of the equilibrium x_0 of (3.44). Since the two subsystems are exponentially stable, the local asymptotic stability of the equilibrium of the composed system (3.38) for sufficiently small ϵ will be ensured (Chapter 7, Corollary 2.3 in [36]). □

Chapter 4

On-Line Parameter Estimation

4.1 Introduction and Definition

The identification of the system starts with investigating its structure. Once the structure has been settled, the system identification will switch into obtaining "the values of certain constant commonly referred to plant or model parameters" [33]. Those parameters will typically be obtained by measurements or calculations based on laws of physics. They can also in many cases be specified in the set of data provided by the manufacturer. In some applications, however, those options are not possible and the only way to determinate the parameters is to examine how the systems input and output signals are related to each other. Such experiments are in the control literature known as parameter estimations. The parameter estimation can either be carried out off-line or on-line. The estimation of the parameters done on-line generates the estimates of the unknown parameters while the system is running. Hence, the name on-line parameter estimation. Such form of parameter estimation will be preferable for the systems where parameters vary with time, for example due to change in the operation condition. The adaptive law which generates the estimates, will most often be represented by a differential equation. It can be constructed by solving a optimization problem where one aims to minimize the deviation between the system measurement, $y(t)$, and the output signal from the parametrized model, $\hat{y}(\theta, t)$. Hopefully, the adaptive law will be defined in such way so that $\hat{y}(\theta, t)$ converge to $y(t)$ as the time goes on. This is being achieved by continuously updating the vector $\theta(t)$ containing the estimates. Obviously, a $\hat{y}(\theta, t)$ getting closer to $y(t)$ implies that the estimate θ is approaching the unknown parameter vector θ^*. The concept of on-line parameter estimation can easily be implied to the issue of identifying the compressor characteristic. The latter is regarded as the system, while inlet flow and pressure rise are considered as the input signal and as output signal, respectively. In the section 4.3, it will be demonstrated that the compressor characteristic can be expressed as *linear parametric model* which allows for application of two fundamental estimation techniques that will be reviewed later in the chapter.

4.2 Mathematical preliminaries

The convergence properties of the two adaptive laws will be evaluated in terms of $\mathcal{L}_p$ stability. For a reader unfamiliar with this concept, some definitions (which has been taken from [33]) will be offered:

4.2.1 Lp Spaces

Let x denote some function of time, with possibilities of being a scalar function or a vector function. It will belong to space $\mathcal{L}_p$ if

$$\|x\|_p \triangleq \left(\int_0^\infty |x(\tau)|^p d\tau \right)^{1/p} \tag{4.1}$$

exists (that is, $\|x\|_p$ is finite) for some $p \in [1, \infty)$. Moreover, if the $\mathcal{L}_\infty$-norm

$$\|x\|_\infty \triangleq \sup_{t \geq 0} |x(t)| \tag{4.2}$$

exists for x, one is saying that x belong to $\mathcal{L}_\infty$. Lastly, if x is a scalar function,$|.|$ will represent the absolute value. On the other hand, if x is supposed to be a vector function defined in $\mathbb{R}^n$, $|.|$ is denoting any norm in $\mathbb{R}^n$

4.2.2 Lp Stability

The linear time-invariant (LTI) system considered for definition of $\mathcal{L}_p$-stability is being described by the convolution of input signal u(t) and system response h(t):

$$y(t) = u * h \triangleq \int_0^t h(t-\tau)u(\tau)d\tau = \int_0^t u(t-\tau)h(\tau)d\tau \tag{4.3}$$

One is saying that the system in (4.3) is $\mathcal{L}_p$-stable if $u \in \mathcal{L}_p \Rightarrow \mathcal{L}_p$ along with $\|x\| \leq c\|u\|$ for some constant $c > 0$. More precisely, if $u \in \mathcal{L}_p$ and $h \in \mathcal{L}_1$ then

$$\|y\|_p \leq \|h\|_1 \|u\|_p \tag{4.4}$$

for some $p \in [1, \infty)$. In the case of $p = \infty$, $\mathcal{L}_p$ - stability (or $\mathcal{L}_\infty$ - stability) is being referred to as bounded-input bounded-output (BIBO) stability.

4.3 Linear Parametric Model

Recall the compressor characteristic:

$$\hat{\Psi}_c(\hat{\phi}) = -k_3\hat{\phi}^3 - k_2\hat{\phi}^2 - k_1\hat{\phi} \tag{4.5}$$

where k_1,k_2 and k_3 are the unknown constants to be generated by the adaptive law and as previously shown, used to construct the the lower bound for the surge controller. By defining

$$y = \hat{\Psi}_c \tag{4.6}$$

as the output signal,

$$z = \begin{bmatrix}\hat{\phi}^3 & \hat{\phi}^2 & \hat{\phi}\end{bmatrix}^T \tag{4.7}$$

as the regressor, and

$$\theta^* = \begin{bmatrix}-k_3 & -k_2 & -k_1\end{bmatrix}^T \tag{4.8}$$

as the vector containing the unknown constants, the equation (4.5) may be expressed as the linear parametric model:

$$y(t) = \theta^{*T} z(t) \tag{4.9}$$

which got its name from letting the unknown vector θ^* to appear linearly in the equation The prediction $\hat{y}$ of y at time t is given as follows:

$$\hat{y}(t) = \theta^T(t) z(t) \tag{4.10}$$

The definition of prediction in (4.10) allows for construction of the prediction (estimation) error:

$$\epsilon_1(t) = y(t) - \hat{y}(t) = y(t) - \theta^T(t) z(t) \tag{4.11}$$

When defining the parameter estimation error, $\tilde{\theta}$, as $\tilde{\theta} \triangleq \theta - \theta^*$, eq. (4.3) can be rewritten on the form:

$$\epsilon_1(t) = y(t) - \hat{y}(t) = \theta^{*T} z(t) - \theta^T(t) z(t) = -\tilde{\theta}^T(t) z(t) \tag{4.12}$$

It has become obvious that there exist a relation between $\epsilon_1(t)$ and $\tilde{\theta}$. An observant reader will notice that none of the elements in z(t) are bounded functions. Neither the signal $\hat{y}(t)$ is guaranteed to be bounded. Consequentially, the upcoming optimization problem may be ill-posed, meaning that small variations in the input data will result in large changes to the solution [8]. This can be solved by normalizing both $z(t)$ and $\hat{y}(t)$ with a signal m (given by $m^2 = 1 + n_s^2$) so that:

$$\bar{y} = \frac{y}{m} \in \mathcal{L}_\infty \quad \text{and} \quad \bar{z} = \frac{z}{m} \in \mathcal{L}_\infty$$

A straightforward choice for n_s is $n_s = z$ and thus $m^2 = 1 + z^T z$. The prediction of $\bar{y}$ is being generated as:

$$\hat{\bar{y}} = \theta^T \bar{z} \tag{4.13}$$

which arises the normalized prediction error to be:

$$\bar{\epsilon}_1 = \bar{y} - \hat{\bar{y}} = \frac{y - \hat{y}}{m} = \frac{y - \theta^T z}{m} \tag{4.14}$$

It will be seen in the upcoming section, the recently defined normalized estimation error and the regressor will play an important part in deriving the adaptive law for θ

4.4 Method of Steepest Descent

The method of steepest descent is according to [5], the simplest version of the gradient method for solving an optimization problem. The method of steepest descent can be classified as line search algorithm, meaning that it is heading for the solution θ^* of the optimization problem

$$\begin{aligned} &\text{minimize} \quad J(\theta) \\ &\text{subject to} \quad \theta \in \mathbb{R}^n \end{aligned} \tag{4.15}$$

by selecting a direction d_k and the length λ_k for the current state θ_k with the goal of improving (in most cases reducing) the present value of the objective function $J(\theta_k)$. When the direction d_k and the length λ_k have been determinated, the search continues to a new state θ_{k+1}. The procedure of choosing the length and the direction is being done in an iterative manner for some initial approximation θ_0 and new states are generated until some conditions are satisfied causing the search to be terminate. What characterizes the method of steepest descent is that the chosen direction always equals the opposite direction of the gradient at the current state, that is $d_k = -\nabla J(\theta_k)$. Equation (4.16) shows how the next state in the steepest descent method is being computed:

$$\begin{aligned} \theta_{k+1} &= \theta_k + \lambda d_k \\ &= \theta_k - \lambda \nabla J(\theta_k) \end{aligned} \tag{4.16}$$

As far as termination conditions are concerned [7] lists up following criteria:

(i) Before computing the next iteration state θ_{k+1}, one has to check if following holds:

$$||\nabla J(\theta_k)|| \leq \epsilon_G \tag{4.17}$$

where ϵ_G is the tolerance of the gradient and is defined by the user. If (4.17) is satisfied, the search is stopped resulting in $\theta^* = \theta_k$.

(ii) Furthermore, if following reduction appears for two consecutive iterations:

$$|J(\theta_{k+1} - J(\theta_k)| \leq \epsilon_A + \epsilon_R |J(\theta_k)| \tag{4.18}$$

the search is terminated and one concludes that $\theta^* = \theta_k$. The parameters ϵ_A,ϵ_R, denotes absolute tolerance and relative tolerance respectively. Like for ϵ_G, ϵ_A and ϵ_R are also being supplied by the user.

The algorithm for solving the optimization problem by applying the method of steepest descent is constructed as in [7]:

Algorithm 1 Steepest Descent Algorithm

1: Select a starting point θ_0 and parameters ϵ_G, ϵ_A,ϵ_R. Set iteration index $k = 0$.
2: Compute $\nabla J(\theta_k)$. Stop if $||\nabla J(\theta_k)|| \leq \epsilon_G$. Otherwise, define a direction vector $d_k = -\nabla J(\theta_k)$.
3: Obtain λ_k and update $\theta_{k+1} = \theta_k - \nabla J(\theta_k)$.
4: Evaluate $J(\theta_{k+1})$. Stop if

$$|J(\theta_{k+1} - J(\theta_k)| \leq \epsilon_A + \epsilon_R |J(\theta_k)|$$

is satisfied for two successive iterations. Otherwise set $k = k+1$,$\theta_k = \theta_{k+1}$ and go to step 2.

The algorithm presented here differs from the one in [7], since it assigns the direction for the next iteration point to be $d_k = -\nabla J(\theta_k)$ rather than $d_k = -\nabla J(\theta_k)/||\nabla J(\theta_k)||$. The stopping criteria in the in Algorithm 1 will not be taken into account when deriving the adaptive law for the surge controller later on. There, one is simply assuming that the search is stopped when $d_k = -\nabla J(\theta_k) = 0$, providing some local minimum. Besides, the optimization problem used to design the adaptive law will be continuous and since Algorithm 1 only is eligible for optimization problems on discrete form, its update equation (Step 3) has to be reformulated. Hence, Algorithm 1 is not fitted for the kind optimization problem needed in this thesis. It has been presented solely with purpose of giving the reader an understanding on how the method of steepest descent may be implemented. By defining infinitesimally step lengths, the continuous version of equation (4.16) will be given by the following differential equation:

$$\dot{\theta} = -\nabla J(\theta(t)), \quad \theta(t_0) = \theta_0 \tag{4.19}$$

The author will follow [33] and scale the direction of steepest descent with the positive definite $n \times n$ non-singular scaling matrix $\Gamma = \Gamma^T$. By letting $\Gamma = \Gamma_1 \Gamma_1^T$ and saying that;

$$\Gamma_1 \bar{\theta} = \theta \tag{4.20}$$

the optimization problem (4.15) (which is now assumed to be continuous) gets an equivalent

$$\begin{aligned} &\text{minimize} \quad J(\bar{\theta}) \triangleq J(\Gamma_1 \theta) \\ &\text{subject to} \quad \bar{\theta} \in \mathbb{R}^n \end{aligned} \tag{4.21}$$

The differential equation generating the trajectory $\bar{\theta}(t)$ for (4.21) becomes:

$$\dot{\bar{\theta}} = -\nabla J\left(\bar{\theta}\right) = -\nabla J\left(\Gamma_1 \bar{\theta}\right) \tag{4.22}$$

Because $\nabla J\left(\bar{\theta}\right) = \frac{\partial J\left(\Gamma_1 \bar{\theta}\right)}{\partial \bar{\theta}} = \Gamma_1^T \nabla J\left(\Gamma_1 \bar{\theta}\right)$ and $\Gamma_1 \bar{\theta} = \theta$, equation (4.22) can be rewritten as:

$$\begin{aligned} \Gamma_1^{-1} \dot{\theta} &= -\Gamma_1^T \nabla J(\theta) \\ \dot{\theta} &= -\Gamma_1 \Gamma_1^T \nabla J(\theta) \\ \dot{\theta} &= -\Gamma \nabla J(\theta) \end{aligned} \tag{4.23}$$

The scaling matrix Γ will from known on be referred to as *adaptive gain*. Although, there various types of objective functions to be chosen from, in order to keep the optimization simple, following objective function has been proposed:

$$J(\theta) = \frac{\bar{\epsilon}_1^2}{2} = \frac{(\bar{y} - \theta^T \bar{z})^2}{2} = \frac{(y - \theta^T z)^2}{2m^2} = \frac{\epsilon^2 m^2}{2} \tag{4.24}$$

with ϵ being constructed to

$$\epsilon = \frac{y - \hat{y}}{m^2} \tag{4.25}$$

The objective function $J(\theta)$ is being minimized with respect to θ for each time t by applying the method of steepest descent (from now and onward referred to as the gradient method). The problem formulated by eq. (4.24) have the property of being convex. As a

result, any local solution of the problem, will also be a global solution. The gradient of the objective function, $J(\theta)$ is found to be

$$\nabla J(\theta) = \frac{\left(y - \theta^T z\right) z}{m^2} = -\epsilon z \tag{4.26}$$

Finally, the adaptive law for generating $\theta(t)$ may now be written as:

$$\dot{\theta} = -\Gamma \epsilon z \tag{4.27}$$

Naturally, a following question arises: "Will θ ever reach θ^*"? The answer that follows is: "It depend on how the input signal z is being constructed. If the input signal $z(t)$ is "rich" enough, the outcoming signal $y(t)$ will contains sufficient information about the unknown θ^*, and the correct estimation of the latter will be reached eventually". However, one might still ask: "how do I know that an input signal I am using for my parameter estimation can be identified as "rich"? Well, one way to examine quality of the input signal is to check whether it satisfy *persistent excitation* condition, meaning:

$$\int_0^{t+T_0} z^2(\tau) d\tau \geq \alpha_0 T_0 \tag{4.28}$$

$\forall t \geq 0$ and where T_0,α_0 are some positive constants. In adaptive control the convergence of $\theta(t)$ towards θ^* is not crucial and the property of persistent excitation will only be of theoretical interest. Therefore, it will not be further explored in this thesis. Besides, the input signal for the estimation for the purpose of adaptive control cannot be chosen freely, making it very challenging, if not impossible, to identify it as a function. [3mm] What will follow now is analysis of the stability properties of the adaptive law (4.27). Consider the statements given by the following theorem [33]

Theorem 2. *The adaptive law* (4.27) *guarantees that:*

(1) $\epsilon, \epsilon n_s, \theta, \dot{\theta} \in \mathcal{L}_\infty$

(2) $\epsilon, \epsilon n_s, \dot{\theta} \in \mathcal{L}_2$

(3) If $n_s, z \in \mathcal{L}_\infty$ *and* z *is PE, then* $\theta(t)$ *converges exponentially to* θ^*

It needs to be remarked that properties (1) and (2) are independent of z *being a bounded signal.*

Proof. Because the unknown vector θ is assumed to be constant during the adaptation scheme, it can be shown that:

$$\dot{\tilde{\theta}} = \Gamma \epsilon z \tag{4.29}$$

The proposed candidate for Lyapunov function is:

$$V\left(\tilde{\theta}\right) = \frac{\tilde{\theta}^T \Gamma^{-1} \tilde{\theta}}{2} \tag{4.30}$$

with the time derivative:

$$\begin{aligned} \dot{V} &= \tilde{\theta} \Gamma^{-1} \dot{\tilde{\theta}} \\ &= \tilde{\theta} \Gamma^{-1} \Gamma \epsilon z \\ &= \tilde{\theta} \epsilon z \\ &= -\epsilon_1 \epsilon \\ &= -\epsilon^2 m^2 \leq 0 \end{aligned} \tag{4.31}$$

From (4.31) it can be concluded that V,$\tilde{\theta}$,$\theta \in \mathcal{L}_\infty$ and because of the relation

$$\epsilon = -\frac{\tilde{\theta}^T z}{m^2} \tag{4.32}$$

(recall eq. (4.12)), it follows that also ϵ,$\epsilon m \in \mathcal{L}_\infty$. Furthermore, the properties of V,$\dot{V}$ gives $\epsilon m \in \mathcal{L}_2$ and thus ϵ, $\epsilon n_s \in \mathcal{L}_2$. By analysing (4.27), it can established that:

$$|\dot{\tilde{\theta}}| = |\dot{\theta}| \leq ||\Gamma|||\epsilon m|\frac{|z|}{m} \tag{4.33}$$

By considering (4.33) and keeping in mind that $\frac{|z|}{m} \in \mathcal{L}_\infty$ together with $\epsilon m \in \mathcal{L}_2 \cap \mathcal{L}_\infty$, it can be concluded that $\dot{\theta} \in \mathcal{L}_2 \cap \mathcal{L}_\infty$ and the statements (1) and (2) of the Theorem 2 has been proven.

For the verification of the statement (2), the reader is referred to Section 4.8 in [33]. □

Although, $\lim_{t\to\infty} V(\tilde{\theta}(t)) = V_\infty$ (given by the properties $V(\tilde{\theta})$ and $\dot{V} \leq 0$ of the Lyapunov-like function $V(\tilde{\theta})$), one cannot simply say that $\dot{V}(t)$ goes to 0 as $t \to \infty$. This implies that ϵ or ϵm may not approach 0 as $t \to \infty$ and the search (provided by the gradient method) will not necessarily end at the global minimum where $\nabla J(\theta) = -\epsilon z = 0$. However if, as stated by [33], one normalizes vector z in such way so that $\dot{z}/m$,$\dot{m}/m \in \mathcal{L}_\infty$, it can be established that $\frac{d}{dt}(\epsilon m) \in \mathcal{L}_\infty$. By considering the latter along with $\epsilon m \in \mathcal{L}_2$ one can show that $\epsilon(t)m(t)$ reaches 0 as $t \to 0$. Because $m^2 = 1 + n_s^2$, $\epsilon(t) \to 0$ as $t \to \infty$ witch corresponds to $\dot{\theta} \to 0$ as $t \to \infty$. Subsequently, $|\nabla J(\theta(t)) \to 0$ as as $t \to \infty$, and the search results in a global minimum.

4.5 Method of Least-Squares

As the name implies, the least-squares method estimates the unknown parameters by minimizing the square deviations between the observed data and their predicted values which are generated by estimating the unknown parameters [54]. According to [2], it is the most frequently used method when it comes to linear regression. which corresponds to finding a line that fits the observed data in the best way. Both [2] and [54] gives examples on how the method of least-squares can be assigned into the regression analysis. The popularity of this method is not limited to the field of linear regression, however. It is also commonly applied in system identification, specially if the system equation can be expressed as an linear parametric model. Certainly, the identification of such system will have many similarities with regression. The method of least-squares is also suitable to identify systems where the unknown parameters do not appear linearly to the regression vector. However, this particular type of problems will not be covered in this report, and the reader is referred to [38] for the description. There are several different approaches for the least squares method, some of them being ordinary least-squares (which is the simplest one), the weighted least-squares, the partial least squares and the alternating least-squares. The weighted least squares will later on be addressed as "the least squares with forgetting factor". The descriptions of the the partial least squares and the alternating least-squares is offered in [1] and [21], respectively. The method of least squares can be based on various types of cost functions each treating the past data differently. For instance,

$$J(\theta) = \frac{1}{2}\int_0^t \epsilon(\tau)^2 d\tau = \frac{1}{2}\int_0^t \frac{(y(\tau) - \theta(t)z(\tau))^2}{m^2(\tau)} d\tau \tag{4.34}$$

is the cost function with respect to θ at time t, that penalizes all the past estimation errors from $\tau = 0$ up to time t. Meanwhile,the more complicated cost function

$$J(\theta) = \frac{1}{2}\int_0^t e^{-\beta(t-\tau)}\frac{(y(\tau) - \theta^T(t)z(\tau))^2}{m^2(\tau)}d\tau + \frac{1}{2}e^{-\beta t}(\theta - \theta_0)^T Q_0(\theta - \theta_0) \quad (4.35)$$

where $Q_0 = Q_0^T > 0$,$\beta \geq 0$ and $\theta_0 = \theta(0)$, emphasizes more recent errors and includes penalty on initial parameter error $\theta - \theta_0$. The cost function applied to design the estimator will differs slightly from (4.35). It will treat all past data equally (i.e the forgetting factor β is set to zero) but will still penalize the initial parameter error $\theta - \theta_0$. It will be termed $J_{LS}(\theta)$ to avoid confusion with earlier mentioned cost functions and takes the form:

$$J_{LS}(\theta) = \frac{1}{2}\int_0^t \frac{(y(\tau) - \theta^T(t)z(\tau))^2}{m^2(\tau)}d\tau + \frac{1}{2}(\theta - \theta_0)^T Q_0(\theta - \theta_0) \quad (4.36)$$

which because of the property z/m, $y/m \in \mathcal{L}_\infty$, $J(\theta)_{LS}$ is convex function of θ over $\mathbb{R}^3$ at each time t. The minimum of the function can be found by computing its gradient and setting it equal to zero,i.e:

$$\nabla J(\theta)_{LS} = 0 \ \ \forall t \geq 0 \quad (4.37)$$

The result is:

$$\nabla J(\theta)_{LS} = Q_0\left(\theta(t) - \theta_0\right) - \int_0^t \frac{y(\tau) - \theta^T(t)z(\tau)}{m^2(\tau)}z(\tau)d\tau \quad (4.38)$$

The non-recursive least squares algorithm, which yields from eq. (4.38), is as follows:

$$\theta(t) = P(t)\left(Q_0\theta_0 + \int_0^t \frac{y(\tau)z(\tau)}{m^2(\tau)}d\tau\right) \quad (4.39)$$

where

$$P(t) = \left(Q_0 + \int_0^t \frac{z(\tau)z^T(\tau)}{m^2(\tau)}d\tau\right)^{-1} \quad (4.40)$$

In most cases, one would like to avoid calculating the inverse in (4.40) when computing the matrix P. The alternative is the following differential equation:

$$\dot{P} = -P\frac{zz^T}{m^2}P, \quad P(0) = P_0 = Q_0^{-1} \quad (4.41)$$

which can be obtained by using the identity:

$$\frac{d}{dt}PP^{-1} = \dot{P}P^{-1} + P\frac{d}{dt}P^{-1} = 0 \quad (4.42)$$

This way of computing the matrix P is valid because the trajectory $P(t)$ will exist for all t due to $Q_0 \geq 0$ together with zz^T being positive semi-definite. That is, the inverse in (4.40) will always be positive definite meaning that one does not need to worry about the issue of division by zero. By differentiating (4.39) with respect to t, inserting expression (4.41) in the calculations and keeping in mind that $\epsilon m^2 = y - \theta^T z$, one will get the following adaptive law:

$$\dot{\theta} = P\epsilon z \quad (4.43)$$

The adaptive scheme involving equations (4.41) and (4.43) is according to [33], referred to as *"pure" least squares algorithm* in the identification literature. It has many similarities with the well-known Kalman-filter. For that reason, the matrix $P = P^T \geq 0$ is commonly known as *covariance matrix*. If one would prefer to incorporate discounting of past data (that is, one would like to include the forgetting factor β), one will obtain the same adaptive law as in (4.43). However, the differential equation for the matrix P will become:

$$\dot{P} = \beta P - P\frac{zz^T}{m^2}P, \quad P(0) = P_0 = Q_0^{-1} \tag{4.44}$$

The disadvantage of choosing the *pure least-squares algorithm* as the adaptive scheme is that it may suffer from *covariance wind-up*. This particular problem occurs when the matrix P^{-1} grows without bounds, since

$$\frac{d}{dt}P^{-1} = \frac{zz^T}{m^2} \tag{4.45}$$

will always be positive semi-definite. The boundless rise of P^{-1} will result, as stated by [33], in an arbitrarily small P and thus slow down the adaptation in some directions. One way to preventing covariance wind-up from occurring, is to equip the pure least-squares algorithm with so-called *covariance resetting*. This new, modified version of pure leas-squares algorithm is described as follows:

$$\begin{aligned} \dot{\theta} &= P\epsilon z \\ \dot{P} &= -\frac{Pzz^TP}{m^2}, \quad P\left(t_r^+\right) = P_0 = \rho_0 I \end{aligned} \tag{4.46}$$

The matrix P is reset to its initial condition at time t_r^+, for which P is considered too small, more specifically $\lambda_{min}(P(t)) \leq \rho_1$ and $\rho_0 > \rho_1 > 0$. Here, $\lambda_{min}(P(t))$ denotes the minimum eigenvalue of P at time t and the ρ_0, ρ_1 are some freely defined constants. This process of resetting the covariance matrix P will always keep it above a certain lower-bound and hence maintain the efficiency of the adaptive scheme. As remarked by [33], the pure least-square algorithm with covariance resetting cannot be derived by setting $\nabla J(\theta) = 0$, as for the traditional least-squares methods. It will, however, be characterized as a least-square method between its resetting points. Although, one may risk to experience the covariance wind-up when using pure least-squares approach, one will always be guaranteed to reach parameter convergences to constant values as shown by the following theorem:

Theorem 3. *The pure least-squares algorithm guarantees that:*

(1) $\epsilon, \epsilon n_s, \theta, \dot{\theta}, P \in \mathcal{L}_\infty$

(2) $\epsilon, \epsilon n_s, \dot{\theta} \in \mathcal{L}_2$

(3) $\lim_{t\to\infty} \theta(t) = \bar{\theta}$*, where* $\bar{\theta}$ *is a constant vector*

(4) If $n_s, z \in \mathcal{L}_\infty$ *and* z *is PE, then* $\theta(t)$ *converges exponentially to* θ^*

Proof. By considering (4.45), it is concluded that $\dot{P} \leq 0$ implying $P(t) \leq P_0 \ \forall t$. Therefore, the matrix $P(t) = P^T(t)$ has the limit defined as:

$$\lim_{t\to\infty} P(t) = \bar{P} \tag{4.47}$$

where $P = P^T$ is a constant matrix assumed to be positive semi-definite. Now, recall the expressions:

$$\dot{P} = -P\frac{zz^T}{m^2}P, \quad \frac{d}{dt}P^{-1} = \frac{zz^T}{m^2}$$

It may be established that:

$$\frac{d}{dt}P^{-1} = -P^{-1}PP^{-1} \tag{4.48}$$

Furthermore, by using $\dot{\theta} = \dot{\tilde{\theta}}$ and $\epsilon = -\frac{\tilde{\theta}^T z}{m^2} = -\frac{z^T\tilde{\theta}}{m^2}$, following equation can be constructed:

$$\begin{aligned}\frac{d}{dt}(P^{-1}\tilde{\theta}) &= -P^{-1}\dot{P}P^{-1}\tilde{\theta} + P^{-1}\dot{\tilde{\theta}} \\ &= \frac{zz^T}{m^2}\tilde{\theta} + P^{-1}\dot{\theta} \\ &= \frac{zz^T}{m^2}\tilde{\theta} + \epsilon z \\ &= -\epsilon z + \epsilon z = 0\end{aligned} \tag{4.49}$$

Because, $\frac{d}{dt}(P^{-1}\tilde{\theta}) = 0$, the function $P^{-1}(t)\tilde{\theta}(t)$ will remain unchanged in the time domain implying that $P^{-1}(t)\tilde{\theta}(t) = P_0^{-1}\tilde{\theta}(0)$ which may be rewritten as $\tilde{\theta}(t) = P(t)P_0^{-1}\tilde{\theta}(0)$. By taking into consideration the limit defined in (4.47), it can be stated that $\lim_{t\to\infty}\tilde{\theta}(t) = \bar{P}P_0^{-1}\tilde{\theta}(0)$ which result in $\lim_{t\to\infty}\tilde{\theta}(t) = \theta^* + \bar{P}P_0^{-1}\tilde{\theta}(0) \triangleq \bar{\theta}$. Thus, the statement (3) of Theorem 3 has been proven. Because the trajectory $\theta(t)$ satisfies $\lim_{t\to\infty}\tilde{\theta}(t) = \theta^* + \bar{P}P_0^{-1}\tilde{\theta}(0) \triangleq \bar{\theta}$, one can conclude that θ,$\tilde{\theta} \in \mathcal{L}_\infty$. Furthermore, keeping in mind that $z/m \in \mathcal{L}_\infty$ along with $\epsilon m = \tilde{\theta}^T z/m$, one will get that ϵ, $\epsilon n_s \in \mathcal{L}_\infty$ as stated by (1) in Theorem 3. In order to verify the statement (2) of the same theorem, consider the following Lyapunov-like function:

$$V(\tilde{\theta}, t) = \frac{\tilde{\theta}^T P^{-1}(t)\tilde{\theta}}{2} \tag{4.50}$$

Its derivative along the parameter θ and time domain t is:

$$\begin{aligned}\dot{V} &= P^{-1}\tilde{\theta}\dot{\tilde{\theta}} + \frac{\tilde{\theta}^T\dot{P}^{-1}(t)\tilde{\theta}}{2} \\ &= \epsilon\tilde{\theta}^T z + \frac{\tilde{\theta}zz^T\tilde{\theta}}{2m^2} \\ &= -\epsilon^2 m^2 + \frac{\epsilon^2 m^2}{2} = -\frac{\epsilon^2 m^2}{2}\end{aligned} \tag{4.51}$$

which gives $V \in \mathcal{L}_\infty$ as well as $\epsilon m \in \mathcal{L}_2$ and one can conclude that ϵ,$\epsilon n_s \in \mathcal{L}_2$. The properties P,$\frac{Y}{m}$,$\epsilon m \in \mathcal{L}_2$ together with $\epsilon m \in \mathcal{L}_2$, implies that $\dot{\theta} \in \mathcal{L}_\infty \cap \mathcal{L}_2$ Thus, the proof of (2) in Theorem 3 has also been completed.

For the proof of the statement (4), consult Section 4.8 in [33]. □

Chapter 5

Observer for Inlet Flow

5.1 Introduction

As concluded earlier, the non-linear controller for CCV together with estimation of the compressor characteristic will rely on feedback from inlet flow at the compressor duct, ϕ. It is, however, a well known fact that there are several issues related to flow measurement. A flow sensor is costly in general,the signals transmitted from the instrument are often corrupted with noise and occasionally the flow may even be unobtainable for measurement. The factors motivated the control community to develop a observer which will predict the trajectory of flow by considering the dynamics of the system. It needs also to be pointed out, that the observer is not restricted to any specific control law. In the term of compressor systems, the literature offers quite little about mass flow observers when comparing with the large amount of publication concerning the control laws applying measurement of mass flow as a feedback. A popular type of observer is the one based on circle criterion (see [35] for the definition) which has been briefly discussed in [11]. Apparently, an observer type can be divided into two classes: a full order observer or the reduced order observer. Their differences lie in whether they include the impeller dynamics in the observer equation, with the reduced observer being the one where those dynamics are being omitted. The feasibility of the system encountered in this thesis is limited to the compressors with constant impeller speed. For that reason, the impeller dynamics will disappear and the full order observer will become irrelevant for the system. Hence, the reduced order observer will be selected as the observer type. According to [4], an observer must satisfy following conditions if the circle criterion is to be fulfilled. First, the linear part of the observer must be strict positive real (SPR), which will follow if the linear matrix inequality (LMI) is being satisfied (the definition of LMI can be found both in [4] and [11]). Second, the non-linearities of the observer equation must be given by non-decreasing functions of linear combination of unmeasured states. Different versions of reduced order mass flow observer (full order observer is included as well) has been gathered in [10]. The observer types has been generated based upon whether one assuming that the pressures at the compressor duct and at the plenum are being modelled or measured.

5.2 GES flow observer

The observer type discussed in this subsection, will be a GES flow observer which was reported by [12] and section 4.3 in [10]. The proposed observer is applicable for the system encountered in this thesis, in the sense that its design is independent of the compressor characteristic. Fed with the measurements of plenum pressure and pressure at the compressor outlet, the observer will estimate the inlet flow and seems to be independent of whether the system input appears in the mass flow or pressure dynamics. An important tool in observer design is the observer (estimation) error defined to be:

$$\tilde{w}_i = w_i - \bar{w}_i \tag{5.1}$$

where w_i is the inlet mass flow and $\bar{w}_i$ is the estimate of the latter. The analysed observer is suited for the compression systems where no uncertainty is related to the pressure measurements, or at least is so insignificant that it may be disregarded. Keeping in mind the Greitzer model described by the notation in Section 2 and the given assumption

Assumption 1. $p_p > p_o, \forall t \geq t_0$

the observer

$$\dot{z} = \frac{A_c}{L_c}(p_c(w_i) - p_p - u) - k_{\bar{m}}\bar{w}_i + k_{\bar{m}}w_0(p_p) \tag{5.2a}$$

$$\bar{w}_i = z + k_{\bar{m}}\frac{V_p}{a_0^2}p_p \tag{5.2b}$$

will make the the equilibrium $\tilde{w}_i = 0$ globally exponentially stable. Hence, the name GES observer. Here, $k_{\bar{m}} > 0$ denotes the observer which is to be determinated by the designer. Note that Assumption 1 will result in $w_o(p_p) \in \mathbb{R}, \forall t \geq t_0$ which guarantees that $\dot{z} \in \mathbb{R}, \forall t \geq t_0$. The stability property of the introduced observer can be shown by first obtaining the observer dynamics:

$$\begin{aligned}
\dot{\bar{w}}_i &= \frac{A_c}{L_c}(p_c(w_i) - p_p - u) - k_{\bar{m}}\bar{w}_i + k_{\bar{m}}w_0(p_p) + k_{\bar{m}}\left(\frac{a_o^2}{V_p}(w_i - w_o(p_p))\right) \\
&= \frac{A_c}{L_c}(p_c(w_i) - p_p - u) - k_{\bar{m}}\bar{w}_i + k_{\bar{m}}w_0(p_p) + k_{\bar{m}}w_i - k_{\bar{m}}w_o(p_p) \\
&= \frac{A_c}{L_c}(p_c(w_i) - p_p - u) + k_{\bar{m}}\tilde{w}_i
\end{aligned} \tag{5.3}$$

and the observer error dynamics are found to be:

$$\begin{aligned}
\dot{\tilde{w}}_i &= \dot{w}_i - \dot{\bar{w}}_i \\
&= \frac{A_c}{L_c}(p_c(w_i) - p_p - u) - \frac{A_c}{L_c}(p_c(w_i) - p_p - u) - k_{\bar{m}}\tilde{w}_i \\
&= -k_{\bar{m}}\tilde{w}_i
\end{aligned} \tag{5.4}$$

Next, consider the Lyapunov-function candidate for estimated mass flow error given by:

$$V(\tilde{w}_i) = \frac{1}{2}\tilde{w}_i^2 \tag{5.5}$$

The time derivative of V with respect to estimation error becomes $\tilde{w}_i$:

$$\begin{aligned}\dot{V}(\tilde{w}_i) &= \tilde{w}_i\dot{\tilde{w}}_i \\ &= -k_{\bar{m}}\tilde{w}_i^2\end{aligned} \tag{5.6}$$

By analyzing eq. (5.5) and eq. (5.6), it can be concluded that the estimation reaches global exponential stability at the equilibrium $\tilde{w}_i = 0$. It needs also to be remarked that by characterizing the equilibrium $\tilde{w}_i = 0$ as GES, the trajectory of the estimation error will be bounded by:

$$|\tilde{w}_i(t)| < |\tilde{w}_i(t_0)|e^{-k_{\bar{m}}(t-t_0)} \tag{5.7}$$

, meaning that the rate of convergence is given by the magnitude of $k_{\bar{m}}$.

5.3 Non-dimentionalization of the observer equations

In order to fit the observer for the systems discussed earlier, there will be a need to non-dimentionalize the equations related to the observer. The non-dimentionalization has been performed in an equal manner as in Chapter 2.4, i.e using the normalization factors $\rho U A_c$ for mass flow, $\frac{1}{2}\rho U^2$ for pressure and $\frac{1}{\omega_H}$ for time. The non-dimentional equivalent to eq. (5.2a) becomes:

$$\begin{aligned}\dot{z} &= \frac{A_c}{L_c}(p_c(w_i) - p_p - \bar{u}) - k_{\hat{m}}\bar{w}_i + k_{\bar{m}}w_o(p_p) \\ \dot{z} &= \dot{w}_i - k_{\bar{m}}\bar{w}_i + k_{\bar{m}}w_0(p_p) \\ \frac{\rho U A_c d\left(\frac{z}{\rho U A_c}\right)}{\frac{d\tau}{\omega_H}} &= \frac{\rho U A_c d\left(\frac{w_i}{\rho U A_c}\right)}{\frac{d\tau}{\omega_H}} + \rho U A_c\left(-k_{\bar{m}}\frac{\bar{w}_i}{\rho U A_c} + k_{\bar{m}}\frac{w_o(p_p)}{\rho U A_c}\right) \\ \frac{\omega_H\rho A_c d\left(\frac{z}{\rho U A_c}\right)}{d\tau} &= \frac{\omega_H\rho U A_c d\left(\frac{w_i}{\rho U A_c}\right)}{d\tau} + \rho U A_c\left(-k_{\bar{m}}\frac{\bar{w}_i}{\rho U A_c} + k_{\bar{m}}\frac{w_o(p_p)}{\rho U A_c}\right) \\ \frac{d\left(\frac{z}{\rho U A_c}\right)}{d\tau} &= \frac{d\left(\frac{w_i}{\rho U A_c}\right)}{d\tau} + \frac{1}{\omega_H}\left(-k_{\bar{m}}\frac{\bar{w}_i}{\rho U A_c} + k_{\bar{m}}\frac{w_o(p_p)}{\rho U A_c}\right) \\ \dot{\alpha} &= \dot{\phi} - \frac{k_{\bar{m}}}{\omega_H}\bar{\phi} + \frac{k_{\bar{m}}}{\omega_H}\Phi_T \\ \dot{\alpha} &= B(\Psi_c - \psi - u) - \frac{k_{\bar{m}}}{\omega_H}\bar{\phi} + \frac{k_{\bar{m}}}{\omega_H}\gamma_T\sqrt{\psi}\end{aligned} \tag{5.8}$$

with $\bar{u}$ being the system input given by the variables containing dimensions. Due to the lack of notation for the non-dimensionalized variable z, it has been termed α by the author.

Non-dimensionalization of eq. 5.2b is shown as follows:

$$\begin{aligned}
\bar{w}_i &= z + k_{\bar{m}} \frac{V_p}{a_0^2} p_p \\
\rho U A_c \frac{\bar{w}_i}{\rho U A_c} &= \rho U A_c \frac{z}{\rho U A_c} + k_{\bar{m}} \frac{V_p}{a_o^2} \frac{\rho U^2}{2} \left(\frac{p_p}{\frac{\rho U^2}{2}} \right) \\
\frac{\bar{w}_i}{\rho U A_c} &= \frac{z}{\rho U A_c} + k_{\bar{m}} \frac{V_p U}{2 A_c a_o^2} \left(\frac{p_p}{\frac{\rho U^2}{2}} \right) \\
\bar{\phi} &= \alpha + k_{\bar{m}} \frac{V_p U}{2 A_c a_o^2} \psi
\end{aligned} \tag{5.9}$$

Finally, the estimated inlet flow dynamics expressed with dimensionless variables are found to be:

$$\begin{aligned}
\dot{\tilde{w}}_i &= \frac{A_c}{L_c}(p_c(w_i) - p_p - u) + k_{\bar{m}} \tilde{w}_i \\
\frac{\rho U A_c d\left(\frac{\bar{w}_i}{\rho U A_c}\right)}{\frac{d\tau}{\omega_H}} &= \frac{1}{2}\rho U^2 \frac{A_c}{L_c} \left(\frac{p_c}{\frac{1}{2}\rho U^2} - \frac{p_p}{\frac{1}{2}\rho U^2} - \frac{\bar{u}}{\frac{1}{2}\rho U^2} \right) + k_{\bar{m}} \rho U A_c \left(\frac{\tilde{w}_i}{\rho U A_c} \right) \\
\frac{d\left(\frac{\bar{w}_i}{\rho U A_c}\right)}{d\tau} &= \frac{U}{2\omega_H L_c} \left(\frac{p_c}{\frac{1}{2}\rho U^2} - \frac{p_p}{\frac{1}{2}\rho U^2} - \frac{\bar{u}}{\frac{1}{2}\rho U^2} \right) + \frac{k_{\bar{m}}}{\omega_H} \left(\frac{\tilde{w}_i}{\rho U A_c} \right) \\
\dot{\tilde{\phi}} &= B(\psi_c - \psi - u) + \frac{k_{\bar{m}}}{\omega_H} \tilde{\phi}
\end{aligned} \tag{5.10}$$

The version of equations (5.8) and (5.9) expressed by deviation variables will be used for simulation in Chapter 7. Control law for the closed-couple valve will now employ feedback from the estimated flow $\bar{\phi}$ rather than measured flow ϕ. This implies:

$$\begin{aligned}
u|_{\phi=\bar{\phi}} &= -c_2(\bar{\phi} - \phi_0) \\
&= u - c_2 \tilde{\phi}
\end{aligned} \tag{5.11}$$

where $\tilde{\phi}$ is the observer error defined by dimensionless mass flows. By letting $\breve{(\cdot)}$ represent the deviations from the equilibrium when the estimated mass flow is being applied by the controller, the closed loop system augmented with the observer is given by the equations:

$$\begin{bmatrix} \dot{\breve{\phi}} \\ \dot{\breve{\psi}} \end{bmatrix} = \begin{bmatrix} B(\breve{\Psi}_c - \breve{\psi} - u) \\ \frac{1}{B}(\breve{\phi} - \breve{\Phi}_T(\breve{\psi}) \end{bmatrix} + \begin{bmatrix} \left(\frac{k_{\bar{m}}}{\omega_H} + Bc_2\right) \tilde{\phi} \\ 0 \end{bmatrix} \tag{5.12}$$

which were obtained by combining (2.20), (5.10) and (5.11). Based on the Assumption 1, the region of attraction for overall system will be $D = \{(\breve{\phi}, \breve{\psi}) \in \mathbb{R}^2 | \breve{\psi} > p_o - p_0)\}$.

Until now, the chapter has been dedicated to discussing the observer only for the case of CCV actuation. In the case of PAASCS, the observer will be expressed by the equations:

$$\begin{aligned}\dot{\alpha} &= B(\Psi_c - \psi) - \frac{k_{\bar{m}}}{\omega_H}\bar{\phi} + \frac{k_{\bar{m}}}{\omega_H}\gamma_T\sqrt{\psi} \\ \bar{\phi} &= \alpha + k_{\bar{m}}\frac{V_p U}{2A_c a_o^2}\psi\end{aligned} \tag{5.13}$$

So, it is almost identical to the one studied in the past, only not to include the system input. Due to the observer not concerning which system equation control input belongs to, the stability analysis for PAASCS will be equal to those given for CCV actuation. The later discussed separation principle will not be relevant for PAASCS, because it does not assume feedback from inlet mass flow. It will still need an observer, however, to provide mass flow estimate for further estimation of the compressor characteristic. The version of equation set (5.13) expressed by deviation variables will be used for simulation in Chapter 7.

5.4 A Separation Principle

What is to be understood with the separation principle in the term of the observer design, is that the controller which will turn the system GES and the observer may be tuned separately. For the linear systems this property will be ensured because of the superposition principle. For the non-linear systems, on the other hand, it will not hold in general, as stated by [10]. Here, it will be showed that the separation principle will indeed hold for the interconnected system of active surge control and the observer despite the non-linearities in the compressor and the valves.
First,let

$$\Sigma_1 : \dot{x}_1 = f_1(x_1), \;\; f_1 : D_1 \to \mathbb{R}^{n-1} \tag{5.14}$$

represent the error dynamics of the closed-loop system in (3.10). Moreover, the observer error dynamics which were given in eq. (5.4) (being non-dimensionalized of course) are denoted by the following:

$$\Sigma_2 : \dot{x}_2 = f_2(x_2), \;\; f_2 : \mathbb{R} \to \mathbb{R} \tag{5.15}$$

As mentioned earlier, instead off the measured mass flow, the control law for CCV will now depend on mass flow from the observer. Meaning, that the overall system arises to be:

$$\Sigma : \dot{x} = f(x) + g(x), \;\; f : D \to \mathbb{R}^n \tag{5.16}$$

with $x = [x_3^T \;\; x_2]^T$, $x_3 = [\breve{\phi} \;\; \breve{\psi}]^T$, $f(x) = [f_1^T(x_3) \;\; f_2(x_2)]^T$ and $g(x) = [f_1^T(x) \;\; 0]^T$ where the function $g(x)$ results from including the mass flow estimate in the control law. Therefore, equation (5.16) is alternative representation of the system described by eq. (5.12). Next, consider the assumptions given in [12]:

Assumption 2. *The Lyapunov function $V_1(x_1)$ satisfies*

$$c_{11}||x_1||^2 \leq V_1(x_1) \leq c_{21}\left\|x_1\right\|^2 \tag{5.17}$$

$$\dot{V}_1(x_1) \leq -c_{31}\left\|x_1\right\|^2 \tag{5.18}$$

$$\left\|\frac{\partial V_1(x_1)}{\partial x_1}\right\| \leq c_{41}\left\|x_1\right\| \tag{5.19}$$

$\forall x_1 \in D_1$ *for some positive constants* $c_{i1} > 0$

Assumption 3. $\|g_1(x)\| \leq \beta \|x_2\| \quad \forall x \in D$
for some constant $\alpha > 0$

The listed will assumptions become basis for the following theorem [12].

Theorem 4. *Given the systems* Σ_1, $Sigma_2$ *and* Σ *as described above. Under Assumption* (2) *and Assumption* (3)*, the system* Σ *defined in* (5.16) *will have a Lyapunov function V(x) that will stay within the bounds*

$$c_1 \|x\|^2 \leq V(x) \leq c_2 \|x\|^2 \tag{5.20}$$

$$\dot{V}(x) \leq -c_3 \|x\|^2 \tag{5.21}$$

$\forall x \in D$. *Meaning that system* Σ *can be classified as GES in the space D.*

The proof the Theorem 4 can be found in [12].

Chapter 6

Adaptive Compressor Control in the Literature

The chapter aims to give the reader an overview on the previous work done on adaptive anti-surge control. The research on adaptive control in sections 6.1, 6.2 and 6.3 has respectively been published in [10], [9] and [44]. The differences between the approaches not only lies in the principles, the adaptive controllers has been derived from, but also in the selection of the actuator. Common for them all is that the backbone of the adaptive controller is an adaptive law consisting of differential equations. Non of approaches in this chapter require knowledge of the system equilibrium, as the methods in the previous chapter, but in return they produce much more complex adaptive laws. Whether the adaptive law estimates the unknown system parameters or just updates the control parameters will vary. Although disturbances in the flow and pressure have not been given any attention in the past, the controller designed in sec. 6.3, will demonstrate its robustness against them.

6.1 Adaptive Extension of Active Surge Control Using Drive Torque

The idea of including an adaptive part to the surge control was explored by [10]. There, the compressor considered for implementation of the adaptive control is standard Greitzer surge model which was covered in Section 2. A new feature is to have the ability of adjusting the impeller speed of the compressor, something that turn outs to be quite beneficial in terms of surge control. The drive unit responsible for supplying the compressor with centrifugal force will be regarded as the control actuator. This opens for two choices for control input: the impeller speed ω and the drive torque τ_d and [10] have studied both of them. Other examples of using the drive torque as an input for surge control are [17] and [27] where the latter was first to introduce this approach. The actuation by drive torque has be modified with adaptive control by [10], mainly due to uncertainty related to the load torque τ_l. As a consequence, ω will now be considered as a system state along with inlet mass flow w_i and plenum pressure p_p. This implies a necessity of incorporating the impeller dynamics in the Greitzer model, something that was pioneered by [22]. Before

discussing the extended model, it needs to be pointed out that ω is limited to a positive value. The arising model consists of three differential equations which are:

$$\begin{aligned} \dot{p_p} &= \frac{c_p^2}{V_p}(w_i - w_t) \\ \dot{w_i} &= \frac{A_c}{L_c}(p_c(w_i, \omega) - p_p) \\ \dot{\omega} &= \frac{1}{J}(\tau_d - \tau_l) \end{aligned} \tag{6.1}$$

The differential equation for the impeller speed was, according to [10], constructed by "evaluating the angular momentum balance for the spinning shaft. Apart from the earlier defined parameters and states, J is the moment of inertia of rotating parts, τ_d symbolizes the impeller speed, τ_l represent the load torque (also referred to as compressor torque) and $p_c(w_c, \omega)$ is the well known compressor characteristic, which is now the function of both the inlet flow and the impeller speed. The load torque which occurs because of the presence of fluid flow in the impeller and friction of rotating mechanical parts, has been approximated by the Euler equation to be:

$$\tau_l(w_c, \omega) = \tau_c(w_c, \omega) + \tau_f(\omega) \tag{6.2}$$

and the friction τ_c along with the viscous friction $\tau_f(\omega)$ are being provided by the equations:

$$\tau_c = k_c|w_c|\omega \tag{6.3}$$

$$\tau_c = k_f\omega \tag{6.4}$$

where $k_c = \omega r_i^2$ and k_f is the friction constant. Other parameters to be defined are the impeller radius r_i and slip factor σ which ranges from zero to one.

Two control laws for the drive torque which is considered as the input of the system consisting of equation set (6.1) , has been obtained in [10] by applying the method of backstepping, the same approach as for the closed-coupled valve. The proposed control laws are given by:

$$\tau_d = -c_1(\bar{\omega} + c_2\bar{w_i}) - c_2\frac{JA_c}{L_c}(p_c(w_i, \omega) - p_p) + \tau_l(w_i, \omega) \tag{6.5}$$

$$\tau_d = -c_1(\bar{\omega} + c_2\bar{w_i}) - c_2\frac{JA_c}{L_c}(p_c(w_i, \omega) - p_p) - c_2k_c|w_i|\bar{w_i} - c_2k_f\bar{w_i} + \tau_d^e \tag{6.6}$$

Both laws are partially expressed with variables $\bar{w_i} = w_i - w_{i,0}$ and $\bar{\omega} = \omega - \omega_0$ representing deviations from respective equilibrium points. Furthermore, if the constants c_1 and σ er determinated to be positive and sufficiently large and c_2 is chosen to satisfy:

$$c_2 \geq \frac{\frac{\partial(w_{i,0}, \omega_0)}{\partial w_{i,0}} + \delta}{\frac{\partial(w_{i,0}, \omega_0)}{\partial w_{i,0}}}$$

the equilibrium point is guaranteed to reach asymptotic stability in the domain

$$D = \{(\bar{p_p}, \bar{w_i}, \bar{\omega}) \in \mathbb{R}^3 \mid \bar{p_p} \geq p_{p,0}\ ,\ -\infty < c_2\bar{w_i} \leq \omega_0\ ,\ \omega_0 \leq \bar{\omega} < \infty\} \tag{6.7}$$

with $\bar{p}_p = p_p - p_{p,0}$ being the deviation variable for plenum pressure. The proofs for the control laws involves the method of backstepping and have been provided by [10]. However, both of them are rather comprehensive, are several pages long and therefore will not be included in this report. An observant reader will notice that the first two terms are equal for the two control laws. This terms are the result of assigning ω as an virtual control at the third step in the backstepping procedure. The remaining terms are distinguish for both control laws because they cancel the load pressure τ_l in the system equation differently. The control law expressed in equation (6.5) cancels it completely (τ_l will disappear from the diff. equation for impeller speed when the proposed control law has been inserted) while the control law shown in (6.6) will cancel it partially. By leaving some terms involving τ_l, one will gain a control law handling the system in more robust way, since the time derivative for its corresponding Lyapunov function will contain an additional stabilizing term, making it more negative.

Occasionally, the compression system will contain some uncertainties. For the case of $p_c(w_c, \omega)$ and τ_l being unknown, [10] suggest additional two control laws where each of the them are being omitted. Another possibility, is to replace the unknown constants appearing in the control law, with their estimates. By assigning θ_1,θ_2 and θ_3 as estimates for JA_c/L_c,k_c and k_f,respectively, and letting:

$$\tau_d = \tau_{s1} + \tau_{s2}, \quad \tau_{s1} = -c_1(\bar{\omega} + c_2\bar{w}_c)$$

the update equations for the control law in (6.5) becomes:

$$\begin{aligned} \tau_{s2} &= \theta_2|w_c| + \theta_3\omega - c_2\theta_1(p_c(w_c,\omega) - p_p) \\ \dot{\theta_1} &= c_{\theta 1}c_2(\bar{\omega} + c_2\bar{w}_c)(p_c(w_c,\omega) - p_p) \\ \dot{\theta_2} &= -c_{\theta 2}(\bar{\omega} + c_2\bar{w}_c)|w_c|\omega \\ \dot{\theta_3} &= -c_{\theta 3}(\bar{\omega} + c_2\bar{w}_c)\omega \end{aligned} \tag{6.8}$$

In addition, the set of upadate equations corresponding to the adaptive law in (6.6) becomes:

$$\begin{aligned} \tau_{s2} &= -c_2\theta_2|w_c|\bar{w}_c + c_2\theta_3\bar{w}_c - c_1\theta_1(p_c(w_c,\omega) - p_p) + \tau_d^e \\ \dot{\theta_1} &= c_{\theta 1}c_2(\bar{\omega} + c_2\bar{w}_c)(p_c(w_c,\omega) - p_p) \\ \dot{\theta_2} &= -c_{\theta 2}(\bar{\omega} + c_2\bar{w}_c)|w_c|\bar{w}_c \\ \dot{\theta_3} &= -c_{\theta 3}(\bar{\omega} + c_2\bar{w}_c)\bar{w}_c \end{aligned} \tag{6.9}$$

Both adaptive controllers ensures convergence of the system states to their stable equilibrium points under the condition that the initial estimates lies sufficiently close. For the verification of this statements, please consult [10].

6.2 High-Gain Type Adaptive Control For Surge Stabilization

Up to this point, the reader has become familiar with the idea of modifying the compressor system with adaptive active surge control by on-line estimating the unknown system parameters which participates in the expression for the system input. This time, however,

another approach will be introduced. First, the control law defined later on, will not contain system parameters and hence the whole idea of generating their estimates will be left out. Second, the control law will be in the form of a high-gain adaptive contoller, termed λ-tracker, which has been covered in depth in [32]. And third, instead of adding to the system a new device assigned as a control actuator, the control duties will be left to the already existing throttle. [9] considers the following system for adaptive surge control:

$$\begin{aligned} \dot{x_1}(t) &= -B[x_2(t) - \Psi(x_1(t))] \\ \dot{x_2}(t) &= \frac{1}{B}[x_1(t) - u(t)\Gamma(x_2(t))] \end{aligned} \tag{6.10}$$

which is equal to the non-dimensionalized Greitzer surge model. Here, x_1 is the flow rate at the compressor duct, x_2 is the pressure at the plenum and the functions $\Psi(x_1(t))$ and $\Gamma(x_2(t))$ represents the compressor characteristic and the throttle characteristic, respectively. The notation form [9] has been kept for future stability analysis. As for the system output, equation:

$$y(t) = x_2(t) - \Psi(x_1(t)) \tag{6.11}$$

is considered. The input signal $u(t)$ represent the throttle section open and is, according to [9], "defined as the ratio of the flow area A_t and its maximum value $A_{\text{t,max}}$ This results in $u(t)$ containing the bounds $0 \leq u \leq 1$. For later analysis, it convenient to rewrite the system as:

$$\begin{aligned} \dot{x_1}(t) &= -B[x_2(t) - \Psi(x_1(t))] \\ \dot{x_2}(t) &= \frac{1}{B}[x_1(t) - u(t)\Gamma(x_2(t))] - \frac{\Gamma(x_2(t))}{B}v(t) \end{aligned} \tag{6.12}$$

where

$$v(t) = u(t) - u_0 \tag{6.13}$$

is the control law which will be specified right away and u_0 is the value of u when the system is stabilized at the equilibrium point. The control law for the system in (6.12) will be given by the adaptive λ-tracker:

$$\begin{aligned} v(t) &= k(t)y(t) \\ \dot{k}(t) &= \mu\sigma_\epsilon(|y(t)|) \\ k(0) &= k_0 \end{aligned} \tag{6.14}$$

which when implemented, will drive the output to zero within the tolerance

$$|y(t)| = |x_2(t) - \Psi(x_1(t)) \leq \epsilon \tag{6.15}$$

For the set of equations in (6.14), $k(t)$ is the adaptive gain, $k_0 \geq 0$ is an arbitrary initial value and μ is a parameter that adjusts the speed of the adaptation. Additionally, $\sigma_\epsilon(.) : \mathbb{R}^+ \to \mathbb{R}^+$ denotes the distance function:

$$\sigma_\epsilon(|y|) = \begin{cases} 0, & \text{if } 0 \leq |y| \leq \epsilon \\ |y| - \epsilon, & \text{if } |y| \geq \epsilon \end{cases} \tag{6.16}$$

For the system in (6.12), following assumptions are being made

Assumption 4. *The compressor characteristic $\Psi(x_1)$ is defined for $x_1 \leq x_1^+$, where $x_1^+ \geq 0$ is an unknown value that gives $\Psi(x_1^+) = 0$ and is locally Lipschitz on its domain of definition. Furthermore, $\Psi(x_1) \geq 0$ for $x_1 \leq x_1^+$ and*

$$\lim_{t \to -\infty} \Psi(x_1) = +\infty$$

Assumption 5. *Function $\Gamma(x_2)$ is locally Lipschitz, strictly increasing and such that:*

$$x_2 \Gamma(x_2) \geq 0$$

It is worth mentioning, that the assumptions 4 and 5 are typical for any compressor and valve characteristic.

Assumption 6. *Reference value u_0 can be chosen within interval $[u^-, u^+]$ where $0 \leq u^-$ and $u^+ \leq 1$. In addition, there exists a (possibly empty) subset $U^{bad} \subset [u^-, u^+]$, containing finitely many points, such that for all*

$$u_0 \in U_0 \doteq \{u : u^- \leq u \leq, u \notin U^{bad}\}$$

the system of equations:

$$\begin{aligned} x_2 - \Psi(x_1) &= 0 \\ x_1 - u_0 \Gamma(x_2) &= 0 \end{aligned}$$

has a unique solution, $P = (x_1^*, x_2^*)$, which defines an isolated equilibrium point for the system.

As for the set U_0 in the Assumption 6, it simply represents the values of u_0 for which the compressor may not recover from stall condition.

Assumption 7. *There is the set*

$$X_{amm} = \{x : x_1 \leq x_1^+, x_2^- \geq 0\}$$

which denote the admissibility region in the $x_1 - x_2$ plane (see Figure 2 in [9]) and where x_2^- is an arbitrarily small positive value. Let X_0 be a subset of X_{amm}, depending on u_0 so that the unique isolated equilibrium point $P \in X_0$ and for each initial condition $x(0) \in X_0$ the corresponding uncontrolled solution $u(t) = u_0$ remains admissible. In other words, $x(t) \in X_{amm}$ and it is bounded, namely, $||x(t)|| \leq M$ for some positive M depending on u_0.

Next, the Lemma 1 (which has been validated in [9]) is formulated as follows:

Lemma 1. *Consider the system expressed in* (6.12)*, under Assumptions 4-7 with the control law $v(t) = k(t)[x_2(t) - \Psi(x_1(t))] = k(t)y(t)$, where $k(t) \geq 0$ is a non-decreasing continuous function. Then, for each $x(0) = x_0 \in X_0$, solution x(t) is bounded and admissible, i.e $||x(t)|| \leq M$ and $x(t) \in X_{amm}$*

is fundamental for the upcoming Theorem 5 which will address the stability properties of the closed loop system containing the earlier defined λ-tracker.

Theorem 5. *Given the system in* (6.12) *under the Assumptions 4-7 together with the adaptive law in* (6.14)*. Then, for $t \to \infty$:*

(i) $k(t) \to k_\infty < +\infty$

(ii) $y(t) \to I_\epsilon = [-\epsilon, \epsilon]$

Proof. By inserting the output equation $y \doteq x_2 - \Psi(x_1)$ in (6.12), one will get:

$$\begin{aligned} \dot{x_1} &= -By \\ \dot{x_2} &= \frac{1}{B}[x_1 - u_0\Gamma(y + \Psi(x_1))] + B\frac{d\Psi(x_1)}{dx_1}y - \frac{1}{B}\Gamma(y + \Psi(x_1))ky \end{aligned} \tag{6.17}$$

It has been stated in Lemma 1 that $k(t)$ is non-decreasing function. Therefore it either grows without bounds or it converges to $k_\infty < \infty$ as $t \to \infty$. Now, it will be shown that the limit is indeed finite. By contradiction, lets assume that $k(t) = k_\infty = +\infty$ and consider $V = y^2/2$ as the Lyapunov-like function for the system. The time derivative of V becomes:

$$\begin{aligned} \dot{V} &= y\dot{y} \\ &= y\left[\frac{1}{B}[x_1 - u_0\Gamma(y + \Psi(x_1))] + B\frac{d\Psi(x_1)}{dx_1}y\right] - \frac{1}{B}\Gamma(y + \Psi(x_1))ky^2 \\ &\leq \alpha - \frac{1}{B}\Gamma(y + \Psi(x_1))ky^2 \end{aligned}$$

The existence of $\alpha > 0$ is assured by Lemma 1, by the continuity of the state transformation and by the fact that $d\Psi/dx_1$, although possibly non-continuous, is bounded since Ψ has the property of being locally Lipschitz (as stated in the Assumption 4). Next, by the definition of the set X_{amm}, x_2 is bounded by x_2^- and thus $\Gamma(y + \Psi(x_1)) \geq \Gamma(x_2^-) \doteq \nu > 0$. For $k > \alpha/(\nu\epsilon^2)$ and for $|y| \geq \epsilon$,one will get that $\dot{V} \leq -\beta < 0$. Therefore if $k(t) \to +\infty$, then there exists a t' such that for $t \geq t'$,$k(t) \geq \alpha B/(v\epsilon)^2$, and then $V(t) \leq V('t) - \beta(t - t')$ as long as $|y(t)| > \epsilon$. Since $V \geq 0$, there must exists a $\bar{t} \geq t'$ such that $|y(t)| \leq \epsilon$ which results in $\sigma_\epsilon(|y(t)|) = 0$ for $t > \bar{t}$. Hence, for $t > \bar{t}$, one have that $\dot{k}(t) = 0$ and it can be concluded that $k(t)$ cannot have an infinite limit. The integration of the adaptive law for k(t) results in:

$$\lim_{t \to -\infty} k(t) = k(0) + \mu \int_0^\infty \sigma_\epsilon(|y(t)|)d\tau = k_\infty < +\infty \tag{6.18}$$

Lemma 1 implies that the states $x_1(t)$ and $x_2(t)$ are bounded which corresponds to the output $y(t)$ being bounded. In this case, Barbalat Lemma [47] states:

Because $\lim_{t \to -\infty} k(t) = k_\infty < \infty$ and the fact that $k'(t)$ is absolutely continuous (due to $\sigma_\epsilon(|y(t)|)$ being absolutely continuous) then $\dot{k}(t) = \mu\sigma_\epsilon(|y(t)|) \to 0$ which implies that $y(t) \to I_\epsilon$ as $t \to 0$ □

The tolerance ϵ should be chosen carefully, in particular when the compression system is affected with measurement noise. Certainly, one would desire y to be as closed to zero as possible when steady-state is reached. One way to go about it is to select a very small value for ϵ. However, too small ϵ may cause the controller gain to increase without limits. On the other hand, a greater ϵ will reduce the precision in the controller. As a guidance, [9] proposes to set ϵ equal to the maximum of the disturbance absolute value if the latter is obtainable. Figure 6.1 reports both simulated and experimental data when the adjective

λ-tracker has been added to the real plant with a throttle being a low inertia butterfly valve which is assumed to have a parabolic characteristic. Following data are being used: $B = 0.378$, $u_0 = 0.087$ (which corresponds to a steady butterfly angle of $\theta = 20°$), $\mu = 0.7288$, $\epsilon = 0.1$ and $k(0) = 0$

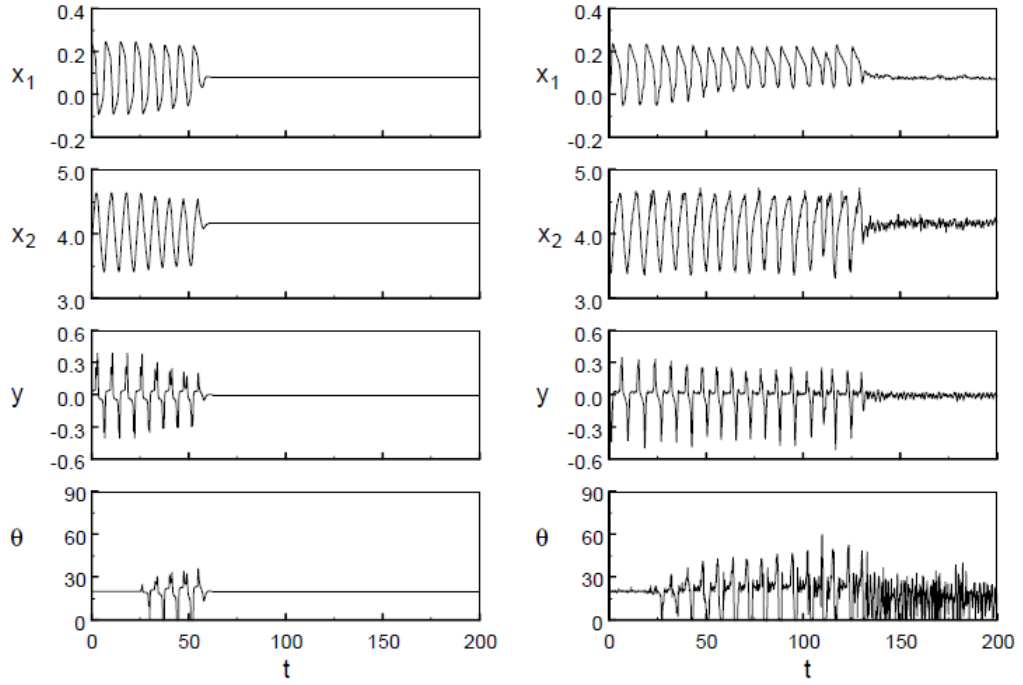

Figure 6.1: Results of the control: simulated(left) and experimental (right) [9]

At the beginning of the experiments the compressor is set into surge, creating oscillations in plenum pressure and mass flow. The controller is put into action at $t = 25$ and quickly stabilizes the system. A remark made by [9] is that the adaptation time is larger for the real plant than it is for the numerical model. This is the consequence of having the disturbances and unmodelled non-linearities affect the dynamics of the system. To compensate for those interferences, one will to have increase the steady-state gain from $k_\infty = 0.845$ for the numerical model to $k_\infty = 2.2$ for the real plant. Under some circumstances, the controller may be unable to recover the compressor from surge due to too strict control bounds, particularly too small value for for $A_{t,\max}$. Analysis provided by [9] shows that this failure is caused by the inherent plant limitations, instead of the proposed control structure. Further discussion about this topic has , however, been left out from this thesis in favour of brevity.

6.3 Adaptive Fuzzy Control of Compressor Surge

A considerable part of the control literature is the one dealing with fuzzy control. It seems that the latter has also founds its way also to the field of compressors, with [3] being an example. This section is a summary of work presented in [44] where the pure-surge version

of the Moore-Greitzer model is the control target. The model parameters, in particular the compressor characteristic, will in many situations be poorly known, as stated numerous times through this thesis. [44] regards the compressor characteristic as the uncertain parameter and propose to estimate it as an fuzzy system later to be estimated by the adaptive law. That estimate will then be a part of the control law for the system. The paper takes the CCV as actuator for which the adaptive fuzzy surge controller is being designed by the backstepping method. Like for [10], the conduct of designing the controller will not be covered in this section but can be be followed in [44]. It is worth mentioning that resulting closed loop system, will from physical point of view be identical to the one discussed in section 3.3.1. The author is fully aware that some readers may be unfamiliar with the concept of fuzziness, specially when it comes to control systems. Therefore, the author will offer some very basic explanations of fuzzy set theory and fuzzy logic, two topics that will be relevant when mathematically describing the fuzzy system. Those explanations has been taken from [16] which offers a comprehensive overview of fuzzy control theory. After the description of the fuzzy systems has been given, the equation composing the adaptive controller will be presented. The controller will later be visualized in a block diagram. At the end, some simulations will be shown where the performance of the adaptive fuzzy controller will be verified.

Now, proceeding with explanation of the fuzzy logic. As the reader may recall, in traditional (Boolean) logic an arbitrary thing can be represented by either having a value of 1(true) or 0(false). In the means of fuzzy logic, the same thing can be represented by a value ranging from 0 to 1, that is "partially true or partially false". Let's use the age of a human as an example. In traditional logic, a person can be viewed as either old or young, representing 1 and 0, respectively. Not surprisingly, it will often be difficult to determinate the age for which a person turns from being young to being old. Hence, the traditional logic may not be relevant for all real-word situations. In the fuzzy logic, a persons age can be evaluated in the range from absolutely young (newborns) which is defined as *completely false* to absolutely old (120 years) defined as *completely true*. For instance, a 40 years old male or female is considered to be 50% absolutely young and 50% absolutely old. Said differently, this persons age is considered as 0.5 *false* and 0.5 *true*.

The concept of fuzziness can also be applied to set theory. The fuzzy set is a set for which an element will have a partial membership. The grade of membership can be measured with a membership function which often range from 0 to 1. In such analogy, 1 will denote a "full member" while 0 will denote "non-member". [16] explains that there is no universal rule for quantifying the membership function. Hence, it will more or less be selected in a subjective manner or "by using ones work experience, scientific knowledge and actual need for the particular application in question", as stated by [16]. The principle of fuzzy sets will be further explained by again using an example from [16]. Let

$$S_f = \{s \in \mathbb{R}^+| \text{ s is large}\} \tag{6.19}$$

be a fuzzy set. Clearly, S_f will be a subset of (universe) set $\mathbb{R}^+$ which contains all positive real numbers. To avoid the confusion whether 0 is a positive number or not, the universe set has been defined as

$$\mathbb{R}^+ = \{x \in \mathbb{R} | x \leq 0\} \tag{6.20}$$

In fact, all fuzzy sets will be subsets of an equal or larger universe set. If S_f was to be viewed in the means of standard set theory (where an element is either being a member of

a set or not), it would be poorly defined since ”large ” is a rather vague description of a number. A following membership function will be used as tool to evaluate ”greatness” of a value

$$\mu_{Sf} = \begin{cases} 0 & \text{if} s \leq 0 \\ 1 - e^{-s} & \text{if} s > 0 \end{cases} \tag{6.21}$$

Moreover, the function has been visually displayed in Figure 6.2

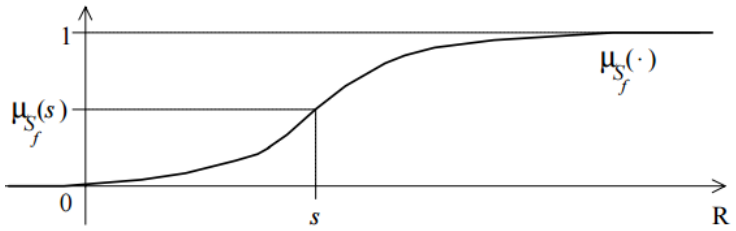

Figure 6.2: A membership function for a positive and large real number [16]

When analyzing Figure 6.2, it becomes obvious that an element with an increasing value, will converge towards full membership.

[44] defines a fuzzy system with the following:

Definition 1. *A fuzzy system is the mapping from the input vector* $x = [x_1, \ldots, x_n] \in X_1 \times \ldots \times X_n \subseteq \mathbb{R}^n$ *to the output vector* $y \in \mathbb{R}$. *The* ith *rule of the logic fuzzy system has the form:*

Rule i: if x_1 *is* F_{i1},x_n *is* F_{in}, *then* $y = \omega_i$ *where* $i = 1, \ldots, m$ *is the number of fuzzy logic rules,* ω_i *is the statement of the* ith *fuzzy rule and* $F_{ij}(j = 1, \ldots, n)$ *represents a fuzzy set in universe of discourse* X_i. *The candidate for the membership function* $\mu_{Fij}(x_j)$ *will be the Gauss function*

$$\mu_{Fij}(x_j) = exp\left(-\left(\frac{x_j - a_{ij}}{b_{ij}}\right)^2\right) \tag{6.22}$$

where a_{ij} *and* b_{ij} *are parameters to be designed. Let*

$$W^T = [\omega_1, \omega_2, \ldots, \omega_m]$$
$$P(x) = [p_1(x), p_2(x), \ldots, p_m(x)]^T$$
$$p_i(x) = \frac{\prod_{j=1}^{n} \mu_{Fij}(x_j)}{\sum_{i=1}^{m}\left(\prod_{j=1}^{n} \mu_{Fij}(x_j)\right)}$$

so that the fuzzy system can be formulated by the equation:

$$y(x) = W^T P(x) \tag{6.23}$$

where W *is called* parameter vector *and* P(x) *is called* fuzzy function basis function vector

In order to keep the fuzzy system $y(x)$ simple, [44] proposes to assign $\mu_{Fij}(x_j)$ to a fixed value, which will follow from setting a_{ij} and b_{ij} to constant values. Those two parameters will, according to [44], define ω_i as a tunable parameter.

Now, moving to the discussion of adaptive surge control. Equations describing the purge-surge version of the Moore-Greitzer model are

$$\begin{aligned}\dot{\psi} &= \frac{1}{4B^2 l_c}(\phi - \Phi_T(\psi)) \\ \dot{\phi} &= \frac{1}{l_c}(\Psi_c(\phi) - \psi)\end{aligned} \tag{6.24}$$

where the compressor characteristic is still the cubic function expressed by (1.5). Consult [23] or [39] for the defition of the parameter l_c When constructing the adaptive surge controller, [44] decided to compensate for possible disturbances in inlet mass flow and plenum pressure. The model in eq. (6.24) extended with interferences from disturbances is given by:

$$\begin{aligned}\dot{\psi} &= \frac{1}{4B^2 l_c}(\phi - \Phi_T(\psi) + d_\phi(\tau)) \\ \dot{\phi} &= \frac{1}{l_c}(\Psi_c(\phi) - \psi + d_\psi(\tau))\end{aligned} \tag{6.25}$$

The influence of CCV will now be included in the system equations. The closed-loop version of (6.25) becomes:

$$\begin{aligned}\dot{\psi} &= \frac{1}{4B^2 l_c}(\phi - \Phi_T(\psi) + d_\phi(\tau)) \\ \dot{\phi} &= \frac{1}{l_c}(\Psi_c(\phi) - \Psi_v(\phi) - \psi + d_\psi(\tau))\end{aligned} \tag{6.26}$$

where $\Psi_v(\phi)$ is the earlier defined CCV characteristic still to be considered as the system input u. [44] aimed the inlet mass flow and pressure disturbances as the control object and came up with following control law for the system :

$$u = k_2 e_2 + e_1 + \hat{f}_a(\psi, \phi) - u_{r2} \tag{6.27}$$

where

$$u_{r2} = -\hat{B}_2 \tanh\left(\frac{e_2}{\eta_2}\right) \tag{6.28}$$

is the robustness designed for the pressure disturbance and

$$e_1 = \psi - \psi_d \tag{6.29a}$$

$$e_2 = \phi - \alpha \tag{6.29b}$$

are the deviation variables. In addition, k_2 and η_2 are the design parameters and $\hat{B}_2$ is the estimate of the unknown upper bound of pressure disturbance, symbolized as B_2, which is being continuously updated by the adaptive law defined in eq. (6.35). Notice that both ψ and ϕ are regarded as feedback signals for the controller u. The parameter ψ_d appearing in eq. (6.29b) and which [44] defines as "the set value of pressure rise in the compressor",

is regarded as reference signal for the system. The virtual control law , α, which plays a part in the backstepping procedure, has been constructed as:

$$\alpha = -k_1 e_1 + \Phi_T(\psi) + 4B^2 l_c \dot{\psi}_d + u_{rl} \tag{6.30}$$

and with the assumption that ψ_d is continuous and bounded. Equation (6.30) contain the tunable parameter k_1 and the robustness designed for flow disturbance which is symbolized by u_{rl} and has been defined as:

$$u_{r1} = -\hat{B}_1 \tanh\left(\frac{e_1}{\eta_1}\right) \tag{6.31}$$

where η_1 is the design parameter and $\hat{B}_1$ is the estimate of the unknown upper bound of flow disturbance, symbolized as B_1, which will be continuously updated by the adaptive law defined in eq. 6.34. The estimation of the compressor characteristic as a fuzzy system will now be followed up by expressing the function $\hat{f}_\alpha(\psi, \phi) = \Psi_c(\phi) - \psi - l_c\dot{\alpha}$ as:

$$\hat{f}_\alpha(\psi, \phi) = \hat{W}^T P \tag{6.32}$$

where the estimate $\hat{W}$ is being generated by the adaptive law:

$$\dot{\hat{W}} = \lambda e_2 P \tag{6.33}$$

with λ being the adaptive gain. In comparison to the two adaptive law defined in Sec. 4.4, one can view W as the vector consisting of the unknown parameters and vector P and e_2 as the regressor and (mass flow) estimation error, respectively. The estimates $\hat{B}_1$ and $\hat{B}_2$ are being adjusted by the adaptive laws:

$$\dot{\hat{B}}_1 = e_1 \tanh\left(\frac{e_1}{\eta_1}\right) \tag{6.34}$$

$$\dot{\hat{B}}_2 = e_2 \tanh\left(\frac{e_2}{\eta_2}\right) \tag{6.35}$$

The closed-loop system in (6.25) coupled with the adaptive controller above will become stable and the tracking error will be ultimately bounded. The structure of the adaptive controller is being visualized by the block diagram in Figure 6.3.

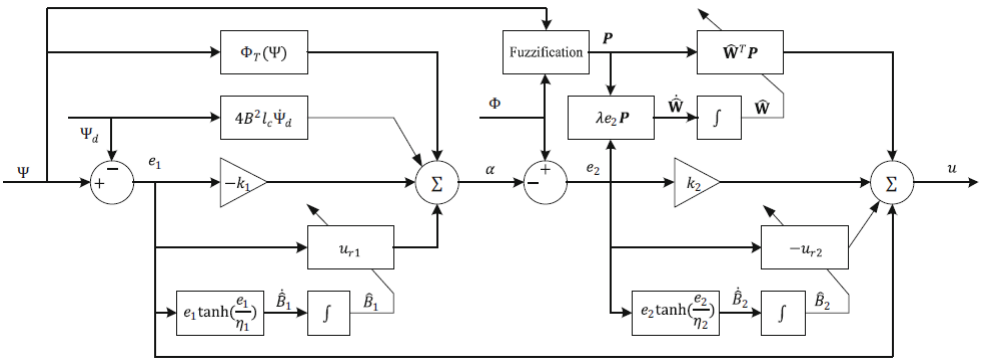

Figure 6.3: The block diagram of the whole adaptive controller [44]

The adaptive controller was validated by [44] through simulations in MATLAB. Three different experiments were carried out by [44] in order to validate the performance of the adaptive fuzzy controller. It is the third one that will be presented in this thesis, however. This is because this experiment will test the controller to its full extent. System parameters during the simulation are: $B = 1.8$, $l_c = 1$, $H = 0.18$, $W = 0.25$ and $\psi_{CO} = 0.3$. The throttle opening has been turned down from 0.65 to 0.6 at $t = 100$, so that the compressor would enter deep surge if uncontrolled. [44] has chosen following control parameters: $k_1 = 0.5$, $k_2 = 1$,$\eta_1 = 0.05$, $\eta 2 = 0.05$ and $\lambda = 2$. Dividing the flow and pressure coefficients into 9 grades (ranging from 0 to 1) results in a membership function given as:

$$\mu_{Fij} = \exp\left(-\left(\frac{x_j - a}{b}\right)^2\right) = \exp(-(x - 0.1)^2), \quad i = 1, \ldots, 9 \tag{6.36}$$

Following disturbances in intlet flow and plenum pressure has been added to the system:

$$d_\phi(\tau) = 0.02\sin(0.1\tau) + 0.02\cos(0.4\tau)$$
$$d_\psi(\tau) = 0.02\sin(0.1\tau) + 0.02\cos(0.4\tau)$$

Simulation result for the adaptive controller are illustrated by Figures (6.4) and 6.5.

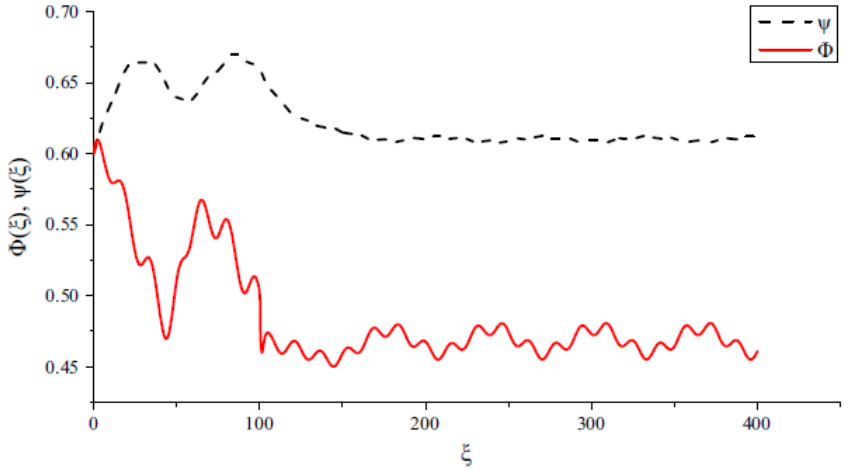

Figure 6.4: Simulation results [44]

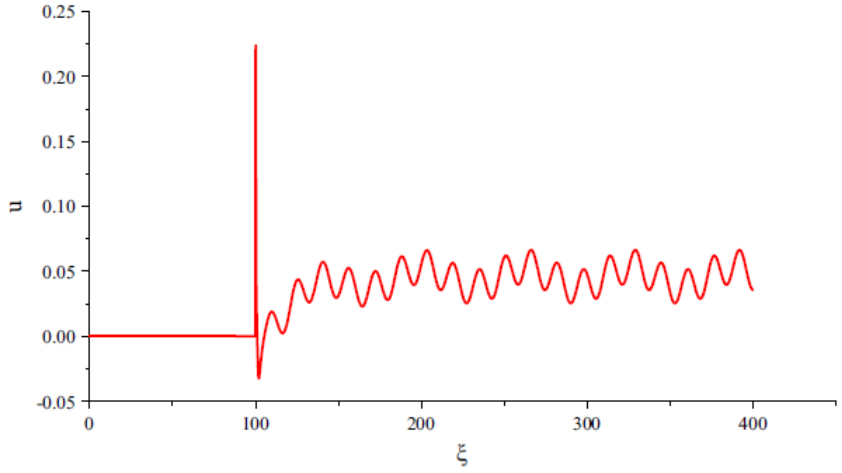

Figure 6.5: Controller output [44]

Clearly, the adaptive controller stabilizes the compressor in the effective manner and works exactly in the way as one would expect from the active surge controller: enlarges the region of stable points of the compressor and in the same time improves its performance. Besides, it handles the disturbances well and thus shows its robustness. One can see that when first activated, the controller will experience a momentary jump caused by fuzzy system not being adapted to adjustment at the beginning (the controller will adapt quickly to the new environment). Afterwards and for a very short period of time, the controller will assign CCV to a negative value. This will result in a negative pressure drop, something that, obviously, cannot be realized. As a solution to this issue, [44] suggests to preset an initial offset to CCV.

Chapter 7

Simulation

7.1 Preliminaries

The results of modified adaptive controller will be presented in the following. The controller was implemented for the cases of CCV and PAASCS. As for the latter, the equations used to build the model are: (3.23), (3.24) and (3.11). In the case of CCV, the model consists of the equations (3.10), (3.15) and (3.11). The compressor map applied in the simulations has been defined in eq. (3.12) As the reader may recall, the listed equations are all given with respect to dimensionless deviation variables. Since the actual equilibrium is unknown, one will have to include the adaptive law (3.41) into the closed-loop system. Note that when the inlet flow cannot be measured, its estimate will appear in the system equations listed above. It seems reasonable to compare the performances of the standard P-controllers (for which the compressor characteristic is known) with the performance of their adaptive version, in order to evaluate the performances of the latter. Such approach has also been followed up in this thesis. Furthermore, the performance of the equilibrium estimation and the accuracy of both estimations of the compressor map and the observer will also be verified through simulations.

The simulations will be given in several bulks. At first, the model will be simulated open-loop both at stable operation and during surge. Equations used during the open-loop simulation are (2.21), (2.22) along with (1.5) which expresses the characteristic for the compressor. In order to verify those conditions, the measurements of inlet flow and plenum pressure will be displayed. What follows is a set of simulations for the system containing a CCV where the modifications discussed in previous chapters will be included. The same type of exercise will be performed afterwards for PAASCS. Both the controller based on gradient method and least-squares method will be tested. The simulations include:

- the inlet flow and plenum pressure measurements for both the standard P-controller and adaptive controller.
- trajectories for the estimates of constants k_1, k_2 and k_3. The convergences for the trajectories can then be compared with the actual values for the constants. These will be calculated in advance.

- the estimates of the equilibrium coordinates provided by the adaptive law in section 3.4.
- the observer output in the form of flow estimate will be compared with the actual flow measurement.

7.2 System specifications

First, an overview of parameter values, used throughout the simulations, will be given. The parameters will have equal values for both actuators.

Symbol	Value	Units
U	68	m/s
V_p	0.1	m^3
L_c	0.41	m
ψ_{c0}	0.352	-
H	0.18	-
a_0	340	m/s
A_c	0.0038	m_s^2
W	0.25	-

Table 7.1: Specifications for the compression system

7.3 Open-loop simulation

7.3.1 Stable operation

The throttle gain is set to $\gamma_T = 0.8$ and the inlet flow is available for measurement. The system is predicted to be stable since the equilibrium point is placed at the negative slope of the compressor characteristic. For the detailed location of the equilibrium point, the reader is referred to Figure 2.2. The measurements of inlet flow and plenum pressure are illustrated by the Figure 7.1 and Figure 7.2 respectively.

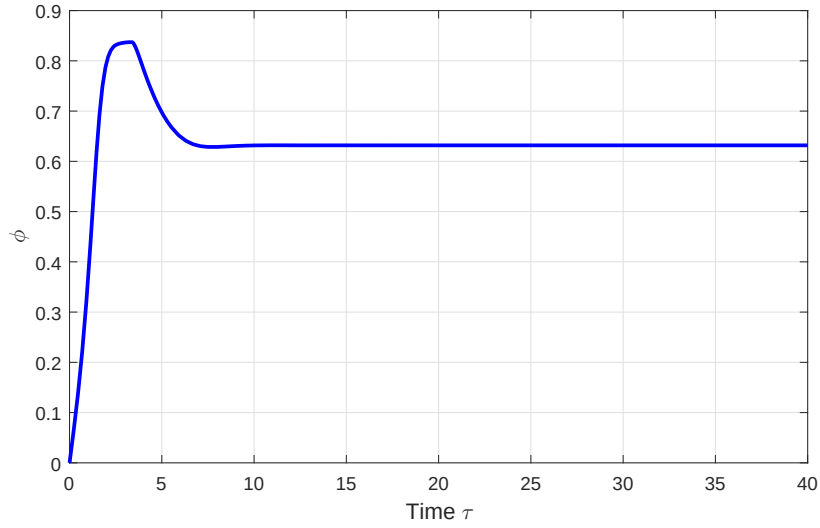

Figure 7.1: Inlet flow for stable operation expressed with a dimensionless standard variable

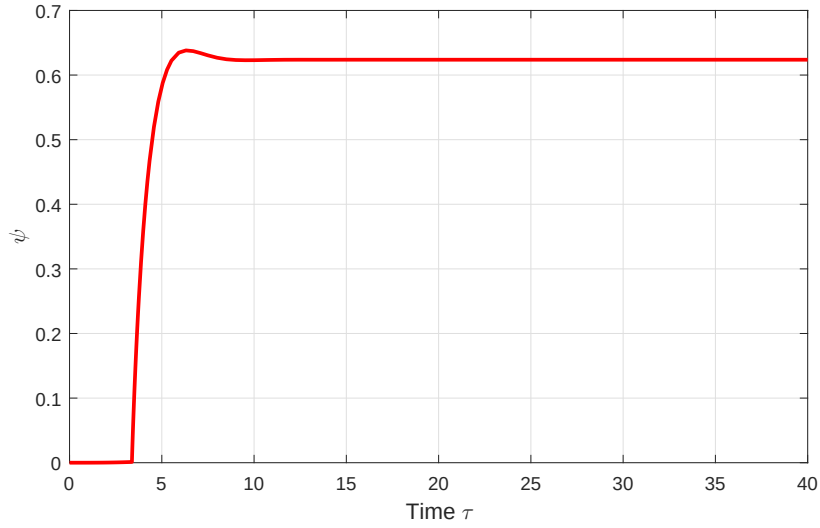

Figure 7.2: Plenum pressure for stable operation

7.3.2 Surge Condition

The gain of the throttle has been reduced from $\gamma_T = 0.8$ to $\gamma_T = 0.5$. The inlet flow is still available for measurement. The Figure 2.2 predicts that the compressor goes into surge due to equilibrium being located the compressor characteristic of positive slope. This is verified by the measurements of inlet flow and plenum pressure depicted by Figure 7.3 and Figure 7.4 respectively.

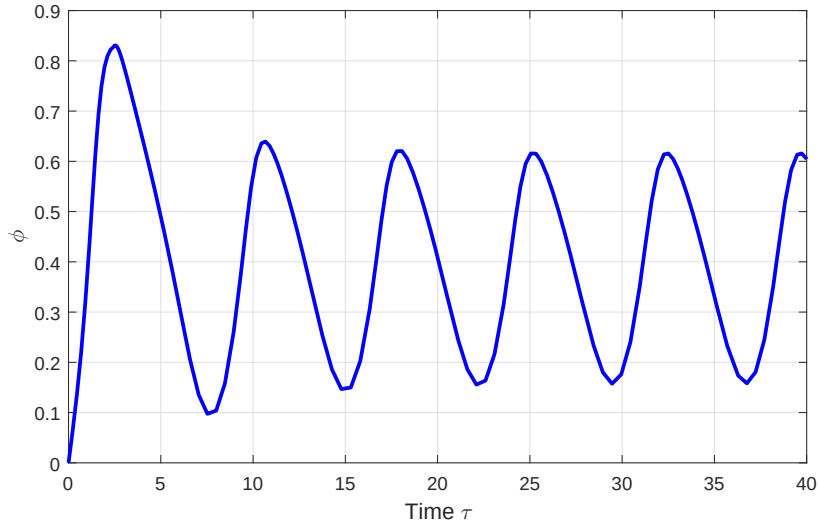

Figure 7.3: Inlet flow during surge expressed with a dimensionless standard variable []

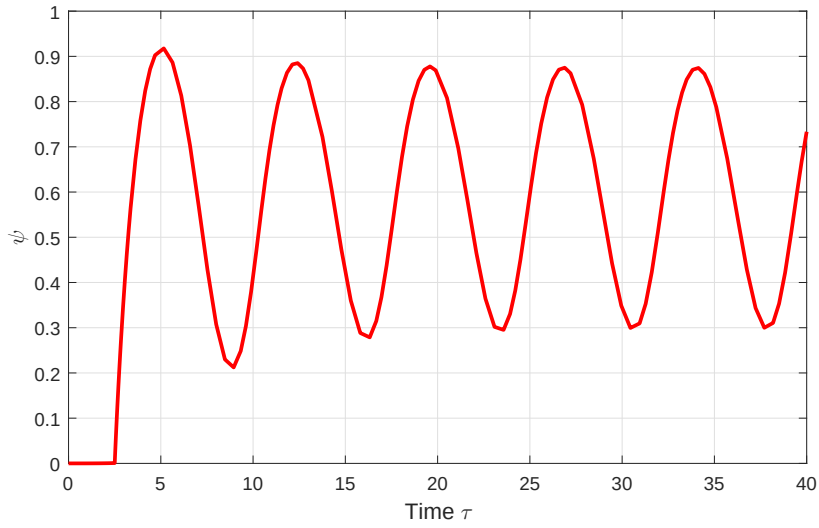

Figure 7.4: Plenum pressure during surge expressed with a dimensionless standard variable

7.4 Closed-loop simulation

7.4.1 Calculations of the compressor characteristic coefficients

In the beginning, one is assuming that the compressor characteristic is available and that the throttle gain has been adjusted to $\gamma_T = 0.5$ (and will remain unchanged throughout

the rest of the simulations). This gives and an equilibrium point being equal to

$$x_o = \begin{bmatrix} \phi_0 \\ \psi_0 \end{bmatrix} = \begin{bmatrix} 0.4133 \\ 0.6833 \end{bmatrix} \tag{7.1}$$

as seen in Figure 2.2. The values of the equilibrium point opens up for following calculations of the coefficients belonging to the compressor characteristic:

$$\begin{aligned} k_1 &= \frac{3H\phi_0}{2W^2}\left(\frac{\phi_0}{W} - 2\right) = \frac{3 * 0.18 * 0.4133}{2 * 0.25^2}\left(\frac{0.4133}{0.25} - 2\right) = -0.6192 \\ k_2 &= \frac{3H}{2W^2}\left(\frac{\phi_0}{W} - 1\right) = \frac{3 * 0.18}{2 * 0.25^2}\left(\frac{0.4133}{0.25} - 1\right) = 2.8219 \\ k_3 &= \frac{0.18}{20.25^3} = 5.7600 \end{aligned} \tag{7.2}$$

The coordinates for the equilibrium point along with the computed values of the coefficients will be used as a benchmark for evaluation of the estimators. The coefficients will also be assembled to form the proportional gain for P-controller later to be compared with its adaptive version. The evaluation of the equilibrium estimates will only be done in the case of PAASC. The reason for this is the fact that in regard to CCV, the equilibrium coordinates obtained from eq. 7.1 will only be used as an approximation. Computation of the true equilibrium point will involve solving the 3rd order polynomial equation in (3.29). This is quite challenging and has consequently been left out from the work of this thesis. Hence, the approximation will only be used for construction of the gain for the P-controller.

7.4.2 Simulations of the single compression system with CCV as the actuator

The controller will be activated at $t = 30$ in order to prevent the system from oscillating. The controller gain is chosen to have the structure

$$c_1 = k_2^2 - k_1 \tag{7.3}$$

which certainly satisfies the bound:

$$c_1 > \frac{k_2^2}{4k_3} - k_1 \tag{7.4}$$

since k_3 will always have a positive value. The proportional gain is calculated to:

$$c_{1p} = k_2^2 - k_1 = 2.8219^2 - (-0.6192) = 8.5823 \tag{7.5}$$

As for the adaptive controller, the controller gain is as follows:

$$c_{2b} = \hat{k}_2^2(t) - \hat{k}_1(t) \tag{7.6}$$

where $\hat{k}_2^2(t)$ and $\hat{k}_1(t)$ are respectively the on-line estimates of k_1 and k_2 at time t. Those estimates are being provided either by the method of steepest descent represented by

eq.(4.27) or least-squares method represented by equations (4.43) and (4.41). Both estimation methods are being activated at $t = 0$. The equations used for constructing the flow observer included to the closed loop are

$$\begin{aligned} \dot{\alpha} &= B(\breve{\Psi}_c - \breve{\psi} - u) - \frac{k_{\bar{m}}}{\omega_H}\breve{\phi} + \frac{k_{\bar{m}}}{\omega_H}\gamma_T\sqrt{\breve{\psi}} \\ \breve{\phi} &= \alpha + k_{\bar{m}}\frac{V_p U}{2A_c a_o^2}\breve{\psi} \end{aligned} \tag{7.7}$$

Recall that $\breve{(\cdot)}$ denotes the deviation from the equilibrium when applying the inlet flow estimate. In addition, the observer gain has been set to $k_{\bar{m}} = 100$

Method of Steepest Descent (Gradient Method)

By defining the adaptive gain for the compressor map estimation and equilibrium estimation, respectively as

$$\Gamma_1 = \begin{bmatrix} 1500 & 0 & 0 \\ 0 & 275 & 0 \\ 0 & 0 & 100 \end{bmatrix} \quad \text{and} \quad P = \begin{bmatrix} 0.05 & 0.05 \\ 0.05 & 0.05 \end{bmatrix}$$

the system response in the following way:

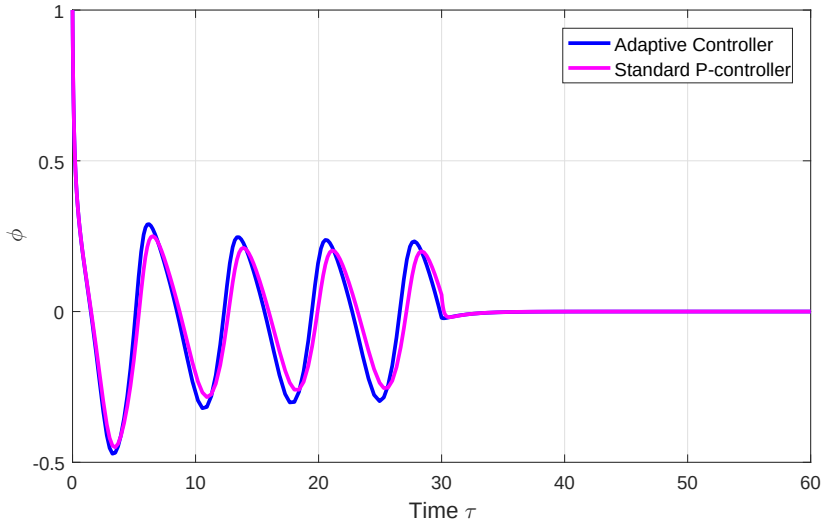

Figure 7.5: Stabilization of the inlet flow with both the standard P-controller and the adaptive controller

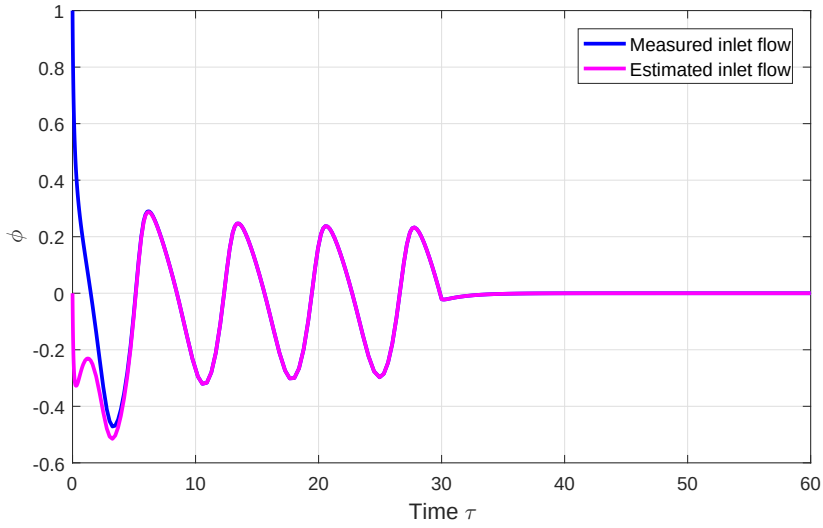

Figure 7.6: Comparing inlet flow measurement with its estimate

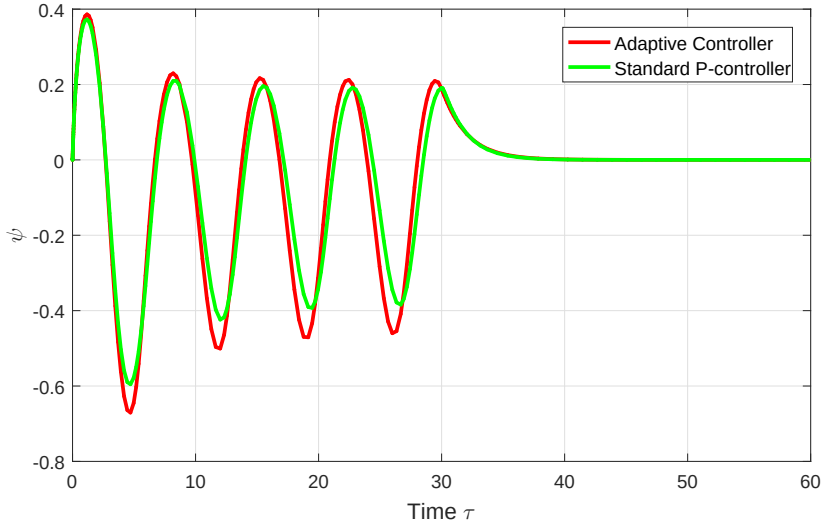

Figure 7.7: Stabilization of the plenum pressure with both the standard P-controller and the adaptive controller

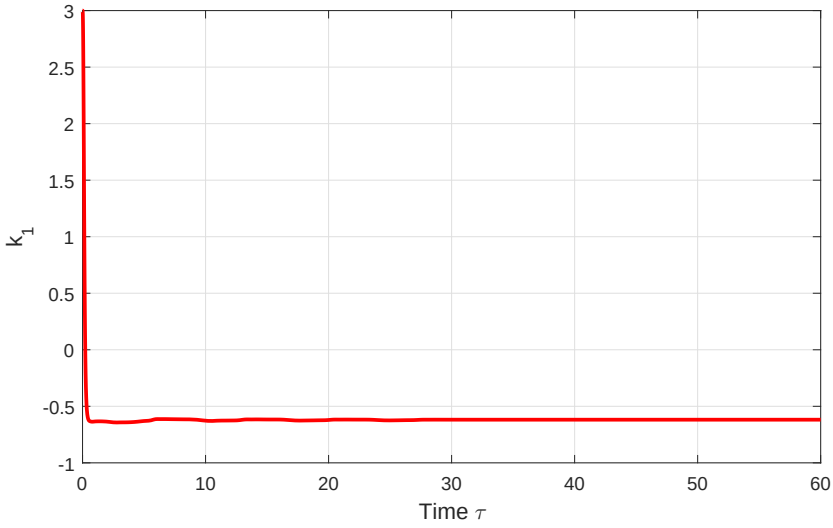

Figure 7.8: Trajectory of the estimate for k_1

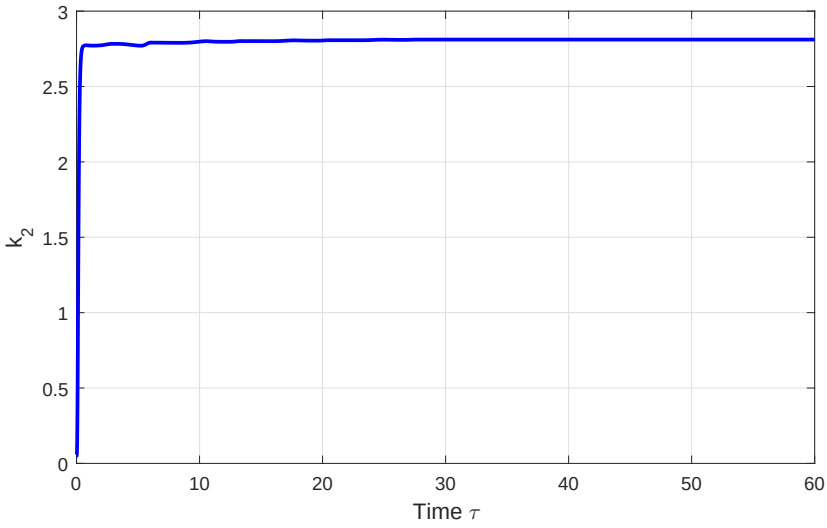

Figure 7.9: Trajectory of the estimate for k_2

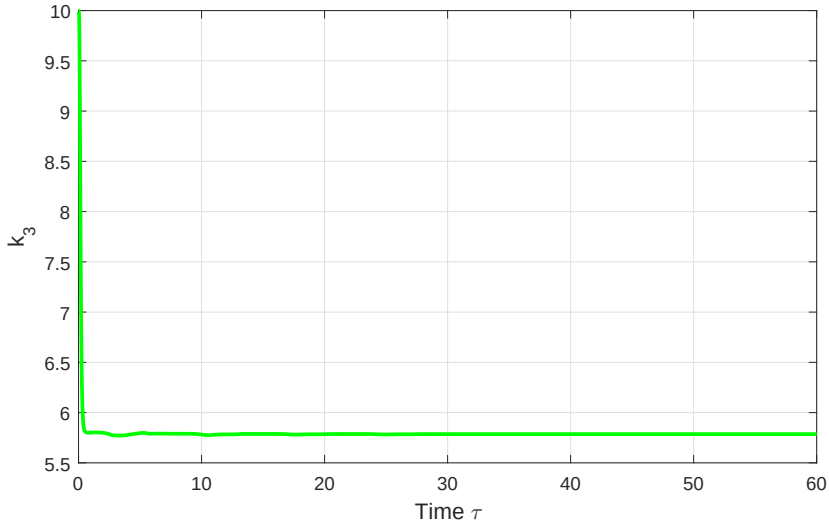

Figure 7.10: Trajectory of the estimate for k_3

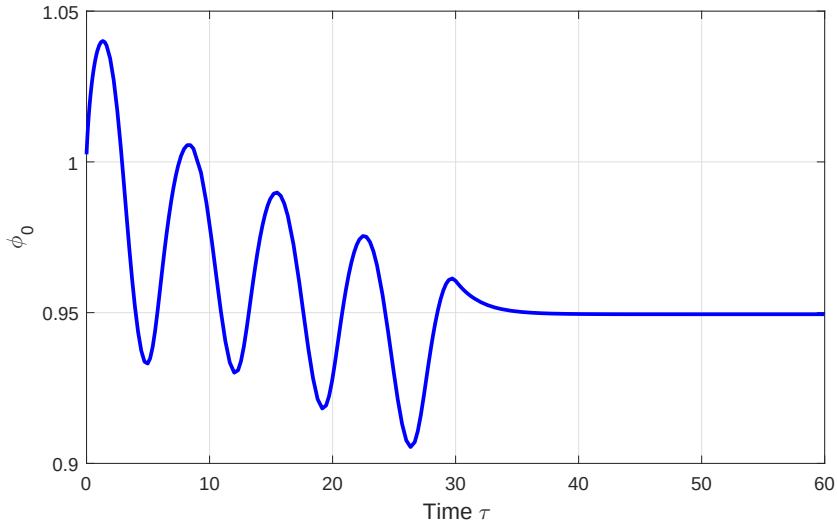

Figure 7.11: Trajectory of the estimate for ϕ_0

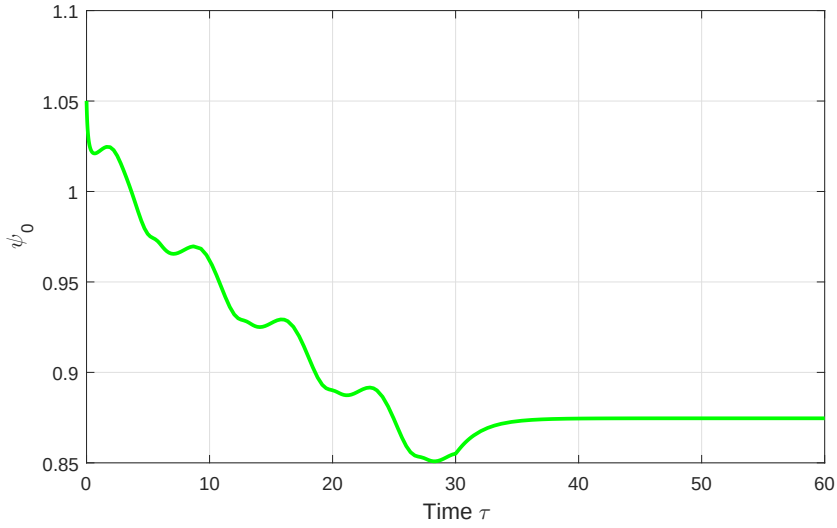

Figure 7.12: Trajectory of the estimate for ψ_0

Least-squares

By choosing

$$P_0 = \begin{bmatrix} 10000 & 0 & 0 \\ 0 & 10000 & 0 \\ 0 & 0 & 10000 \end{bmatrix} \quad \text{and} \quad P = \begin{bmatrix} 0.05 & 0 \\ 0 & 0.04 \end{bmatrix}$$

as the initial value for matrix P (for compressor map estimation) and the adaptive gain for equilibrium estimation, the system will response in the following way:

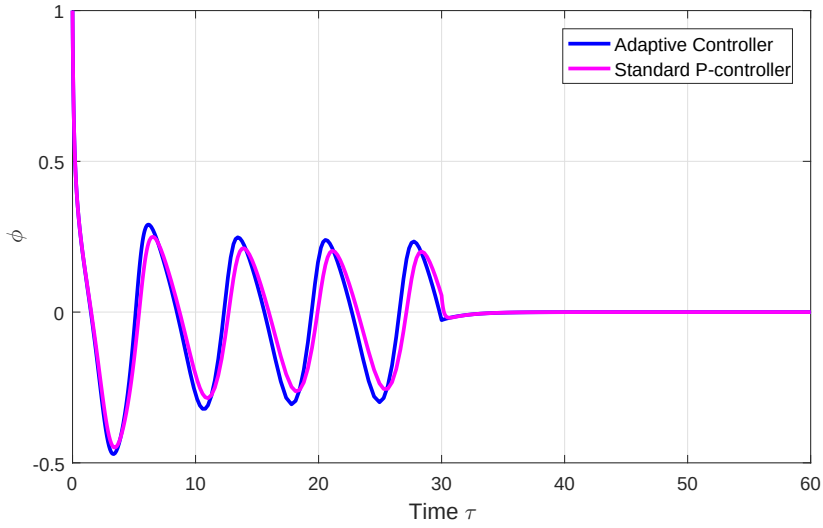

Figure 7.13: Stabilization of the inlet flow with both the standard P-controller and the adaptive controller

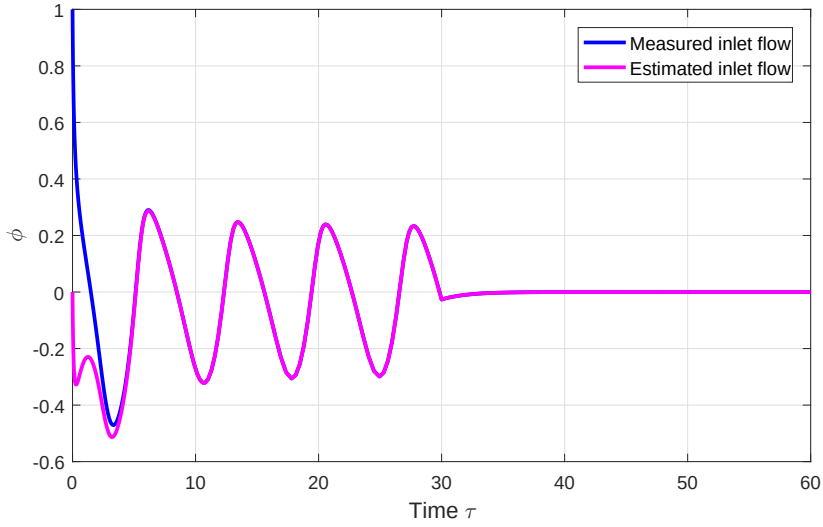

Figure 7.14: Comparing inlet flow measurement with its estimate

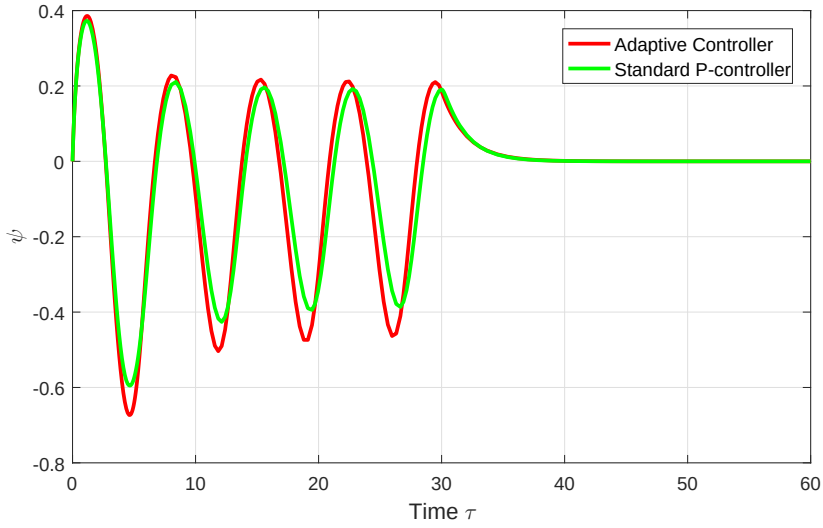

Figure 7.15: Stabilization of the plenum pressure with both the standard P-controller and the adaptive controller

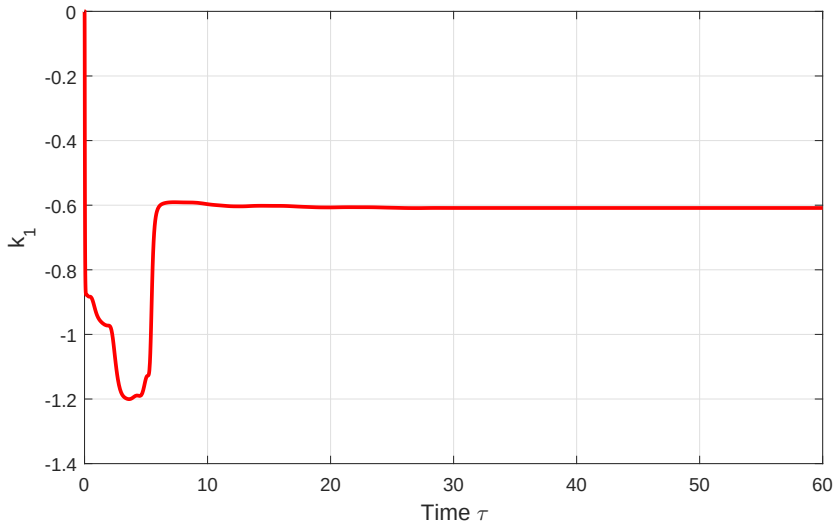

Figure 7.16: Trajectory of the estimate for k_1

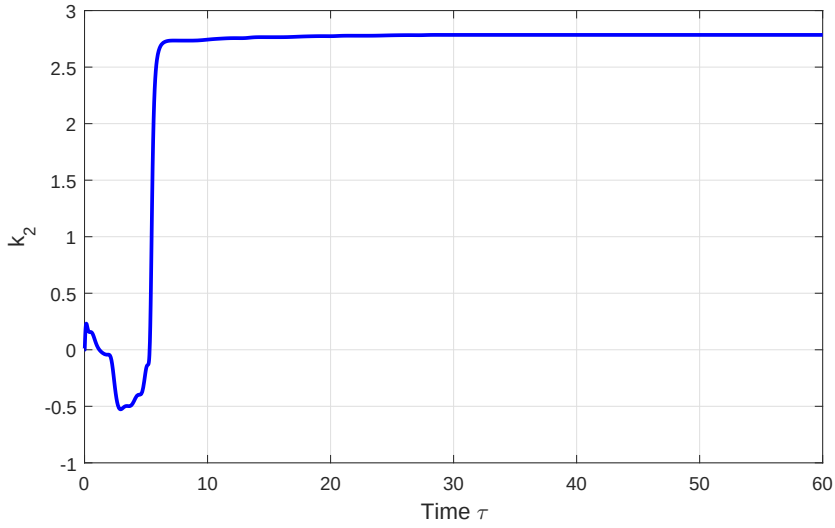

Figure 7.17: Trajectory of the estimate for k_2

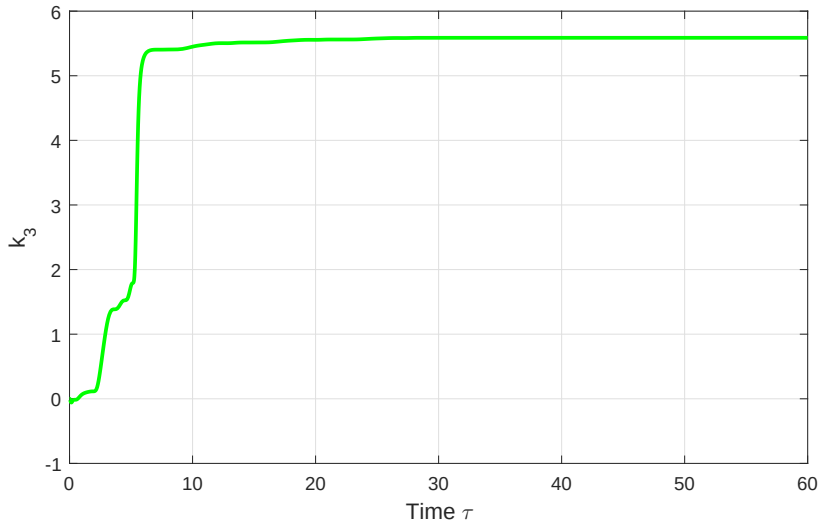

Figure 7.18: Trajectory of the estimate for k_3

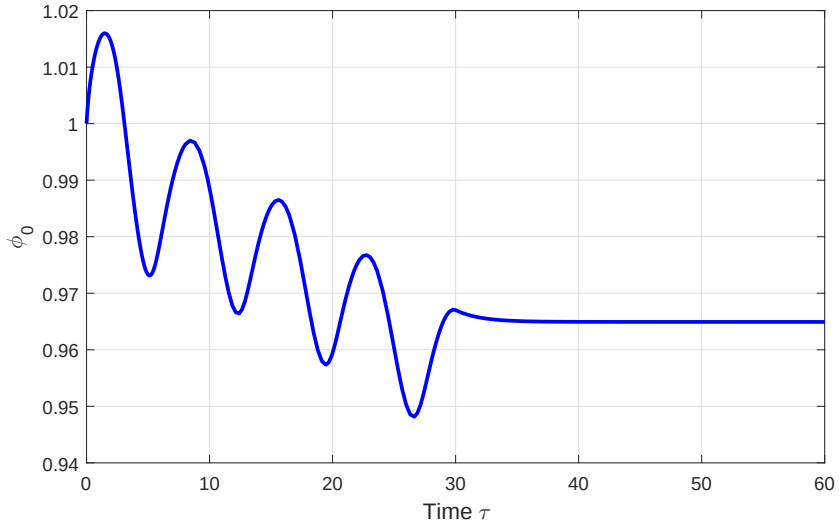

Figure 7.19: Trajectory of the estimate for ϕ_0

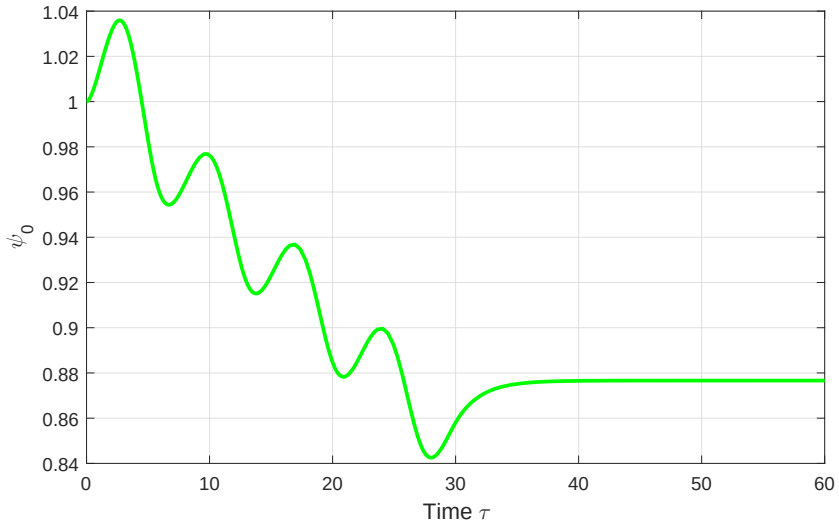

Figure 7.20: Trajectory of the estimate for ψ_0

7.4.3 Simulations of PAASCS

The controller will be activated at $t = 30$ in order to prevent the system from oscillating. The controller will be on the form

$$\phi_u = -B^2 c_2(\Psi_c - \psi) \tag{7.8}$$

where the constant c_2 has been chosen to

$$c_2 = k_2^2 - k_1 \tag{7.9}$$

which certainly satisfies the bound:

$$c_1 > \frac{k_2^2}{4k_3} - k_1 \tag{7.10}$$

since k_3 will always have a positive value. The proportional gain is calculated to:

$$K_p = B^2(k_2^2 - k_1) = 0.6418(2.8219^2 - (-0.6192)) = 5.5085 \tag{7.11}$$

As for the adaptive controller, the controller gain is as follows:

$$K_{pa} = B^2(\hat{k}_2^2(t) - \hat{k}_1(t)) \tag{7.12}$$

where $\hat{k}_2^2(t)$ and $\hat{k}_1(t)$ are respectively the on-line estimates of k_1 and k_2 at time t. Those estimates are being provided either by the method of steepest descent represented by eq.(4.27) or least-squares method represented by equations (4.43) and (4.41). Both estimation methods are being activated at $t = 0$. The equations used for constructing the flow observer included to the closed loop are

$$\begin{aligned} \dot{\alpha} &= B(\breve{\Psi}_c - \breve{\psi}) - \frac{k_{\bar{m}}}{\omega_H}\breve{\phi} + \frac{k_{\bar{m}}}{\omega_H}\gamma_T\sqrt{\breve{\psi}} \\ \breve{\phi} &= \alpha + k_{\bar{m}}\frac{V_p U}{2A_c a_o^2}\breve{\psi} \end{aligned} \tag{7.13}$$

In addition, the observer gain has been set to $k_{\bar{m}} = 100$

Method of Steepest Descent (Gradient Method)

By defining the adaptive gain for the compressor map estimation and equilibrium estimation, respectively as

$$\Gamma_1 = \begin{bmatrix} 1500 & 0 & 0 \\ 0 & 275 & 0 \\ 0 & 0 & 100 \end{bmatrix} \quad \text{and} \quad P = \begin{bmatrix} 0.05 & 0 \\ 0 & 0.05 \end{bmatrix}$$

the system response in the following way:

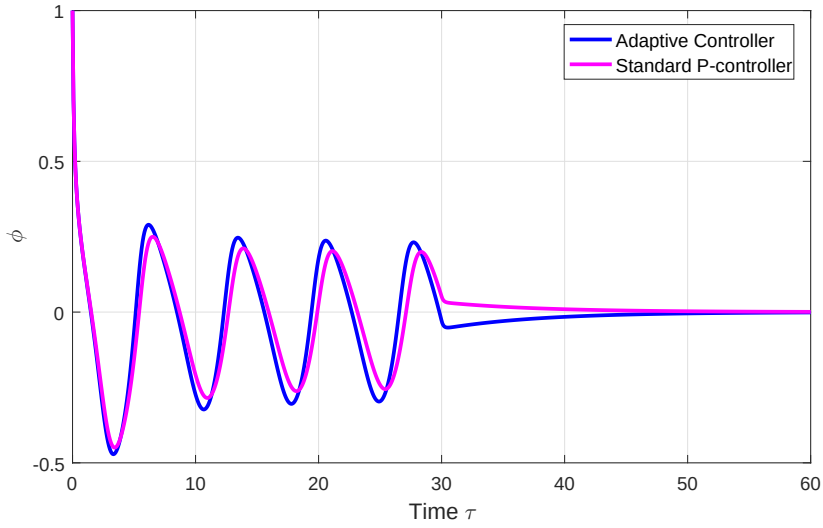

Figure 7.21: Stabilization of the inlet flow with both the standard P-controller and the adaptive controller

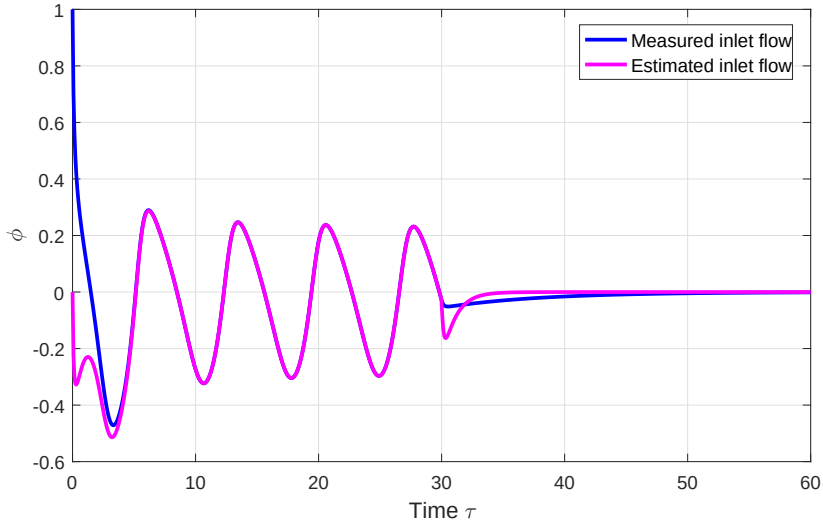

Figure 7.22: Comparing inlet flow measurement with its estimate

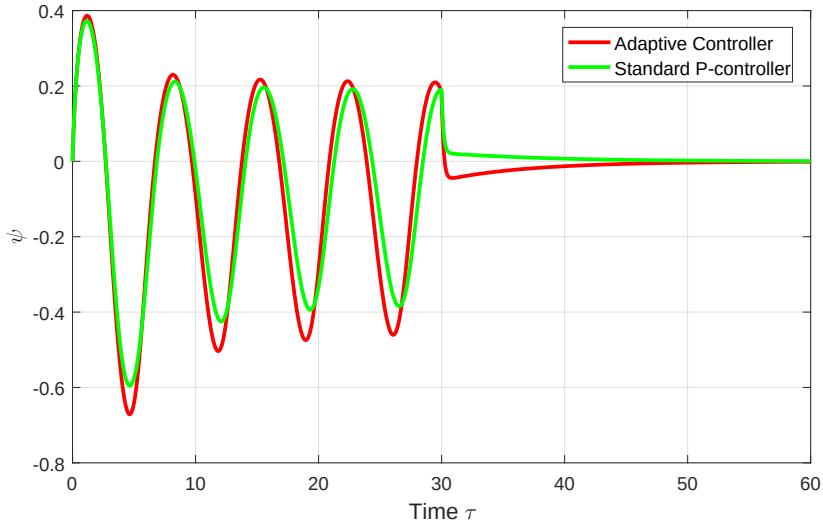

Figure 7.23: Stabilization of the plenum pressure with both the standard P-controller and the adaptive controller

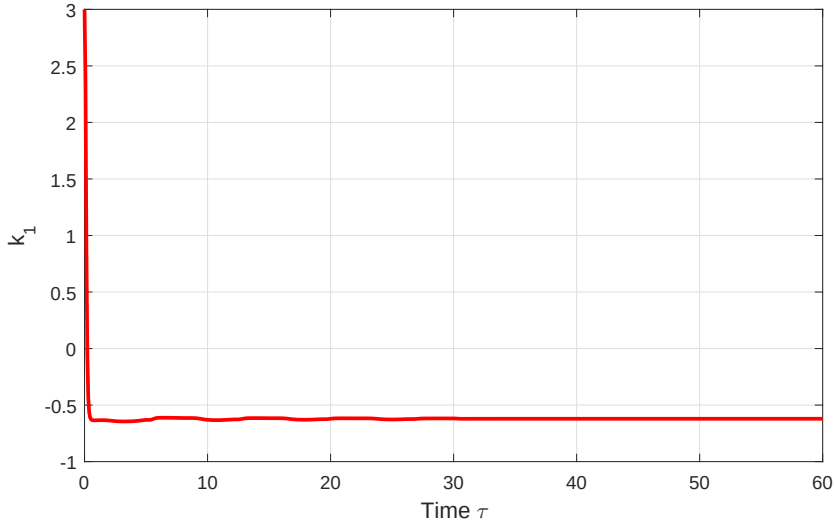

Figure 7.24: Trajectory of the estimate for k_1

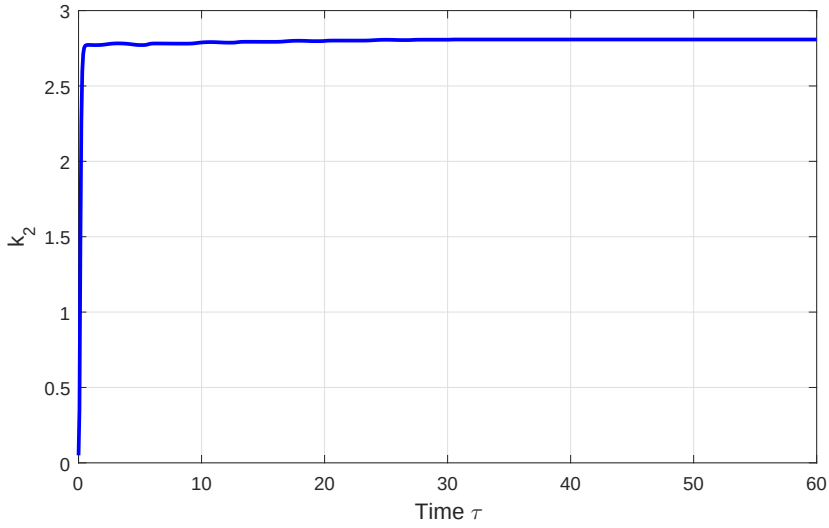

Figure 7.25: Trajectory of the estimate for k_2

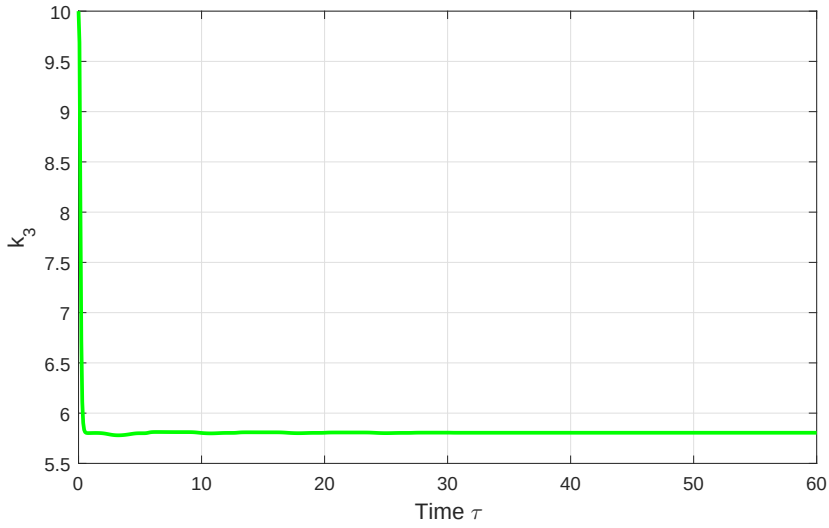

Figure 7.26: Trajectory of the estimate for k_3

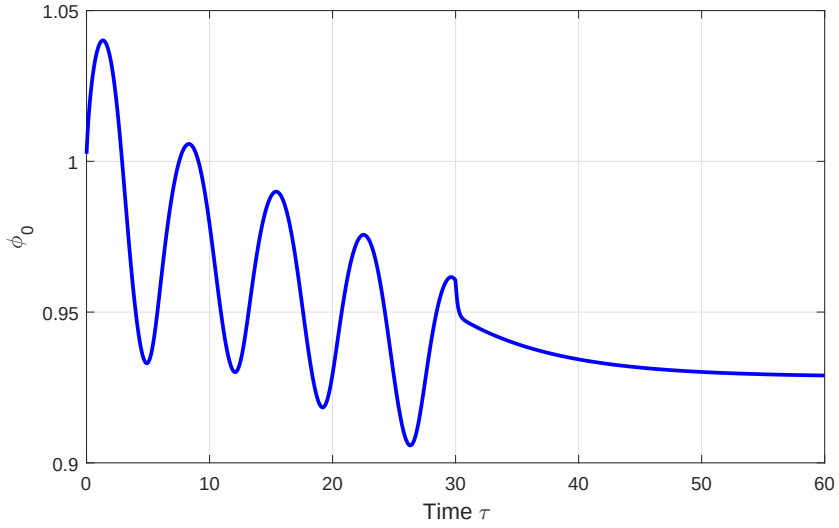

Figure 7.27: Trajectory of the estimate for ϕ_0

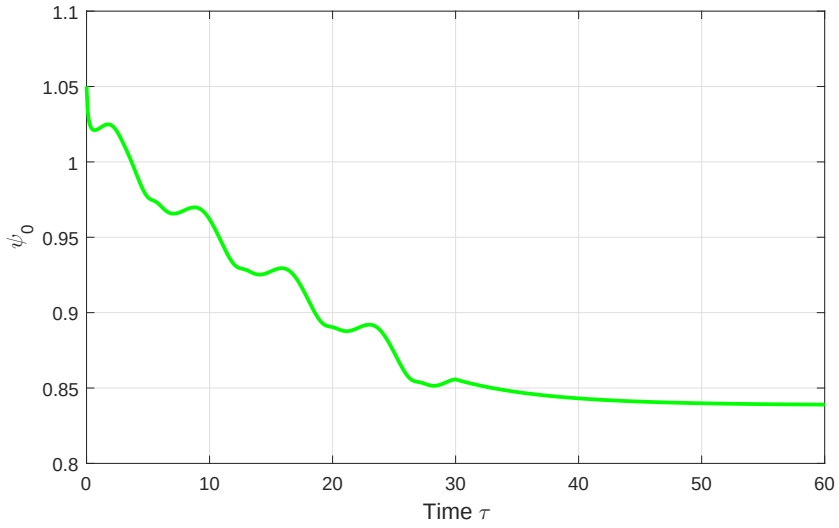

Figure 7.28: Trajectory of the estimate for ψ_0

Least-squares

By choosing

$$P_0 = \begin{bmatrix} 10000 & 0 & 0 \\ 0 & 10000 & 0 \\ 0 & 0 & 10000 \end{bmatrix} \quad \text{and} \quad P = \begin{bmatrix} 0.05 & 0 \\ 0 & 0.04 \end{bmatrix}$$

as the initial value for matrix P and the adaptive gain for equilibrium estimation, the system will response in the following way:

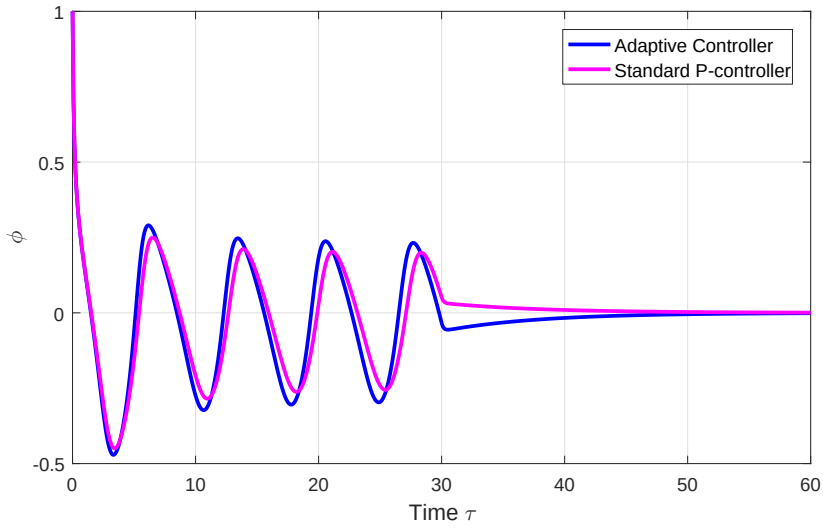

Figure 7.29: Stabilization of the inlet flow with both the standard P-controller and the adaptive controller

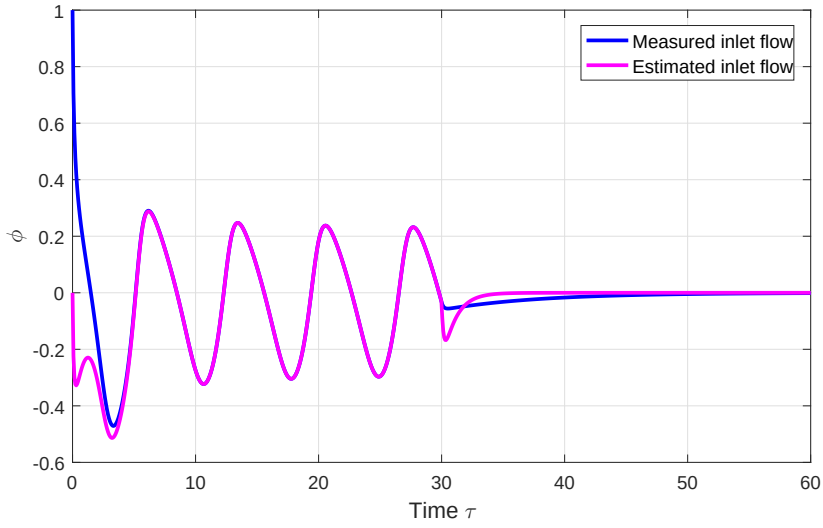

Figure 7.30: Comparing inlet flow measurement with its estimate

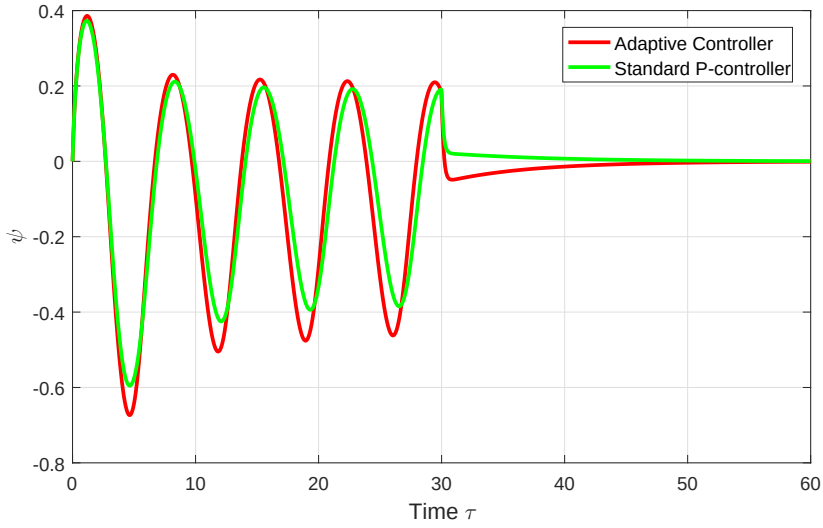

Figure 7.31: Stabilization of the plenum pressure with both the standard P-controller and the adaptive controller

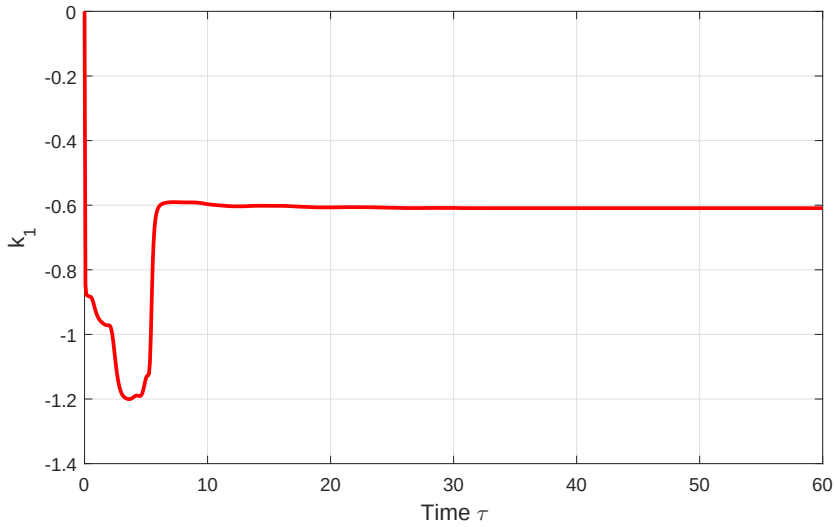

Figure 7.32: Trajectory of the estimate for k_1

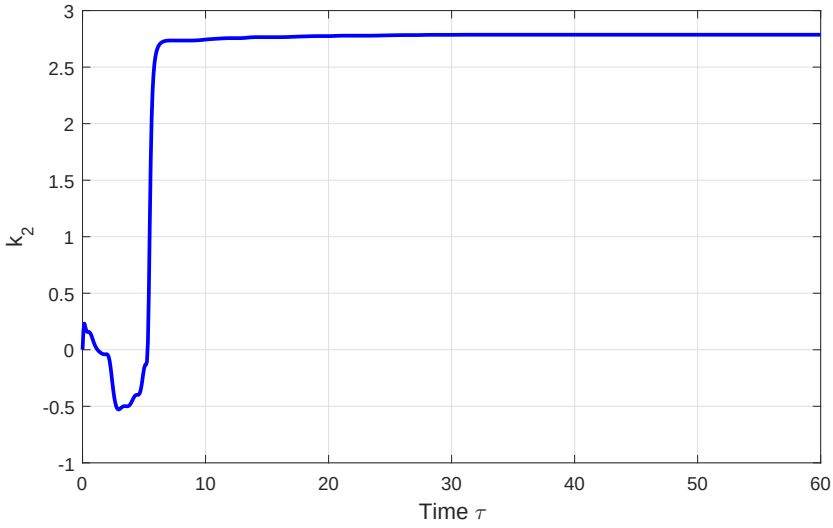

Figure 7.33: Trajectory of the estimate for k_2

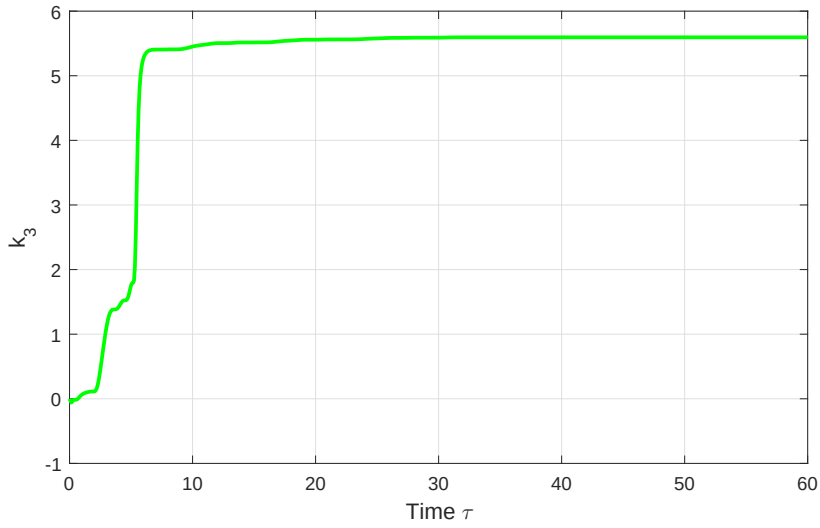

Figure 7.34: Trajectory of the estimate for k_3

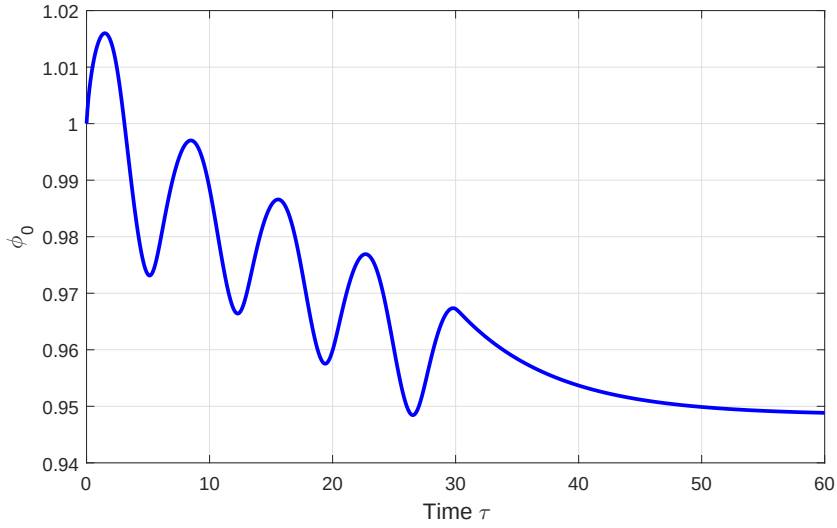

Figure 7.35: Trajectory of the estimate for ϕ_0

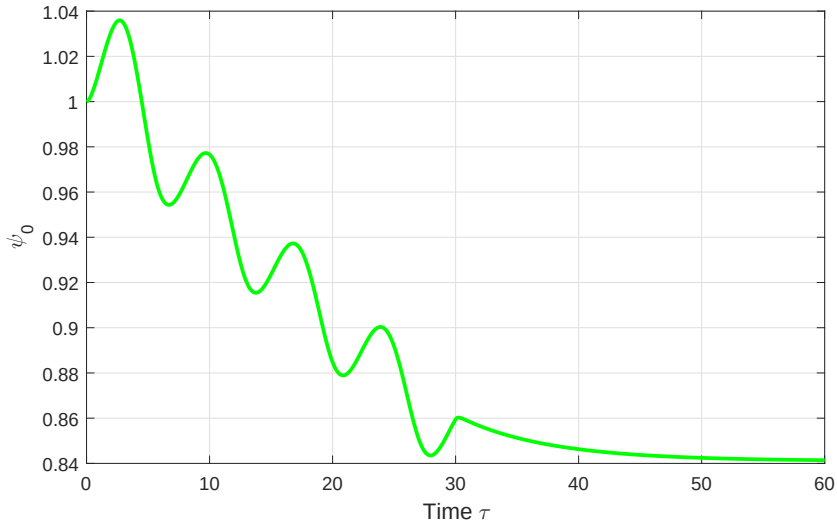

Figure 7.36: Trajectory of the estimate for ψ_0

Evaluation of the results will be done in Section 8 and 9.

Chapter 8

Discussion

The simulations presented in Chapter 7 arises several issues that requires some attention.

Probably, the most important issue that needs to be discussed is the estimation of the equilibrium point. A study of Figures 7.27, 7.28, 7.35 and 7.36 reveals some gap between the actual coordinates for the equilibrium point and their estimates supplied by the adaptive law which [6] proposed. This discovery contradicts with the statement made by [6] where one is predicting that $\hat{\theta}_0$ will be equal to x_0. The reason for this divergence is possibly that the model which supplies the adaptive law with system states uses the outcome of the adaptive law itself to compute those states. In fact, a experiment was run by the author where the equilibrium of the system is known beforehand meaning that the model will generates the states independently of the adaptive law. Under such conditions, the adaptive law produces estimates which manage to exponentially converge to the actual equilibrium. The effect of this inaccuracy in equilibrium estimates will spread to the adaptive controller. Therefore, the performances of the adaptive controller and standard P-controller (for which equilibrium point is known) will differ from each other, even when k_1, k_2 and k_3 were estimated almost perfectly. Of course, one solution of avoiding such error in equilibrium estimates, would be to dismiss the deviation variables in favour of the standard variables in order to express the compression system. In return, the deviation variables are the key tool in order to obtain a simplified parameter estimation of the compressor characteristic and cannot simply be omitted. Thus, the uncertainty regarding the estimation of the equilibrium point is an inevitable drawback of methods introduced in this thesis.

Comparison of the adaptive and standard P-controller leads to a conclusion that large departure of estimates from the actual equilibrium, does not have much of an sizeable influence on the system dynamics. Still, amplitude of surge oscillations tends out be larger for inaccurate equilibrium estimation than for the case where the equilibrium is known exactly. Frequency of the oscillations is the same for both cases. Moreover, the performance of the adaptive controller seems to be somewhat poorer than it is for the P-controller. It still manages, however, to bring the system states exponentially to the origin. Obviously, the are two factors which will influence the performance of the adaptive law: the tuning matrix P and its initial estimate. In order to get a satisfying result, [6] proposes a slow

adaptation (see eq. (3.41)), an advice that has been followed up in this thesis. A reasonable value for the initial estimate can be selected by considering the operating range of the system.

Now, the focus is set on the adaptive controller itself. Although some effort has been put in terms of tuning the adaptive gain, there still exist some parameter estimation error $\tilde{\theta}$ at steady-state for both estimation methods. This implies that the fluctuation of mass flow, does not fulfil persistent excitation condition. As the reader may recall from section 4.1, the convergence of θ toward θ^* is not a priority. Instead, the objective is to come up with such estimates so that the the controller drives the system to a stable equilibrium. Based on the presented simulations in Chapter 7, it can be concluded that the implemented adaptive controller satisfies this goal.

The discussion continues to comparing the two estimation methods. Simulations shows that the estimates reaches their convergence somewhat faster for the gradient method compared with least-squares. This result seems to be incidental, but it needs to be noted that more care had to be put in tuning the adaptive gain for the gradient method than it did for the least-squares. As for the latter, the accuracy of the estimates can be improved by by more aggressively penalizing the estimation error ϵ; the elements for the initial matrix P_0 are set to a very high value. The same approach was tried for the gradient method, only to provide poorer estimates for the constants k_1, k_2 and k_3. The performance of the adaptive controller also worsened. Even if the penalizing of the estimation error with very large matrix P works very well in this particular case of the least-squares, it is not to be expected in general.

Actually, for all simulations, the gain for the adaptive controller remain constant during the stabilization of the system. The reason is that the parameter estimation is being performed prior to the activation of the controller. The delay in activating the controller has been incorporated not only to illustrate its effect but also to provide a highly varying flow measurement signal for the parameter estimation. Ironically, flow signal oscillating due to surge, appears to be very well suited for parameter estimation. The suggested adaptive control embedded for the compression systems can be classified as *indirect adaptive control*. The hallmark for the indirect adaptive control is that the plant parameters are estimated on-line and later used to compute the controller parameters. [33] mentions that in academic environments, the indirect adaptive control is being referred to as *explicit adaptive control* since the design is based on explicit model of the plant. The alternative to indirect adaptive control is obviously *direct adaptive control*. This strategy is characterized by parameterizing the plant model in terms of the control parameters which er estimated directly "without intermediate calculations involving plant parameter estimates" as stated [33]. Such approach has been termed *implicit adaptive control* because the design depends on estimating the implicit plant model.

Chapter 9

Conclussion

This thesis has provided new results in the field on adaptive control of surge in axial and centrifugal compressors. Traditional surge controllers often rely on system parameters. Many of them can be regarded as uncertain in special cases. The literature has already been aware of this uncertainties and have suggested several adaptive controllers that estimates the unknown parameters and/or updates the control settings so that the system requirements are met. In this thesis, two types of surge actuators are being studied: closed-coupled valve (CCV) and a piston. Both actuators were previously operated by standard P-controllers for which the gains can be constructed by the coefficients from the compressor map. For a large part of compressor systems, the compressor map will be poorly known.

The alternative adaptive controller developed in this work, provided the estimates for the compressor map by using two very simple identification approaches. Both methodologies generated very accurate estimates and the resulting adaptive controllers managed to stabilize the compression system in a satisfactory way. To apply the suggested estimation strategies, however, some specific adjustments had to be done upon the compressor model. Primarily, the adjustments consisted of expressing the compressor model in terms of deviation variables. Such action required knowledge of the coordinates of the system equilibrium. If not known, it could either be approximated to some reasonable value or can explicitly be found by using an adaptive scheme. To the best authors knowledge, such adaptation scheme has ,until now, newer been used in the context of compressors. The results through simulations showed that this methodology had rather poor accuracy or at least requires a comprehensive amount of tuning. Still, the result were considered sufficient for the applications in this thesis. Further research on estimating the compressor operating point is, however, appreciated and welcomed by the author. The lack of the accuracy for the equilibrium estimation would also influence the performance of the adaptive controller. For that reason, the adaptive controller differed slightly from the P-controller when it came to stabilizing the compressor. [3mm] The compression system together with the adaptive controller was also accompanied by the observer which provided the estimates of the mass flow for the adaptive controller. The observer was included in both choices of actuation. Results showed that the observer provided an very accurate estimate for mass flow in the case of CCV-actuation. As for the case of assigning the piston as the

actuator, the estimate lost its accuracy in the part where the mass flow was recovered from the oscillations. However, the overall performance of the observer was still found to be acceptable.

Bibliography

[1] H. Abdi. Partial least-squares (PLS) regression. *Encyclopedia of Social Science Research Methods*, 2003. SAG.

[2] H. Abdi. The method of least-squares. *Encyclopedia of Measurement and Statistics*, 1:530–532, 2007.

[3] S. Al-Malawi and J. Zhang. Compressor surge control using a variable throttle area and fuzzy logic control. *Transaction of the Institute of Measurement and Control*, 34(4), 2010.

[4] M. Arcak and P. Kokotovic. Nonlinear observers: a circle criterion. *Automatica*, 37:1913 – 1923, 2001.

[5] M. Bartholomew-Biggs. *Nonlinear optimization with engineering applications*, volume 19. Springer, 2008.

[6] A.S Bazanella, P.V. Kokotovic, and A.E. Silva. On the control of dynamic systems with unknown operating point. *International Journal of Control*, 73(7):600 – 605, 2000.

[7] A.D Belegundu and T.R. Chandrupatla. *Optimization concepts and applications in engineering*. Prentice Hall, 2011.

[8] F.B Belgacem and S.M Kaber. Quadratic optimization in ill-posed problems. *Inverse Problems*, 24(5), 2008.

[9] F. Blanchini and P. Giannattasio. Adaptive control of compressor surge instability. *Automatica*, 38:1373–1380, 2002.

[10] B. Bøhagen. *Active surge Control of centrifugal compressor systems*. PhD thesis, Norwegian University of Science and Technology,Department of Engineering Cybernetics, 2007.

[11] B. Bøhagen and J.T. Gravdahl. Circle criterion observer for a compression system. *Proceedings of the 2007 American Control Conference*, pages 3553 – 3559, 2007.

[12] B. Bøhagen, O. Stene, and J.T Gravdahl. A ges flow observer for compression systems: Design and experiment. *Proceedings of the 2004 American Control Conference*, pages 1528–1533, 2004.

[13] M. Boyce. Axial-flow compressors. *boycepower.com*, pages 163 – 195.

[14] M. Boyce. Principles of operation and performance estimation of centrifugal compressors. *Proceedings of the Twenty-Second Turbomachinery Symposium*, pages 161–177, 1993.

[15] M. Boyce. *Centrifugal compressors: a basic guide*. PennWell, 2003.

[16] G. Chen and T.T Pham. *Fuzzy sets. fuzzy logic and fuzzy control systems*. CRC Press, 2001.

[17] A. Cortinovis, D. Pareschi, M. Mercangoez, and T. Besselmann. Model predictive anti-surge control of centrifugal compressors with variable speed drives. *Proceedings of the 2012 IFAC Workshop on Automatic Control in Offshore Oil and Gas Production*, pages 251–256, 2012.

[18] B. de Jager. Rotating stall and surge avoidance: a survey. *Proceedings of the 34th IEE Conference on Decition and Control*, 2:1857–1862, 1995.

[19] H.W. Emmons, C.E. Pearson, and H.P. Grant. Compressor surge and stall propagation. *Transactions of the ASME*, 77:455–469, 1955.

[20] A.H Epstein, J.E.F Williams, and E.M Greitzer. Active suppresion of aerodynamic instabilities in turbomachines. *Joournal of Propulsion and Power*, 5:204–211, 1989.

[21] J. Felsenstein. An alternating least-squares approach to inferring phylogenies from pairwise distances. *Systematic Biology*, 46, 1997.

[22] D.A Fink, N.A. Cumpsty, and E.M Greitzer. Surge dynamics in a free-spool cenreifugal compressor system. *Journal of Turbomachinery*, 1993.

[23] J.T. Gravdahl. *Modeling and control of surge and rotating stall in compressors*. PhD thesis, Norwegian University of Science and Technology,Department of Engineering Cybernetics, 1998.

[24] J.T Gravdahl and O. Egeland. Compressor surge control using a closed-coupled valve and backstepping. *Proceedings of the American Control Conference*, 1997.

[25] J.T Gravdahl and O. Egeland. *Compressor surge and rotating stall: modelling and control*. Springer, 1999.

[26] J.T Gravdahl and O. Egeland. *Modelling and simulation for automatic control*. Marine Cybernetics, Trondheim,Norway, 2002.

[27] J.T Gravdahl, O. Egeland, and S.O Vatland. Drive torque actuation is active surge control of centrifugal compressors. *Automatica*, 38(11):1881–1983, 2002.

[28] E.M. Greitzer. Surge and rotating stall in axial flow compressors, part 1: Theoretical compression system model. *Journal of Engineering for Power*, pages 190–198, 1976.

[29] E.M. Greitzer. Coupled compressor diffuser flow instability. *Journal off aircraft*, 1977.

[30] D. Gysling, D. Dugundji, E. Greitzer, and A. Epstein. Dynamic control of centrifugal compressor surge using tailored structures. *Journal of Turbomachinery*, 113(4):710–722, 1991.

[31] K.E Hansen, P. Jørgensen, and P.S Larsen. Experimental and theoretical study of surge in a small centrifugal compressor. *Journal of Fluids Engineering*, 103:391–395, 1991.

[32] A. Ilchmann. *Non-identifier-based high gaina adaptive control*. Springer, 1993. Lecture Notes in Control and Information Science.

[33] P.A Ioannou and J. Sun. *Robust adaptive control*. Prentice Hall, 1996.

[34] A. Jerzak. An introduction to centrifugal compressor modelling and load sharing. Norwegian University of Science and Technology,Department of Engineering Cybernetics, 2016.

[35] H. Khalil. *Nonlinear systems*. Prentice Hall, 3rd edition, 2002.

[36] P.V. Kokotovic, H.K. Khalil, and O'Reilly. *Singular Pertubation Methods in Control: Analysis and Design*. Academic Press, 1986.

[37] K. Louie, H. Clark, and P.C.D Newton. Analysis of differential equation models in biology: A case study for clover meristem populations. *New Zealand Journal of Agricultural Research*, 41:567–576, 1998.

[38] K. Madsen, H.B. Nielsen, and O Tingleff. *Methods for non-Linear least-squares problems*. Informatics and Mathematical Modelling, Technical University of Denmark, 2nd edition, 2004.

[39] F.K Moore and E.M Greitzer. A theory of post-stall transients in axial compressor systems: Part i - development of equations. *Journal of Engineering for Gas Turbines and Power*, 108:68–76, 1986.

[40] K. Nakagawa, M. Fujiwara, T. Nishioka, S. Tanaka, and Y. Kashiwabara. Experimental and numerical analysis of active supression of centrifugal compressor surge by suction-side valve control. *JSME International Journal, Series B*, 37(4):878–885, 1994.

[41] M.J Nieuwenhuizen. Parameter analysis and identification of the greitzer model by analogy with the van der pol equation. Master's thesis, Technische Universiteit Eindhoven,Department Mechanical Engineering, 2008.

[42] T. Øvervåg. Centrifugal compressor loadsharing with the use of mpc. Master's thesis, Norwegian University of Science and Technology,Department of Engineering Cybernetics, 2013.

[43] J.E Pinsley, G.R Guenette, A.H Epstein, and Greitzer E.M. Active stabilization of centrifugal compressor surge. *Journal of Turbomachinery*, 113:723 – 732, 1991.

[44] H. Sheng, W. Huang, T. Zhang, and X. Huang. Robust adaptive control of compressor surge using backstepping. *Arabian Journal of Science and Engineering*, 39(12):9301 – 9308, 2014.

[45] J.C. Simon, L. Valavani, A.H. Epstein, and E.M Greitzer. Evaluation of approaches to active compressor surge stabilization. *Journal of Turbomachinery*, 115:57 – 67, 1993.

[46] J.S Simon and L. Valavani. A lyapunov based nonlinear control scheme for stabilizing a basic compression system using a closed-coupled control valve. *Proceedings of the 1991 American Control Conference*, pages 2398–2406, 1991.

[47] J.F. Slotine and W. Li. *Applied non-linear control*. Prentice Hall, 1991.

[48] J. Sorokes. Selecting a centrifugal compressor. *Chemical Engineering Progress*, 109(6):44 – 51, 2013.

[49] N. Uddin and J.T. Gravdahl. Piston actuated-surge control of centrifugal compressor including integral action. *Proceedings og the 11th International Conference on Control, Automation and Systems*, 2011a.

[50] N. Uddin and J.T. Gravdahl. Active surge control using pistion actuation. *Proceedings of the ASM 2011 Dynamic Systems and Control Conference*, 2011b.

[51] N. Uddin and J.T Gravdahl. Bond graph modeling of centrifugal compressor systems. *Simulations: Transaction of the Society for Modeling and Simulation*, 91:998–1013, 2015.

[52] N. Uddin and J.T. Gravdahl. Active compressor surge control system by using piston actuation: implementation and experimental results. *11th IFAC Symposium on Dynamics and Control of Process Systems, including Biosystems*, pages 347 – 352, 2016.

[53] N. Uddin and J.T. Gravdahl. Two general feedback control laws for compressor surge stabilization. *24th Mediterranean Conference on Control and Automation*, pages 689–695, 2016.

[54] S. van der Geer. Least-squares estimation. *Encyclopedia of Statistics in Behavioral Science*, 2:1041–1045, 2005.

[55] N. Westerhof, N. Stergiopulos, and M. Noble. *Snapshots of hemodynamics*. Springer, 2nd edition, 2010.

[56] F. Willems and B. de Jager. Modeling and control of compressor flow instabilities. *IEE Control Systems*, 19:8–18, 1995.

[57] J.F Williams and X. Huang. Active stabilization of compressor surge. *Journal of Fluid Mechanics*, 204:245–262, 1989.

[58] S. Yeung and R. Murray. Reduction of bleed valve rate requirements for control of rotating stall using continous air injection. *Proceedingds of the 1997 IEEE International Conference on Control Application*, pages 693–690, 1997.